

NATIONAL CENTRE FOR NUCLEAR RESEARCH

DOCTORAL THESIS

---

# Modelling the primordial universe with quantum spacetimes

---

*Author:*  
Jaime DE CABO MARTÍN

*Supervisor:*  
Dr. hab. Przemysław  
MAŁKIEWICZ  
*Auxiliary supervisor:*  
Prof. Patrick Peter

*A thesis submitted in fulfillment of the requirements  
for the degree of Doctor of Philosophy*

*in the*

Department of Fundamental Research



June 15, 2023



## Declaration of Authorship

I, Jaime DE CABO MARTÍN, declare that this thesis titled, “Modelling the primordial universe with quantum spacetimes” and the work presented in it are my own. I confirm that:

- This work was done wholly or mainly while in candidature for a research degree at the National Centre for Nuclear Research.
- Where any part of this thesis has previously been submitted for a degree or any other qualification at the National Centre for Nuclear Research or any other institution, this has been clearly stated.
- Where I have consulted the published work of others, this is always clearly attributed.
- Where I have quoted from the work of others, the source is always given. With the exception of such quotations, this thesis is entirely my own work.
- I have acknowledged all main sources of help.
- Where the thesis is based on work done by myself jointly with others, I have made clear exactly what was done by others and what I have contributed myself.

Signed:

---

Date:

---



NATIONAL CENTRE FOR NUCLEAR RESEARCH

## *Abstract*

### **Modelling the primordial universe with quantum spacetimes**

Jaime DE CABO MARTÍN

The understanding of the origins and evolution of the Universe is the fundamental goal of cosmology. The available mathematical description breaks down at the very beginning of the evolution - the big-bang singularity, which is a long-standing issue of the classical cosmology, hindering the comprehension of the nature of the Universe at its earliest stage.

This doctoral thesis investigates a simple cosmological model of Friedmann-Lemaître-Robertson-Walker universe, filled with a perfect fluid, and furnished with primordial inhomogeneous scalar perturbations. The quantization of the background spacetime by means of covariant quantization methods is our proposal for a novel approach to studying the early universe. Our research shows that this model resolves the initial singularity by replacing it by the so-called big-bounce, a propitious alternative to the current paradigm based on inflation.

The quantum effects in the dynamics of the perturbations can lead to nonequivalent evolutions. We observe that an ambiguity arises due to the quantization of the background space-time, leading to physically inequivalent evolutions at the quantum level despite being equivalent classically. This results in ambiguous predictions for the amplitude power spectrum of primordial perturbations. This result of our research raises new questions and challenges for the development of quantum cosmology. In addition, we study the physical predictions that follow from the final quantum state of perturbations amplified by the big bounce and constrain our model with observational results. Our research shows that the final quantum state of perturbations contains a lot of information about the early universe, which can be used to further refine the model and to make more detailed predictions.

Finally, we investigate the homogeneous but anisotropic quantum mixmaster universe. First, we quantize the model and apply to it a semi-quantum approximation. Then we examine the possibility for the existence of a sufficient amount of inflationary dynamics in the semi-quantum model. We show that this model can undergo only limited amount of inflation and thus does not include a robust inflationary mechanism for generating the primordial structure. Our findings provide new insights into the behaviour of anisotropic cosmologies in the quantum regime.

Overall, this doctoral thesis describes a comprehensive investigation into the quantum dynamics of the early universe and its evolution, expanding our viewpoint on the fundamental nature of the Universe.



## *Streszczenie*

### **Modelling the primordial universe with quantum spacetimes**

Jaime DE CABO MARTÍN

Zrozumienie pochodzenia i ewolucji Wszechświata jest podstawowym celem kosmologii. Dostępny matematyczny opis ewolucji załamuje się w samym jej początku - osobliwości wielkiego wybuchu, stanowiącej odwieczny problem klasycznej kosmologii, utrudniający zrozumienie natury Wszechświata w jego najwcześniejszym stadium.

W tej pracy doktorskiej badany jest prosty model kosmologiczny wszechświata Friedmanna-Lemaitre'a-Robertsona-Walkera, wypełnionego płynem doskonałym i rozszerzonego o pierwotne niejednorodne zaburzenia skalarnie. Kwantyzacja czasoprzestrzeni tła przy użyciu uogólnionych kowariantnych metod kwantyzacji to nasza propozycja nowego podejścia do badania wczesnego wszechświata. Nasze badania pokazują, że ten model jest w stanie rozwiązać początkową osobliwość przez zastąpienie jej tzw. wielkim odbiciem, obiecującej alternatywy dla obecnego paradygmatu opartego na teorii inflacji.

Efekty kwantowe w dynamice zaburzeń mogą prowadzić do ich nierównoważnych ewolucji. Dokonujemy obserwacji, że ta niejednoznaczność wynika z tego, że tło kosmologiczne jest skwantowane, co prowadzi do fizycznie nierównoważnych ewolucji na poziomie kwantowym, mimo, że klasycznie były równoważne. Skutkuje to niejednoznacznością przewidywań na spektrum mocy amplitudy pierwotnych zaburzeń. Ten wynik badań stawia nowe pytania i wyzwania dla rozwoju kwantowej kosmologii. Ponadto, badamy przewidywania fizyczne jakich dostarcza stan końcowy zaburzeń wzmocnionych przez wielkie odbicie i ograniczamy nasz model dzięki obserwacjom. Nasze badania pokazują, że końcowy stan kwantowy zaburzeń zawiera wiele informacji o wczesnym wszechświecie, które można wykorzystać do dalszego udoskonalenia modelu wielkiego odbicia i do jeszcze dokładniejszych przewidywań.

Co więcej, badamy jednorodny, anizotropowy kwantowy model wszechświata mixmaster. Najpierw kwantujemy model i wprowadzamy semi-kwantowe przybliżenie. Potem badamy możliwość zajścia wystarczającej ilości samoistnej inflacji na poziomie semi-kwantowym. Pokazujemy, że ten model zawiera ograniczoną ilość inflacyjnej dynamiki i nie zawiera inflacyjnego mechanizmu generacji pierwotnych struktur. Nasze wyniki dostarczają nowych spostrzeżeń na temat zachowania kosmologii anizotropowych w kwantowym reżimie.

Podsumowując, ta rozprawa doktorska opisuje wszechstronne badanie kwantowej dynamiki wczesnego wszechświata i jego ewolucji, poszerzające naszą perspektywę na fundamentalną naturę Wszechświata.



# *Acknowledgements*

## *Agradecimientos*

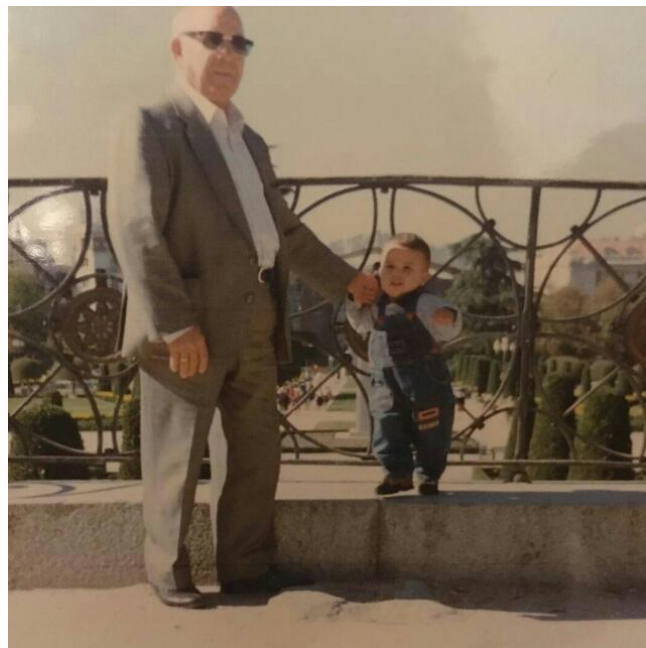
First, I want to express my most sincere gratitude to my supervisor Przemek, for allowing me to be part of and guiding me through the fascinating world of research in theoretical physics and quantum cosmology, something I have dreamed about since I was a teenager. For helping me throughout all my PhD, being always available for any doubt or problem I could have, for the uncountable days of meetings, discussions and explanations, for the great patience he has to teach me his extensive knowledge and the big amount of freedom he gave me during my studies. I cannot imagine a better supervisor than him and I will always consider him as my scientific father. I want to thank my co-supervisor Patrick Peter, for his warm and great hospitality at Institut d'Astrophysique de Paris during which I learned a lot, always being willing to have a scientific conversation and being the perfect host allowing me to enjoy and discover many things about the splendid city of Paris. For passing on his great experience in the field to me, and for the great amount of knowledge I gained during our many meetings throughout the PhD studies. I would also like to thank Jean-Pierre Gazeau for the numerous hours spent together in a enjoyable environment discussing about many different aspects of physics and his highly valuable lessons along our spellbinding collaboration. I would like to thank in general to all the physicist I have had the opportunity to work with and collaborate, who have helped me during the development of my PhD studies, either with a brief work discussion or during my participation in conferences. Finally, I would like to thank the Polish National Science Centre for the financial support during the time of my PhD studies. My work was supported through the research grant 2018/30/E/ST2/00370.

En lo personal, me gustaría agradecer estos cuatro años a mucha gente. Primero a mi madre por su amor y apoyo incondicional durante toda mi vida y toda mi carrera, por ser la persona que más se preocupa por mi y de que todo siempre me vaya a la perfección incluso si eso implica sacrificarse ella en cualquier aspecto, es sin duda la mejor persona que he conocido en mi vida y la mejor madre que alguien puede desear, te quiero muchísimo. A mi padre, igualmente por su cariño y apoyo durante toda mi vida, por hacerme sentir orgulloso presumiendo siempre de su hijo y mi trabajo con todo el mundo y por siempre estar e intentar ayudarme si necesito cualquier cosa, te quiero mucho. A mi abuela Veli por su afecto, por siempre estar para mi y no cansarse nunca de hablarme de cualquier cosa imaginable permitiendome aprender más escuchandola cada vez por muchos años que pasen; y a mi abuelo Eugenio por quererme desde el momento en que nací, estoy seguro que si he dedicado mi vida a las ciencias es gracias a haberlo heredado innatamente de él, y por ello millones de gracias, los quiero y siempre lo haré. Quiero agradecer especialmente a mis abuelos Pablo y Antonia, por ser pilares fundamentales toda mi vida. No me cansaré de decir que deberían ser eternos, y no hay nadie que se merezca el cielo más que ellos. Desearía poder vivir mil vidas con ellos para poder equiparar todo el amor que me han dado y darles las gracias por todo lo que me han enseñado, transmitido y ayudado, los quiero con locura y los tendré presente siempre. En términos generales me gustaría agradecer a mi familia, con la que he compartido buenos momentos toda mi vida, a mis tios Eugenio, Juan, Ana y Esteban, a mis numerosos primos, y a Manuel, a Chus y Rober.

Quiero especialmente agradecer a mi Arantxa, the special one, por todo el amor que me procesa cada día, solo comparable al que yo le tengo, que es infinito, por todos los años que hemos estado juntos desde el momento que nos encontramos y nos

convertimos en inseparables y todos los años de mi vida que espero pasar a su lado. Nunca podré hacer suficiente para merecerte y agradecerte todo lo que haces por mi, te declaro mi más sincero amor eterno, y siempre voy a estar toda mi vida a tu lado, con el objetivo de darte la vida más feliz que tanto mereces. También, es la persona con la voz más bonita que he escuchado en mi vida, desearía despertarme todos los días con tan angelical sonido, y estoy muy orgulloso de sus tres dominadas. También me gustaría agradecer a mi siempre suegro Darío, sin duda de las personas más interesantes que he tenido la oportunidad de conocer, por toda la ayuda que nos ha ofrecido, por preocuparse por hacer posible nuestro perfecto desarrollo de la vida durante nuestros años en Polonia, y por todo el amor y enseñanza que has proporcionado a tu hija Arantxa, sin el cual no sería la gran persona que yo he llegado a conocer.

A mis amigos de toda la vida, de mi pueblo Garciotum, y de la universidad, por la infinidad de increíbles momentos y experiencias vividas juntos, y en especial a Andres, Andrea y Mario, porque, aun aguantándonos muchos años como amigos en España, han tenido el detalle de pasarse por Polonia para ver qué tal nos trataba la vida por aquí y seguir sumando aventuras que espero que nunca falten.



*"Quien nos quiere no nos abandona jamás, y siempre podrás hallarlos aquí ♡"*

# Contents

|                                                                   |            |
|-------------------------------------------------------------------|------------|
| <b>Declaration of Authorship</b>                                  | <b>iii</b> |
| <b>Abstract</b>                                                   | <b>v</b>   |
| <b>Streszczenie</b>                                               | <b>vii</b> |
| <b>Acknowledgements</b>                                           | <b>ix</b>  |
| <b>1 Motivation to study quantum models of the early universe</b> | <b>1</b>   |
| <b>2 Theoretical Framework</b>                                    | <b>5</b>   |
| 2.1 Hamiltonian formalism for General Relativity . . . . .        | 5          |
| 2.1.1 Relativistic perfect fluid . . . . .                        | 6          |
| 2.1.2 The FLRW universe . . . . .                                 | 7          |
| Choice of internal clock . . . . .                                | 8          |
| Background singular solutions . . . . .                           | 9          |
| 2.1.3 Perturbative expansion - scalar modes . . . . .             | 9          |
| 2.2 Anisotropic models . . . . .                                  | 12         |
| 2.2.1 Homogeneous cosmological models . . . . .                   | 13         |
| 2.2.2 Hamiltonian formulation of homogeneous models . . . . .     | 14         |
| 2.2.3 Mixmaster universe . . . . .                                | 15         |
| 2.3 The standard model of cosmological Inflation . . . . .        | 19         |
| 2.4 Coherent states . . . . .                                     | 21         |
| 2.4.1 Generalized Coherent states (GCS) . . . . .                 | 22         |
| Phase space representation . . . . .                              | 23         |
| Weyl-Heisenberg symmetry group . . . . .                          | 24         |
| Affine group . . . . .                                            | 25         |
| 2.4.2 Quantization methods based on coherent states . . . . .     | 27         |
| 2.4.3 Semiclassical formalism . . . . .                           | 28         |
| Semiclassical and semiquantum trajectories . . . . .              | 30         |
| 2.4.4 Application of GCS methods to Quantum Cosmology . . . . .   | 30         |
| <b>3 Unitarily inequivalent quantum cosmological models</b>       | <b>33</b>  |
| 3.1 A quantum background . . . . .                                | 35         |
| 3.1.1 Affine quantization of the background . . . . .             | 35         |
| 3.1.2 Phase space semiquantum approximation . . . . .             | 37         |
| Semiquantum background trajectories . . . . .                     | 38         |
| 3.2 Classical perturbations . . . . .                             | 39         |
| 3.2.1 Fluid parametrization . . . . .                             | 41         |
| 3.2.2 Conformal perturbations . . . . .                           | 42         |
| 3.2.3 Solutions for classical perturbations . . . . .             | 43         |
| 3.3 Quantum perturbations . . . . .                               | 44         |
| 3.3.1 Quantization of fluid parametrization . . . . .             | 44         |

|          |                                                                                            |            |
|----------|--------------------------------------------------------------------------------------------|------------|
| 3.3.2    | Quantization of conformal parametrization . . . . .                                        | 45         |
| 3.4      | Semiquantum perturbations . . . . .                                                        | 45         |
| 3.4.1    | Fluid modes . . . . .                                                                      | 46         |
| 3.4.2    | Conformal modes . . . . .                                                                  | 47         |
|          | Difference between both semiquantum perturbation theories . . . . .                        | 50         |
| 3.5      | Brief discussion of results . . . . .                                                      | 51         |
| <b>4</b> | <b>Ambiguous power spectrum in a quantum bounce</b>                                        | <b>53</b>  |
| 4.1      | The ambiguity . . . . .                                                                    | 54         |
| 4.2      | Spectral indices of the semiquantum models . . . . .                                       | 57         |
| 4.2.1    | Numerical integration . . . . .                                                            | 57         |
| 4.2.2    | Analytical Integration . . . . .                                                           | 58         |
| 4.3      | A tale of two indices . . . . .                                                            | 63         |
| 4.3.1    | Numerical facts . . . . .                                                                  | 64         |
| 4.3.2    | A sharp transition . . . . .                                                               | 65         |
| 4.4      | Brief discussion of results . . . . .                                                      | 67         |
| <b>5</b> | <b>Physical predictions and final state of perturbations in quantum bouncing cosmology</b> | <b>69</b>  |
| 5.1      | Final states distributions . . . . .                                                       | 70         |
|          | Bogolyubov transformations . . . . .                                                       | 70         |
| 5.1.1    | Particle distributions . . . . .                                                           | 71         |
| 5.1.2    | Phase space representation . . . . .                                                       | 72         |
| 5.1.3    | Temporal phase shift . . . . .                                                             | 74         |
| 5.2      | Physical predictions . . . . .                                                             | 77         |
| 5.2.1    | Amplitude and the bounce . . . . .                                                         | 77         |
| 5.2.2    | Phase shift . . . . .                                                                      | 79         |
| 5.3      | Brief discussion of results . . . . .                                                      | 80         |
| <b>6</b> | <b>Can a quantum mixmaster universe undergo a spontaneous inflationary phase?</b>          | <b>83</b>  |
| 6.1      | Quantum mixmaster model and semiquantum portrait . . . . .                                 | 84         |
| 6.1.1    | Quantization and Semiquantum portrait of the isotropy . . . . .                            | 85         |
| 6.1.2    | Quantization and semiquantum portrait of the anisotropy . . . . .                          | 86         |
| 6.1.3    | Semiquantum portrait of the total Hamiltonian constraint . . . . .                         | 88         |
| 6.2      | Semiquantum dynamics . . . . .                                                             | 91         |
| 6.2.1    | Isotropic dynamics . . . . .                                                               | 91         |
| 6.2.2    | Anisotropic dynamics . . . . .                                                             | 93         |
| 6.3      | Accelerated expansion . . . . .                                                            | 95         |
| 6.3.1    | General remarks . . . . .                                                                  | 95         |
| 6.3.2    | Proper analysis . . . . .                                                                  | 96         |
|          | Numerical analysis . . . . .                                                               | 98         |
|          | Analytical analysis . . . . .                                                              | 98         |
|          | Comparison with simple inflaton model replacing anisotropy . . . . .                       | 101        |
| 6.4      | Brief discussion of results . . . . .                                                      | 102        |
| <b>7</b> | <b>Conclusions and prospects for the future</b>                                            | <b>103</b> |
|          | <b>Bibliography</b>                                                                        | <b>105</b> |

*A mis abuelos, mis padres y mi compañera de vida Arantxa*



# 1

## Motivation to study quantum models of the early universe

Unravelling the mysteries of the cosmos is one of the oldest scientific objectives. At least five thousand years ago, in ancient Egypt, human beings already looked up to the sky, trying to find answers to the deepest questions about the cosmos. Throughout history, many civilizations attempted to address issues of cosmology such as the birth, evolution and ultimate fate of the Universe, as well as inquired about its size or their place in it. Modern physical cosmology, as it is now understood, began in the first decades of the twentieth century, with the development of Albert Einstein's general theory of relativity [1-5], and was consolidated by major observational discoveries, such as the ones made by Hubble [6] and Vesto Slipher [7] among others. Due to its success in explaining the observations, General Relativity is nowadays the most widely accepted theory of gravity, and constitutes the basis of the Standard Cosmological Model. In addition, in the beginning of the twentieth century, another theory made its appearance as well: quantum mechanics. The latter, by assuming the discreteness of the nature, has also been extremely successful in explaining different observations and predicting new effects on the smallest scales, that where later verified experimentally. Nevertheless, the ambitious scientific goal of combining quantum theory and General Relativity into a compatible quantum-gravitational description is still an uncompleted work. Such a description should be able of explaining with success both the physics of the largest cosmological scales and the smallest ones where quantum fluctuations control the gravitational interaction. In order to find such a theory, the focus should be put on systems where both gravitational and quantum effects have a significant role and intertwine. Cosmology provides a valuable experimental test and verification of quantum-gravitational theories. Such theories may potentially describe the earliest moments of the history of the Universe and explain the origin of the primordial structure in the universe. Therefore, the early universe is one of the most relevant research areas to focus on. In addition, quantum cosmological theories generally supposes a technically more manageable framework than quantum gravity, since they usually consider spacetimes with a reduced number of degrees of freedom. The results found for these often soluble cosmological systems can be next generalised to more complex systems.

It is widely accepted that the primordial universe can be described as a patch of flat, isotropic and homogeneous space equipped with small Gaussian and adiabatic

density perturbations with a nearly scale-invariant amplitude spectrum. These density perturbations provided the seeds for the later formation of the cosmic structures we observe today (such as galaxies, galaxy clusters and super-clusters, galaxy filaments, walls, voids, etc). This is in accordance with the present observational data on CMB anisotropies [8], which also indicates that the Universe emerged from an initial state where the spacetime was extremely curved and the matter fields were extremely dense. This is known as the cosmological (or big-bang) singularity. According to the celebrated Hawking-Penrose theorems [9], the appearance of singularities is a generic feature of general relativity. However, they are commonly conceived as a breakdown of the underlying theory, since the spacetime geodesics become incomplete, indicating that our theory should be replaced by a more fundamental and complete one. A natural candidate is a quantum cosmological theory of the primordial universe.

Currently, the most popular modelling of the origin of cosmic structure is based on inflation [10]. The theory of inflation introduces effects of quantum gravity as it involves quantisation of the gravitational field perturbations around a classical homogeneous and isotropic cosmological background. Despite its widely acknowledged success, inflation has some well-known drawbacks, among which two we highlight as inherent: (1) it postulates the existence of an unknown scalar particle, the inflaton, in a fine-tuned potential, what might be difficult to implement at high energy physics; (2) inflation does not address the issue of initial singularity, i.e., the inflationary spacetime is geodesic past-incomplete. Alternative theories based on quantum cosmology replace the big-bang scenario by a quantum bounce that starts the cosmological expansion and is preceded by cosmological contraction. They involve even more elements of quantum gravity, making it possible to obtain a more complete description of the primordial universe. However, it should be noted that these models come not only with new technical but also unsolved conceptual problems. As an example of the latter, there is the problem of interpretation of quantum dynamics of gravitational systems (the so-called problem of time [11]), although it is not a concern of the work presented here.

In the realm of quantum cosmology, several approaches have been developed to propose a non-singular quantum model of the universe. One of the first that incorporates the principles of quantum mechanics and general relativity to propose a wave function describing the entire universe is the Hartle-Hawking model [12]. Another intriguing approach is Bohmian cosmology, inspired by the pilot-wave interpretation of quantum mechanics [13, 14]. More recently, Loop Quantum Cosmology (LQC) has emerged as a compelling framework that merges concepts from loop quantum gravity and cosmology providing a viable description of the early universe and addressing the singularity problem [15, 16]. These diverse approaches offer valuable insights into the nature of quantum cosmology and contribute to our ongoing quest for a comprehensive understanding of the origins of the universe's structure.

In order to obtain a more complete description, it would be desirable to construct the most thorough theory of the primordial universe possible. Hence, any restrictive a priori assumption on the primordial matter or the primordial symmetries should be avoided as much as possible. In particular, the last assumption can be relaxed by removing isotropy of the background and employing more generic spatially homogeneous models, such as the Bianchi types. The introduction of anisotropy could give rise to new effects and leave imprints in the evolution of the primordial universe, specially, if there exists interplay between anisotropy and the quantum bounce. In fact, there exist observational data that suggest some kind

of anomalies at large angular scales that might require this kind of anisotropic extension to the standard theories [17]. Therefore, the results of such theories could be, to some degree, confronted with observations.

This thesis explores possible quantum cosmology models of the origin of primordial structure. We show how the introduction of a quantum state for the background spacetime resolves the singularity with a quantum bounce. Generalized coherent states are proposed as novel useful tools for the investigation. They allow to introduce more general quantization methods, in which the possible ambiguities can be parametrized, and present a semi-classical (or semi-quantum) approximation for the cosmological background. We carefully analyse the consequences that the ambiguities arising from the quantum nature of the cosmological background can produce, and investigate whether they can lead to non-equivalent physical predictions. In this context, we intend to emphasize how important the choice of the relevant variable for the perturbations to be quantized actually is. We examine how the quantum bounce amplifies the perturbations and derive the power spectrum for the primordial structure it can generate, in comparison to the inflationary scenario. Finally, we include anisotropic oscillations to the quantum homogeneous background spacetime in order to inspect if the interplay between the bounce, contracting phase and anisotropy is able to generate a universe that reproduces an inflationary dynamics, that is, undergoing sufficiently long accelerated expansion.

The thesis consist of 7 chapters, the first one being the present chapter 1:

Chapter 2 establishes the framework for the research results shown in the next chapters, and introduces the three main theoretical concepts: canonical Hamiltonian formalism of cosmological models, with application to (1) the isotropic FLRW cosmological model filled with perfect fluid, and its expansion to include scalar perturbations, and (2) models with anisotropic background, focusing on the Bianchi IX universe; (3) the use of generalized coherent states for phase space covariant quantization methods and semiclassical description of quantum systems.

Chapter 3 focuses on the derivation of the *semi-quantum* bouncing model for classically equivalent isotropic cosmological models with scalar perturbations. Special attention is paid to the ambiguities that arise from the quantization process.

Chapter 4 consists in the derivation of the power spectrum of scalar perturbations for the semi-quantum models. That includes further investigation of the ambiguity and identification of the relevant quantum parameters producing different predictions.

Chapter 5 describes the study of the final quantum state of the perturbations and physical predictions of the models. Observational data is used to constrain some parameters of the bouncing solutions.

Chapter 6 introduces the semi-quantum analysis of the dynamics of the anisotropic and homogeneous quantum mixmaster universe. The obtained solutions are examined with regard to the existence of inflationary dynamics.

Chapter 7 summarises the presented results and includes a discussion about future research direction.

This thesis is based on the following articles:

- [Chapter 3](#): Jaime d. C. Martin, Przemysław Małkiewicz and Patrick Peter. *Unitarily inequivalent quantum cosmological bouncing models* Phys. Rev. D 105, 023522 (2022).

- Chapter 4: Jaime d. C. Martin, Przemysław Małkiewicz and Patrick Peter. *Ambiguous power spectrum in a quantum bounce* [arXiv:2212.12484] (2023).
- Chapter 5: Jaime d. C. Martin and Przemysław Małkiewicz. *Physical predictions and final quantum state of perturbations in quantum bouncing cosmology* [In preparation] (2023).
- Chapter 6: Hervé Bergeron, Jaime d. C. Martin, Jean-Pierre Gazeau and Przemysław Małkiewicz. *Can a quantum mixmaster universe undergo a spontaneously inflationary phase?* [arXiv:2303.07873] (2023).

In addition, part of the content of the chapters 3-5 is also included in the paper: Jaime d. C. Martin. *The primordial structure from Quantum Cosmological bouncing models*. Contribution to the 2022 Cosmology session of the 56th Rencontres de Moriond. [arXiv:2203.03924] (2022). Moreover, chapter 6 also comprises content that can be found in: Jaime d. C. Martin. *Mixmaster universe: semiclassical dynamics and inflation from bouncing*. Published in Acta Physica Polonica B Proceedings Supplement 16, 6-A20 [arXiv:2302.01111] (2023).

# 2

## Theoretical Framework

### 2.1 Hamiltonian formalism for General Relativity

In this section we introduce the Hamiltonian formulation of General Relativity. We recall the basic elements of the ADM [18] canonical formalism for General Relativity. We first apply the formalism to a Friedmann-Lemaître-Robertson-Walker universe filled with a perfect fluid. For the latter the canonical formalism for relativistic perfect fluids by B. Schutz is used. Afterwards, scalar gravity and matter perturbations are introduced to the model, omitting the vector and tensor perturbations since they undergo independent dynamics. Our presentation of the framework largely follows Ref. [19]. In the next section, the same Hamiltonian formalism is applied to the anisotropic Bianchi IX universe.

The ADM formalism is introduced by writing the following spacetime line element:

$$ds^2 = -N^2 dt^2 + q_{ab}(dx^a + N^a dt)(dx^b + N^b dt) \quad (2.1)$$

where  $a, b = 1, 2, 3$  are spatial coordinate indices,  $N$  and  $N^a$  denote, respectively, the lapse and shift functions, and  $q_{ab}$  is an induced three-metric on the three-dimensional spacelike hypersurface with toroidal topology,  $\Sigma = \mathbb{T}^3$ . In canonical relativity, the spacetime manifold is assumed to admit a foliation  $\mathcal{M} = \Sigma \times \mathbb{R}$  where  $\mathbb{R}$  is a time manifold.

The Hamiltonian of General Relativity is obtained by applying variational principle [18] to the Einstein-Hilbert Action in the ADM variables ( $\Sigma$  is assumed compact, hence there is not boundary terms)

$$S_g = \frac{1}{2\kappa} \int_{\mathcal{M}} R \sqrt{-g} d^4x = \frac{1}{2\kappa} \int_{\mathbb{R}} \int_{\Sigma} ({}^3R - K^2 + K_a^b K_b^a) N \sqrt{q} d^3x dt, \quad (2.2)$$

where  $g_{ab}$  is the spacetime metric,  $R$  is the Ricci scalar curvature of the spacetime,  ${}^3R$  the one of the three-geometries,  $K_{ab} = (\dot{q}_{ab} - D_a N_b - D_b N_a)/2N$  is the extrinsic curvature tensor and  $\kappa = 8\pi G_N$ . The Hamiltonian is a sum of first-class constraints

$$\mathbf{C}_g = \int_{\Sigma} (NC_g + N^a C_{g,a}) d^3x \quad (2.3)$$

with  $N$  and  $N^a$  playing the role of Lagrange multipliers. The gravitational parts of the four constraints can be written in terms of the ADM phase space variables ( $q_{ab}, \pi^{ab} = \sqrt{q}(K^{ab} - Kq^{ab})$ ) as

$$C_g = \frac{\sqrt{q}}{2\kappa} \left( -{}^3R + q^{-1}(\pi_a^b \pi_b^a - \pi^2/2) \right), \quad C_g^b = -\frac{1}{\kappa} D_a(\pi^{ab}) \quad (2.4)$$

where  $D_a$  is the spatial covariant derivative.

### 2.1.1 Relativistic perfect fluid

Regarding the matter part, the phase space can be extended in order to include perfect fluids, each one satisfying a barotropic equation of state  $p = w\rho$ . Schutz was the first to introduce a formalism consisting in a velocity-potential approach to the variational formulation of relativistic perfect fluids [20, 21]. In order to include perfect fluids into a cosmological spacetime, let us introduce some basic thermodynamical quantities:  $p$  - pressure,  $\rho$  - energy density,  $n$  - number density of fluid's particles,  $T$  - temperature,  $\mu = (\rho + p)/n$  - enthalpy per fluid's particle, and  $S$  - entropy per fluid's particle ( $s$  - specific entropy). In terms of these quantities we can express the first law of thermodynamics as:

$$dp = nd\mu - nTdS. \quad (2.5)$$

In the Schutz formalism, the fluid four-velocity is written in terms of six different scalar potentials:

$$U^\nu = \mu^{-1}(\phi,{}^\nu + \alpha\beta,{}^\nu + \theta s,{}^\nu). \quad (2.6)$$

We assume the entropy of the perfect fluid to be constant in time and homogeneous across the space. Therefore, last term of the above expression vanishes. We assume a non-rotational perfect fluid, then  $\alpha = \beta = 0$ , and we can write the four velocity of the fluid as a function of two scalar fields ( $\phi$  defining its flow and the entropy  $\mu$ ) and the four-metric:

$$U^\nu = \mu^{-1}\phi,{}^\nu \quad (2.7)$$

with normalization  $U_\nu U^\nu = -1$ . The Schutz action for perfect fluids reads:

$$S_f = \int_{\mathcal{M}} \sqrt{g} p(w, \phi) d^4x \quad (2.8)$$

In the canonical analysis, the variation of this action with respect to the time derivative of the scalar field gives the fluid conjugate momentum  $p^\phi = -N\sqrt{q}nU^0$ , where we used (2.7) (2.5) and  $n = \partial p / \partial \mu|_S$ . In terms of the phase space variables, the fluid Hamiltonian reads:

$$\mathbf{C}_f = \int_{\Sigma} (\dot{\phi} p^\phi - N\sqrt{q}p(w, \phi)) \quad (2.9)$$

From this Hamiltonian, one sees that we are interested in  $\dot{\phi}$  and the pressure  $p$ . For the equation of state  $p = w\rho$ , the dimensionless parameter  $w$ , called the barotropic index, is a constant defined in the range  $-1/3 < w < 1$ , where, for instance:  $w = 0$  represents non-relativistic dust,  $w = 1/3$  radiation, and  $w = 1$  stiff matter. That equation of state can be shown [22] to be equivalent to

$$p(\mu) = K\mu^{\frac{w+1}{w}}, \quad (2.10)$$

where  $K$  is an arbitrary constant. We assume the above equation for the pressure. This specifies the following expression for the time derivative of the scalar field:

$$\dot{\phi} = N \frac{p^\phi}{\sqrt{q} K \frac{w+1}{w} \mu^{\frac{w+1}{w}-2}} + N^a \phi_{,a}. \quad (2.11)$$

The expression of the specific enthalpy  $\mu$  in terms of the canonical variables can be determined by means of the normalization condition for  $U^\mu$ :

$$\mu^2 = \left( \frac{p^\phi}{\sqrt{q} K \frac{w+1}{w} \mu^{\frac{w+1}{w}-2}} \right)^2 - q^{ab} \phi_{,a} \phi_{,b}. \quad (2.12)$$

Thus, the fluid Hamiltonian is found to read:

$$\mathbf{C}_f = \int_{\Sigma} (N C_f + N^a C_{f,a}) d^3x, \quad (2.13)$$

where the constraints read:

$$C_f = \frac{(p^\phi)^2}{\sqrt{q} K \frac{w+1}{w} \mu^{\frac{w+1}{w}-2}} - \sqrt{q} K \mu^{\frac{w+1}{w}}, \quad C_{f,a} = p^\phi \phi_{,a}. \quad (2.14)$$

Finally, the total gravity and fluid Hamiltonian reads:

$$\mathbf{C} = \mathbf{C}_g + \mathbf{C}_f = \int_{\Sigma} (N(C_g + C_f) + N^a(C_{g,a} + C_{f,a})) d^3x. \quad (2.15)$$

This total constraint is expanded to second order in perturbations around a flat FLRW model in the next section.

### 2.1.2 The FLRW universe

In the case of homogeneous and isotropic Friedmann-Lemaître-Robertson-Walker flat metric

$$ds^2 = -N^2 d\tau^2 + a^2(\tau) \delta_{ab} dx^a dx^b \quad (2.16)$$

the induced three-metric is  $q_{ab} = a^2 \delta_{ab}$ , the shift functions  $N^a$  vanish in the comoving coordinates, and the three constraints  $C_{g,a}$  vanish along with  ${}^3R$  on the flat and homogeneous spatial slices. We define the canonical background variables as<sup>1</sup>:

$$a^2 = \frac{1}{3} \int_{\Sigma} q_{ab} \delta^{ab} d^3x, \quad p_a = \int_{\Sigma} \pi^{ab} \delta_{ab} d^3x, \quad \bar{\phi} = \int_{\Sigma} \phi d^3x, \quad \bar{p}^\phi = \int_{\Sigma} p^\phi d^3x \quad (2.17)$$

where we assumed the coordinate volume of the compact spatial slice  $\mathbb{T}^3$  to be  $\mathcal{V}_0 = \int_{\Sigma} d^3x = 1$ . Then, in these variables the gravitational constraint (2.4) (later called the zeroth order Hamiltonian  $H_g^{(0)}$ ) for the FLRW universe reads:

$$\mathbf{C}_g = -\frac{\kappa_0 N}{12a} p_a^2, \quad (2.18)$$

<sup>1</sup>These variables are considered the zeroth-order variables in the later perturbative expansion.

where  $\kappa_0 = \kappa/\mathcal{V}_0$ . For convenience, let us redefine the canonically conjugate background variables to

$$\tilde{q} = \gamma a^{\frac{3(1-w)}{2}}, \quad \tilde{p} = \frac{\sqrt{6(1+w)}}{2\kappa_0} a^{\frac{3(1+w)}{2}} H, \quad \{\tilde{q}, \tilde{p}\} = 1, \quad (2.19)$$

where  $\gamma = 4\sqrt{6}/(3(1-w)\sqrt{1+w})$ , and  $p_a = 6a^2H/\kappa_0$  with  $H = \dot{a}/(Na)$  the Hubble rate [23]. With the suitable choice of the lapse function,  $N = (1+w)a^{3w}$ , the gravity Hamiltonian can be written in terms of the new variables as:

$$\mathbf{C}_g = -2\kappa_0 \tilde{p}^2. \quad (2.20)$$

Since the canonical background variable  $\bar{\phi}$  is assumed to be homogeneous<sup>2</sup>, for the background fluid Hamiltonian (2.14) we obtain the following expression:

$$\mathbf{C}_f = N \frac{a^3 K}{w} \left( \frac{|\bar{p}^\phi|}{K^{\frac{w+1}{w}} a^3} \right)^{w+1}. \quad (2.21)$$

Making the aforementioned choice of lapse function and conveniently setting the arbitrary constant  $K = w/(w+1)$ , we can write the fluid Hamiltonian as:

$$\mathbf{C}_f = |\bar{p}^\phi|^{w+1}. \quad (2.22)$$

At the same time, we can also perform a canonical transformation of the fluid variables:

$$(\bar{\phi}, \bar{p}^\phi) \mapsto (T, p^T) := \left( \frac{1}{w+1} (\bar{p}^\phi)^{\frac{1}{w}} \bar{\phi}, (\bar{p}^\phi)^{w+1} \right), \quad \{T, p^T\} = 1, \quad (2.23)$$

In these new variables the fluid constraint equals the fluid momentum:

$$\mathbf{C}_f = p^T. \quad (2.24)$$

### Choice of internal clock

Therefore, for this particular choice of the lapse, it is really easy to solve the total background Hamiltonian constraint  $\mathbf{C} = 0$ , and obtain

$$p^T = -\mathbf{C}_g. \quad (2.25)$$

Since the fluid canonical momentum variable equals the gravitational Hamiltonian, we can reduce the symplectic form and obtain

$$\omega \Big|_{\mathbf{C}=0} = d\tilde{q}d\tilde{p} - d(-T)d(-\mathbf{C}_g) \quad (2.26)$$

to understand that the gravitational part of the constraint ( $-\mathbf{C}_g$ ) generates the motion of the variables  $\tilde{q}$  and  $\tilde{p}$  with respect to the internal time ( $-T$ ). The motion occurs in the constraint surface and the Hamiltonian  $-\mathbf{C}_g$  is called the physical Hamiltonian. It is then a standard procedure [24] to promote the fluid variable to the role of internal clock while removing it and its conjugate momentum from the phase space.

<sup>2</sup> $\bar{\phi}$  is the zeroth order part of  $\phi$ . The to-be introduced first order perturbation  $\delta\phi$  is the difference between them. We consider the specific enthalpy  $\mu$  to be a zeroth-order variable, meaning that the second term in the right hand side of Eq. (2.12) vanish and we just have  $\mu^{\frac{w+1}{w}} = \left( \frac{|\bar{p}^\phi|}{K^{\frac{w+1}{w}} a^3} \right)^{w+1}$ .

This kind of procedure was first proposed by Kuchar [25]. Note that we conveniently invert the direction of time with respect to the fluid variable  $-T$  in order to have a positive physical background Hamiltonian:

$$\mathbf{C} = -\mathbf{C}_g = 2\kappa_0 \tilde{p}^2. \quad (2.27)$$

From now on, we shall denote the internal clock by " $\tau$ " and assume it coincides with the FLRW time in (2.16) [26].

### Background singular solutions

The background Hamiltonian (2.27) is mathematically equivalent to the one of a free particle on the half-line. For fluids with parameter range  $-1/3 < w < 1$ , the variable  $\tilde{q}$ , as defined in (2.19), is proportional to a positive power of the scale factor  $a$ . The big-bang singularity takes place at  $\tilde{q} = 0$ , since it corresponds to the vanishing of the scale factor. In addition, we assume that the only physically viable universes are the ones with  $a > 0 \rightarrow \tilde{q} > 0$ . Hence, this implies the existence of two separate branches of solutions: the contraction and the expansion. On the current classical level, the phase space trajectories of the two branches are straight lines with constant momentum which are not connected: the ones of the expanding era emerge from the singularity with  $\tilde{p} > 0$ , while the ones of the contracting era terminate at it with  $\tilde{p} < 0$ . The classical singular solutions are obtained from the background Hamilton equations stemming from (2.27):

$$\tilde{q}(\tau) = \sqrt{8\kappa_0 \mathbf{C}} \tau = (q_B \omega) \tau, \quad \tilde{p}(\tau) = \sqrt{\frac{\mathbf{C}}{2\kappa_0}} = \frac{q_B \omega}{4\kappa_0}, \quad (2.28)$$

where we set the singularity time at  $\tau \rightarrow 0$ , and  $\mathbf{C}$  is a constant by virtue of its definition and the Hamilton equation  $d\tilde{p}/d\tau = 0$ . For later convenience we set the constant to be  $\mathbf{C} = (q_B \omega)^2 / (8\kappa_0)$ . It can be shown [27] that the background Hamiltonian (2.27)  $\mathbf{C} = (1+w)E_f|_{a=1}$  equals  $(1+w)$  times the energy of the fluid contained in the universe when  $a = 1$ . Then, in order to assign the correct trajectory to the background universe, one need to know the value of the energy of the fluid in the whole universe when  $a = 1$ . Such a value can be determined only when one knows the size of the universe, which can be fixed by demanding that the volume of the observable patch be a fixed ratio ( $r^{-1}$ ) of the size of the full universe.

### 2.1.3 Perturbative expansion - scalar modes

Let us now expand the canonical formalism up to second order in perturbations to the FLRW universe. We define the canonical perturbation variables as differences between the ADM and the background variables (2.17):

$$\delta q_{ab} = q_{ab} - a^2 \delta_{ab}, \quad \delta \pi^{ab} = \pi^{ab} - \frac{1}{3} p_a \delta^{ab}, \quad \delta \phi = \phi - \bar{\phi}, \quad \delta p^\phi = p^\phi - \bar{p}^\phi. \quad (2.29)$$

Then,  $a^2$ ,  $p_a$ ,  $\bar{\phi}$ , and  $\bar{p}^\phi$  are zeroth order quantities. The Poisson brackets read  $\{\delta q_{ab}(x), \delta \phi^{a'b'}(x')\} = \delta_{(a}^a \delta_{b)}^{b'} \delta^3(x - x')$ ,  $\{\delta \phi(x), \delta p^\phi(x')\} = \delta^3(x - x')$ . Perturbations of the lapse and the shifts are also introduced:  $N \mapsto N + \delta N$ ,  $N^a \mapsto N^a + \delta N^a$ , thus now  $N$  and  $N^a$  are zeroth order quantities. The total Hamiltonian (2.15), expanded up to second order has the following structure:

$$\mathbf{H} = \mathbf{H}^{(0)} + \int_{\Sigma} \left( NH^{(2)} + \delta NH^{(1)} + \delta N^a H_a^{(1)} \right) d^3x. \quad (2.30)$$

The second order Hamiltonian generates the dynamics of the first order perturbations. It is not a constraint since, in addition to the constraints  $H^{(1)}$  and  $H_a^{(1)}$ , it includes a non-vanishing term,  $NH^{(2)}$ , where the choice of the lapse function  $N$  was defined below (2.19). For that reason, from now on we shall denote our total Hamiltonian by  $\mathbf{H}$  in order to differentiate it from the vanishing (zeroth-order) background Hamiltonian constraint ( $\mathbf{C} = \mathbf{C}_g + \mathbf{C}_f$ ), that has been reduced to (2.27) and is now denoted by  $\mathbf{H}^{(0)} = 2\kappa_0 \tilde{p}^2$ . Observe that the above Hamiltonian lacks first-order terms in perturbations. The dynamics is determined from the variation of the action (2.2)+(2.8), which vanish at first order of the perturbative expansion. This is so because the mean value of the first order perturbation terms after integration over the whole space  $\Sigma$  is zero. It is worth noting that in the perturbations' dynamics the time problem does not arise since the second order Hamiltonian includes the non-vanishing term  $NH^{(2)}$ , meaning the physical observables are not in general constants of motion since they are not required to commute with the Hamiltonian.

The canonically conjugate pair of perturbations are Fourier-transformed,

$$\delta \check{q}_{ab}(\vec{k}) = \int_{\Sigma} \delta q_{ab}(\vec{x}) e^{-i\vec{x}\vec{k}} d^3x, \quad \delta \check{\pi}^{ab}(\vec{k}) = \int_{\Sigma} \delta \pi^{ab}(\vec{x}) e^{-i\vec{x}\vec{k}} d^3x. \quad (2.31)$$

Moreover, the metric perturbations are projected into a new basis with six different perturbation modes  $A_m^{ab}$ , and its dual  $A_{ab}^m$ . In this thesis, we are only interested in scalar perturbations ( $\delta q_1, \delta q_2, \delta \pi^1, \delta \pi^2, \delta \phi, \delta p^\phi$ ), hence, we keep only the scalar modes ( $A_1^{ab}, A_2^{ab}$ ), (vector and tensor perturbations are omitted since they undergo independent dynamics):

$$\delta \check{q}_{ab} = \delta q_{1,2} A_{ab}^{1,2}, \quad \delta \check{\pi}^{ab} = \delta \pi^{1,2} A_{1,2}^{ab}, \quad \text{where} \quad A_{ab}^1 := \delta_{ab}, \quad A_{ab}^2 := \frac{k_a k_b}{k^2} - \frac{1}{3} \delta_{ab}. \quad (2.32)$$

The projector operators are defined in terms of the orthonormal triad  $(\vec{k} \cdot k^{-1}, \vec{v} \cdot k, \vec{w} \cdot k)$ . In the scalar modes only the wavevector  $\vec{k} \cdot k^{-1}$  of this new frame is present. Thus, if we rewrite the diffeomorphism constraint  $H_a^{(1)}$  with respect to such frame, we only keep the scalar mode  $H_{\vec{k}}^{(1)}$  of it, multiplied by the longitudinal scalar mode of the shift vector perturbation  $\delta N^{\vec{k}} = i\delta n \vec{k}$ . In addition,  $H^{(1)}$  is a fully scalar constraint. The non-vanishing second order term is split in its scalar, vector and tensor part since the different modes are decoupled. For us, only the scalar term  $H^{(2S)}$  remains.

Once we have only the scalar modes, the next step is to strongly solve the two scalar constraints by reducing the number of canonical variables and simplifying the form of the non-vanishing second order scalar Hamiltonian. For this purpose the Dirac method is used [28]. It starts with extending the set of constraints by the introduction of gauge-fixing conditions, one for each first-class constraint, in order to obtain a set of second-class constraints. Then, the so-called Dirac brackets are introduced. By means of the latter, we get rid of the first order constraints from the Hamiltonian, and the values of the first order Lagrange multipliers  $\delta N$  and  $\delta n$ , which are different for each set of gauge-fixing conditions, become irrelevant for the

<sup>3</sup>Note that although the zeroth-order terms  $N^a$  and  $C_{g,a}$  vanish, neither of their respective first-order perturbation terms  $\delta N^a$  or  $C_{g,a}^{(1)}$  do.

dynamics in the reduced phase space. Therefore, we isolate the true independent physical degrees of freedom from the kinematical phase space, removing the pure gauge ones. In this way, we obtain the physical scalar Hamiltonian  $H^{(2S)}$  in terms of only two gauge-invariant perturbation variables, called Dirac observables  $(\phi, \pi_\phi)$ . The final total Hamiltonian reads:

$$\mathbf{H}_k = \mathbf{H}^{(0)} - \sum_k N \left( \frac{1}{2} \frac{a^{-3w}}{(1+w)} |\pi_{\phi,k}|^2 + \frac{1}{2} w(1+w) a^{3w-2} k^2 |\phi_k|^2 \right), \quad (2.33)$$

where the zeroth order Hamiltonian  $NH^{(0)}$  is the background Hamiltonian of Eq. (2.27) with the time inversion accounted, and we replaced the integral by the summation since the second order Hamiltonian  $NH_k^{(2)}$  only depends on the discrete wave vector  $k$ . The second order part of the Hamiltonian (2.33) can be written in terms of the redefined background variables (2.19), with the same value of the lapse function we chose for the background zeroth order Hamiltonian,  $N = (1+w)a^{3w}$ , reading:

$$\sum_k \mathbf{H}_k^{(2)} = \sum_k \left( \frac{1}{2} |\pi_{\phi,k}|^2 + \frac{1}{2} w(1+w)^2 \left( \frac{q}{\gamma} \right)^{\frac{4(3w-1)}{3(1-w)}} k^2 |\phi_k|^2 \right), \quad (2.34)$$

From now on, for simplicity, we drop the tilde notation from above  $(\tilde{q}, \tilde{p}) \rightarrow (q, p)$ . The total Hamiltonian (2.27)+(2.34) represents the starting point for the next chapter 3, where we quantize the cosmological system and obtain bouncing solutions and *semi*-quantum dynamics of the truly physical perturbation degrees of freedom. The gauge-invariant perturbation variables have different physical interpretation for different gauge-fixing conditions. It is useful to understand their physical meaning in terms of physical and geometrical quantities. Therefore, we introduce the following quantities associated with the intrinsic geometry and matter for the scalar modes (in Fourier space):

$$\begin{aligned} \delta q &= 3a^4 \delta q_1, & \delta R_k &= 2a^{-4} k^2 (\delta q_1 - \frac{1}{3} \delta q_2), \\ \delta \rho &= a^{-3(w+1)} |\bar{p}^\phi|^{w+1} \left( \frac{\delta p^\phi}{\bar{p}^\phi} - \frac{3\delta q_1}{2a^2} \right), \end{aligned} \quad (2.35)$$

where  $\delta R_k$  and  $\delta \rho$  are the perturbations of the intrinsic curvature of the three-geometry and energy density of the fluid respectively, and  $\delta q$  is the metric density perturbation. In addition, we also keep the perturbation  $\delta \phi_k$  which has the geometrical interpretation of a quantity determining the part of the fluid flow tangential to the three-surface. In terms of these quantities the gauge-invariant perturbations read:

$$\begin{aligned} \phi_k &= \frac{1}{\mathcal{V}_0 \sqrt{2\kappa_0}} \left( \frac{\bar{p}^\phi \delta \phi_k}{\sqrt{w(w+1)} p} + \frac{a^{-\frac{3w-3}{2}}}{\sqrt{\frac{w}{6}}} \frac{a^2}{4\mathcal{V}_0^{\frac{2}{3}} k^2} \delta R_k \right), \\ \pi_{\phi,k} &= \sqrt{2\kappa_0} \left( \sqrt{w(w+1)} \frac{a^{3w+3} p}{|\bar{p}^\phi|^{1+w}} \delta \rho \right. \\ &\quad \left. - \frac{3(1-w)p}{2} \sqrt{\frac{w+1}{w}} \frac{a^2}{4\mathcal{V}_0^{\frac{2}{3}} k^2} \delta R_k - \sqrt{\frac{3}{2w}} \frac{w+1}{2} a^{\frac{3w-3}{2}} \bar{p}^\phi \delta \phi_k \right). \end{aligned} \quad (2.36)$$

Let us now define some of the different gauge-invariant curvature perturbation variables that are widely used in the field of the early universe: The variable  $\mathcal{R}$  is a gauge-invariant quantity that corresponds to the (minus) curvature perturbation on the co-moving hypersurfaces,  $\mathcal{R}_k|_{\delta\phi_k=0} = -\frac{4a^2}{k^2}\delta R_k$ . The variable  $\zeta$  is a gauge-invariant quantity that corresponds to the curvature perturbation on the uniform-density hypersurfaces,  $\zeta_k|_{\delta\rho=0} = \frac{4a^2}{k^2}\delta R_k$ . And finally the Mukhanov-Sasaki variable  $v_k = -\sqrt{\frac{3(w+1)}{w\kappa_0}}a \mathcal{R}_k$ , which, when divided by the scale factor  $v_k/a$ , is generally used to compute the power spectrum of the scalar perturbations, and can then be identified with the curvature perturbation on the co-moving hypersurfaces,  $-\sqrt{\frac{3(w+1)}{w\kappa_0}} \mathcal{R}_k$  (modulo the constant). In terms of our perturbations  $\phi_k$ ,  $\pi_{\phi,k}$  they read:

$$\begin{aligned}\mathcal{R}_k &= -\sqrt{\frac{w\kappa_0}{3}}a^{\frac{3w-3}{2}}\phi_k. \\ \zeta_k &= \sqrt{\frac{\kappa_0}{3w}}\frac{\mathcal{V}_0(w+1)}{2}a^{\frac{3w-3}{2}}\phi_k + \frac{1}{\sqrt{2w(w+1)\kappa_0}}\frac{1}{3p}\pi_{\phi,k}, \\ v_k &= a^{\frac{3w-1}{2}}\sqrt{w+1}\phi_k.\end{aligned}\tag{2.37}$$

For  $\phi \gg \pi_{\phi,k}$  (the initial condition for the expanding Universe) the curvature perturbation variable on the uniform-density hypersurfaces reads:  $\zeta \approx \sqrt{\frac{\kappa_0}{3w}}\frac{\mathcal{V}_0(w+1)}{2}a^{\frac{3w-3}{2}}\phi_k$ .

## 2.2 Anisotropic models

The standard approach to the early universe is based on Friedmann cosmology, that is, it assumes from the very beginning the approximate isotropy and homogeneity of the primordial space. However, it is expected that an approximate FLRW universe, when evolved back in time, at some moment close enough to the big-bang singularity, loses its space-like symmetries. A theory that assumes a fewer number of primordial symmetries allows the construction of a more generic cosmological scenario. A significantly less restrictive model than the standard one exhibits richer and more complex behaviour on approach to the big-bang singularity.

A more general (and widely acknowledged) solution of general relativity in the vicinity of cosmological singularity was studied by Belinskii, Khalatnikov and Lifshitz (BKL) in [29]. In the BKL scenario, as the dynamics of an inhomogeneous spacetime approaches singularity, the time derivatives of the gravitational field dominate over all spatial derivatives for relatively long stretches of time. Hence, the asymptotic dynamics becomes ultralocal and, surprisingly, the evolution of the general gravitational field turns out to become almost identical, at each point separately, with a generic spatially homogeneous model. Therefore, the dynamics of general spatially homogeneous cosmologies appears crucial for understanding generic singularities in GR.

### 2.2.1 Homogeneous cosmological models

The aforementioned kind of models can admit many different homogeneity groups<sup>4</sup>. A manifold  $\Sigma$  is called spatially homogeneous if its three-dimensional subgroup of symmetries acts simply and transitively on the invariant spatial hypersurfaces that it generates<sup>5</sup>. Depending on the Lie algebra of their Killing vectors fields, which determines the local properties of the symmetry group  $G$ , they are classified into the so-called Bianchi types. These models are very useful for studying the resolution of classical singularities through a suitable quantization method, and the ensuing quantum dynamics can be described by applying certain approximations. The Bianchi models admit three independent spatial Killing vectors  $\xi_1, \xi_2, \xi_3$ , which generate the set of isometries of the spatial metric [31]. These Killing vectors satisfy the Lie algebra  $[\xi_i, \xi_j] = -C_{ij}^k \xi_k$ , where  $C_{ij}^k$  are the structure constants of the homogeneity group  $G$  that satisfy the Jacobi identity.

To construct a basis of vector fields  $\{e_i\}$  invariant under the group  $G$  in our homogeneous manifold, we only need to give its components with respect to the Killing vectors. An invariant basis is useful because each spatial metric component  $q_{ij} = q(e_i, e_j)$  is group invariant, meaning it is constant on the homogeneous hypersurfaces. In addition, the structure coefficients of the basis  $e_i$  are also constant on each homogeneous hypersurface. We define the vector fields by requiring  $[\xi_i, e_j] = 0$ . Combining the latter with the condition that  $e_i$  be invariant, that is, has zero Lie derivative with respect to the Killing vectors, we find that  $[e_i, e_j] = C_{ij}^k e_k$ . The dual forms of the invariant basis vector fields are denoted by  $\omega^i$ , where  $\omega^i(e_j) = \delta_j^i$ . The curl of the dual forms satisfy the Cartan equation  $d\omega^k = \frac{1}{2} C_{ij}^k \omega^i \wedge \omega^j$ . Thus, since the  $e_i$  are invariant vectors, the spatial metric can be written as  $ds^2 = q_{ij} \omega^i \omega^j$ . The vector fields  $e_i$  constitute a basis of the tangent frame bundle  $T\Sigma$  of the manifold  $\Sigma$ . The metric and torsion-free (Levi-Civita) connection on such frame bundle is denoted by  $\Gamma_j^i$ , where  $\Gamma_j^i = \Gamma_{kj}^i \omega^k$ . We assume only diagonal metric spatial components in this basis which, in addition, are only time dependent. Hence, the connection coefficients, also defined as  $\nabla_{e_i} e_j = \Gamma_{ij}^k e_k$  for the non-holonomic basis  $e_i$ , are found to read:

$$\Gamma_{ij}^k = \frac{1}{2} \left( C_{ij}^k - C_{jk}^i - C_{ik}^j \right) \quad (2.38)$$

and become antisymmetric in the two lower indices<sup>6</sup>. Therefore, using the definitions above, we obtain the following expression for the Riemann curvature:

$$\begin{aligned} R_{jkl}^i &:= 2\omega^i e_k^a e_l^b \nabla_{(a} \nabla_{b)} e_j = \omega^i \left( \nabla_{e_k} (\omega^m(e_l) \Gamma_{mj}^n e_n) - \nabla_{e_l} (\omega^m(e_k) \Gamma_{mj}^n e_n) - \right. \\ &\quad \left. \omega^m (\nabla_{e_k} e_l) \Gamma_{mj}^n e_n + \omega^m (\nabla_{e_l} e_k) \Gamma_{mj}^n e_n \right) \\ &= \Gamma_{kn}^i \Gamma_{lj}^n - \Gamma_{ln}^i \Gamma_{kj}^n - (\Gamma_{kl}^m - \Gamma_{lk}^m) \Gamma_{mj}^i = \Gamma_{kn}^i \Gamma_{lj}^n - \Gamma_{ln}^i \Gamma_{kj}^n - C_{kl}^m \Gamma_{mj}^i. \end{aligned} \quad (2.39)$$

<sup>4</sup>The symmetry group of the manifold  $\Sigma$  is the group of isometries, i.e. transformations which leave the spatial metric of  $\Sigma$  invariant. The set of isometries of  $\Sigma$  has the structure of a group. The homogeneity group is a three-dimensional subgroup of the latter, which is considered isomorphic to a Lie Group  $G$ .

<sup>5</sup>A group is simple and transitive if the Killing vectors are linearly independent as vector fields. There exist another category of spatially homogeneous manifolds [30] where the spatial hypersurfaces have a transitive but not simple group of isometries, but we do not consider it in this work.

<sup>6</sup>In this case, the connection coefficients are also called the Ricci rotation coefficients.

Using Eq. (2.38) and the spatial metric, it is straightforward to derive the expression for the Ricci scalar in terms of the structure constants:

$$R = -C_{ik}^i C_{jl}^j q^{kl} - \frac{1}{2} C_{jk}^i C_{ik}^j q^{kl} - \frac{1}{4} C_{jk}^i C_{j'l}^{i'} q_{ii'} q^{kl} q^{jj'} \quad (2.40)$$

Following the classification scheme by Ellis and MacCallum [32], we write the structure constants in the form:

$$C_{jk}^i = \epsilon_{jkl} m^{li} + 2\delta_{(k}^i a_{j)} \quad (2.41)$$

to define the symmetric matrix  $m^{li}$  and the triplet  $a_j$ . From now on, we consider exclusively class A models, for which  $a_j = 0$ . Then, substituting the structure constants for the  $m^{li}$  gives:

$$R = \frac{1}{2} \frac{(m_i^i)^2}{q} - \frac{m_{ij} m^{ij}}{q} \quad (2.42)$$

Moreover, it is possible to choose the invariant basis  $\mathbf{e}_i$  to be the one in which the matrix  $m_{ij}$  is diagonal  $m_{ij} = \text{diag}(m^1, m^2, m^3)$ . The only remaining Bianchi models following these assumptions are types I, II, VI<sub>0</sub>, VII<sub>0</sub>, VIII and IX. The domain of the basis vectors fields are extended onto the whole spacetime, and we assume they commute with the normal to the spatial hypersurface vector field,  $e_0$ . The dual to that normal unitary vector is  $Ndt$ , which defines the direction of time. We can also assume that in this basis the spatial metric is diagonal  $q_{ij} = \text{diag}(q_1, q_2, q_3)$ , hence the Ricci scalar reads:

$$\begin{aligned} R &= \frac{1}{2} \frac{(m^i q_i)^2}{q_1 q_2 q_3} - \frac{(m^i)^2 (q_i)^2}{q_1 q_2 q_3} \\ &= \frac{m^1 m^2}{q_3} + \frac{m^1 m^3}{q_2} + \frac{m^2 m^3}{q_1} - \frac{(m^1)^2}{2} \frac{q_1}{q_2 q_3} - \frac{(m^2)^2}{2} \frac{q_2}{q_1 q_3} - \frac{(m^3)^2}{2} \frac{q_3}{q_1 q_2}. \end{aligned} \quad (2.43)$$

## 2.2.2 Hamiltonian formulation of homogeneous models

The models contain a total of six dynamical canonical variables, including the three  $q_i$ , each one playing the role of an effective directional scale factor for each one of the three principal directions, and their respective conjugate three-momentum  $p_i$ . In order to work within the framework of homogeneous models in Hamiltonian formulation, it is much more convenient to switch to a new set of coordinates, called Misner variables [33]. The Misner parametrization is introduced by the following canonical transformation:

$$\begin{pmatrix} q_1 p_1 \\ q_2 p_2 \\ q_3 p_3 \end{pmatrix} = \begin{pmatrix} \frac{1}{6} & \frac{1}{12} & \frac{\sqrt{3}}{12} \\ \frac{1}{6} & \frac{1}{12} & -\frac{\sqrt{3}}{12} \\ \frac{1}{6} & -\frac{1}{6} & 0 \end{pmatrix} \begin{pmatrix} p_\Omega \\ p_+ \\ p_- \end{pmatrix} \quad \text{and} \quad \begin{pmatrix} \ln q_1 \\ \ln q_2 \\ \ln q_3 \end{pmatrix} = \begin{pmatrix} 2 & 2 & 2\sqrt{3} \\ 2 & 2 & -2\sqrt{3} \\ 2 & -4 & 0 \end{pmatrix} \begin{pmatrix} \Omega \\ \beta_+ \\ \beta_- \end{pmatrix}. \quad (2.44)$$

In order to understand the cosmological interpretation of the Misner variables, let us suppose that we set the elements of the diagonal metric  $q_i = a_i^2$ , where  $a_i$  represents the scale factor for one of the three principal directions ( $i = 1, 2, 3$ ). Thus, we have:

$$\Omega = \frac{1}{3} \ln(a_1 a_2 a_3), \quad \beta_+ = \frac{1}{3} \ln\left(\frac{a_1 a_2}{a_3}\right), \quad \beta_- = \frac{1}{2\sqrt{3}} \ln\left(\frac{a_1}{a_2}\right) \quad (2.45)$$

In this way, we clearly see that the variable  $\Omega$  describes the isotropic part of the geometry, whereas  $\beta_\pm$  describe the distortions to isotropy and are called the anisotropic

variables. In Misner variables, the scalar curvature reads:

$$R = e^{-2\Omega} \left( m^1 m^2 e^{4\beta_+} + m^1 m^2 e^{-2\beta_+ + 2\sqrt{3}\beta_-} + m^2 m^3 e^{-2\beta_+ - 2\beta_+ - 2\beta_+ \sqrt{3}\beta_-} \right. \\ \left. - \frac{(m^1)^2}{2} e^{4\beta_+ + 4\sqrt{3}\beta_-} - \frac{(m^2)^2}{2} e^{4\beta_+ - 4\sqrt{3}\beta_-} - \frac{(m^3)^2}{2} e^{-8\beta_+} \right), \quad (2.46)$$

and, regarding the space-time metric, the total line element now reads:

$$ds^2 = -N^2 dt^2 + e^{2\Omega + 2\beta_+} \left( e^{2\sqrt{3}\beta_-} (\omega^1)^2 + e^{-2\sqrt{3}\beta_-} (\omega^2)^2 + e^{-6\beta_+} (\omega^3)^2 \right). \quad (2.47)$$

The elements of the spatial metric are functions of the proper time alone:  $\beta_0(t), \beta_{\pm}(t)$ . In the ADM formalism, the Hamiltonian constraint (2.4) for these diagonal and hypersurface-orthogonal class A Bianchi models, in Misner variables, is found to read:

$$\mathbf{C}_g = \frac{N}{2\kappa_0} \frac{e^{-3\Omega}}{24} \left( (2\kappa_0)^2 (-p_{\Omega}^2 + p_+^2 + p_-^2) + 36e^{4\Omega} (V(\beta_{\pm}) - 1) \right). \quad (2.48)$$

The Poisson brackets of the canonical variables read:  $\{\Omega, p_{\Omega}\} = \{\beta_{\pm}, p_{\pm}\} = 2\kappa_0$ . In what follows, we assume  $2\kappa_0 = 1$ . The vector constraints vanish, and the anisotropic potential of the previous equation is defined as:

$$V(\beta_{\pm}) := -\frac{2}{3} e^{2\Omega} R + 1 \quad (2.49)$$

and, being proportional to the scalar curvature, it depends on the structure constants  $C_{ij}^k$  (and therefore on  $m^i$ ), that is, on the specific choice of the homogeneous model. The gravitational Hamiltonian (2.48) resembles the Hamiltonian of a particle in a 3D Minkowski space-time moving inside a time-dependent potential. From all the remaining possible homogeneous models, the most important one, and unfortunately the most difficult, is the Bianchi type IX, which is commonly known as the *mixmaster universe*.

### 2.2.3 Mixmaster universe

The Bianchi IX model is important because it is a most generic homogeneous model in the sense that all its structure constants  $m^i$  are non-vanishing. Henceforth, we only devote attention to the mixmaster universe, i.e. the Bianchi type IX, within the group of spatially homogeneous class A models.

The manifold corresponding to group the Bianchi type IX is a space invariant under  $SO(3, \mathbb{R})$  symmetry group. This group has as its structure constants

$$C_{jk}^i = \epsilon_{ijk} \iff m^i = 1. \quad (2.50)$$

For simplicity, the three-sphere is taken as the topological prototype of the invariant hypersurfaces, since it is the simply connected covering space of  $SO(3, \mathbb{R})$ . Any metric placed on  $S^3$  of the form  $e_i \cdot e_j = q_{ij}$  and independent of position in any invariant hypersurface is invariant under  $SO(3, \mathbb{R})$ . The proof to that invariance comes from the fact that we can find the three Killing vectors on  $S^3$ , such that  $[\xi_i, e_j] = 0$ , and these Killing vectors are the generators of the  $SO(3, \mathbb{R})$  isometry group, with structure constants being the ones of Eq. (2.50). In the metric, the dual basis one-forms  $\omega^i$

representing these three-spheres spatial hypersurfaces, are usually parametrised as:

$$\begin{aligned}\omega^1 &= (-\sin \varphi d\theta + \cos \varphi \sin \theta d\phi) / \sqrt{m^2 m^3} \\ \omega^2 &= (\cos \varphi d\theta + \sin \varphi \sin \theta d\phi) / \sqrt{m^1 m^3} \\ \omega^3 &= (\sin \theta d\phi + d\varphi) / \sqrt{m^1 m^2}.\end{aligned}\tag{2.51}$$

Since we assume the topology of the spatial hypersurfaces to be  $S^3$ , the coordinate volume is found to be  $\mathcal{V}_0 = \int_{S^3} \omega^1 \wedge \omega^2 \wedge \omega^3 = 16\pi^2 / (m^1 m^2 m^3) = 16\pi^2$ . The choice of the mixmaster universe as our homogeneous model yields the following expression for the scalar curvature (2.46):

$$R = -\frac{1}{2} m^i e^{-2\Omega + 4\beta_+} \left( \left[ 2 \cosh(2\sqrt{3}\beta_-) - e^{-6\beta_+} \right]^2 - 4 \right),\tag{2.52}$$

with the structure constants being the ones of Eq. (2.50). Then the mixmaster anisotropic potential (2.49) is defined as:

$$V_{IX}(\beta_{\pm}) = \frac{1}{2} e^{4\beta_+} \left( \left[ 2 \cosh(2\sqrt{3}\beta_-) - e^{-6\beta_+} \right]^2 - 4 \right) + 1.\tag{2.53}$$

The shape of this potential is plotted in Fig. 2.1. From now on, we simply denote this potential as  $V(\beta)$ .

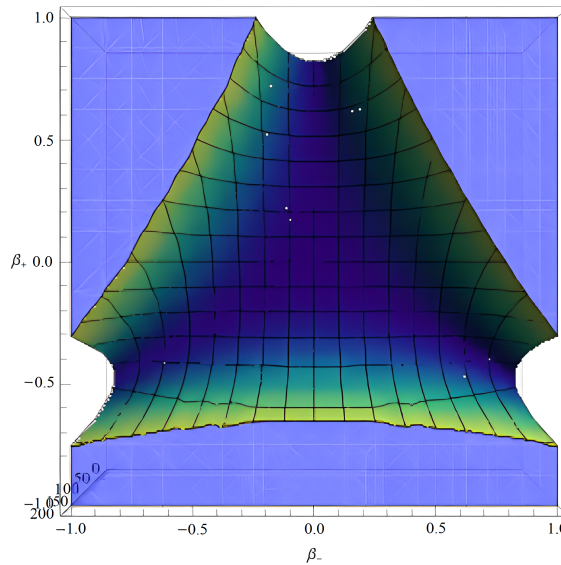


FIGURE 2.1: Representation of the anisotropic potential of Eq. (2.53) for the classical mixmaster universe (Bianchi type IX model).

The classical dynamics of the mixmaster model is described by the Hamiltonian constraint (2.48) with potential (2.53) along the proper time  $t$ . The singularity is reached for  $\Omega \rightarrow -\infty$ . The factor in front of the potential in this Hamiltonian goes to zero at the singular point  $36e^{4\Omega} \rightarrow 0$ , therefore, as the isotropic geometry of the universe contracts, the potential walls move further apart and the particle progressively penetrates larger regions of the anisotropy space  $\beta = (\beta_+, \beta_-)$ . It is legitimate to represent this singularity of the Hamiltonian flow as a boundary of the phase space, redefining the isotropic variables to bring the singular point to finite values

of the canonical coordinates<sup>7</sup>. Then, we introduce the following isotropic canonical coordinates [35]:

$$q = e^{\frac{3}{2}\Omega} = a^{\frac{3}{2}}, \quad p = \frac{2}{3}e^{-\frac{3}{2}\Omega}p_\Omega, \quad (q, p) \in \mathbb{R}_+ \times \mathbb{R}, \quad (2.54)$$

where we also defined the mean scale factor  $a := (a_1 a_2 a_3)^{1/3}$ . The collapse is now represented in the open half-plane ( $q > 0$ ) rather than a plane. This range of the isotropic phase space variables admits the affine group of symmetry transformations<sup>8</sup>. The spacetime line element now reads:

$$ds^2 = -N^2 dt^2 + q^{\frac{4}{3}} e^{2\beta_+} \left( e^{2\sqrt{3}\beta_-} (\omega^1)^2 + e^{-2\sqrt{3}\beta_-} (\omega^2)^2 + e^{-6\beta_+} (\omega^3)^2 \right). \quad (2.55)$$

The Hamiltonian constraint of the classical mixmaster in this new coordinates can be written a sum of an isotropic and anisotropic part:

$$\begin{aligned} \mathbf{C} &= -\mathbf{C}_{iso} + \mathbf{C}_{ani} \\ \mathbf{C}_{iso} &= \frac{N}{24} \left( \frac{9}{4} p^2 + 36q^{\frac{2}{3}} \right), \quad \mathbf{C}_{ani} = \frac{N}{24} \left( \frac{\mathbf{p}^2}{q^2} + 36q^{\frac{2}{3}} V(\boldsymbol{\beta}) \right), \end{aligned} \quad (2.56)$$

where  $\mathbf{p} := (p_+, p_-)$ . The Hamilton equations (for  $N = 24$ ) read:

$$\begin{aligned} \dot{q} &= \frac{9}{2} p, \quad \dot{p} = -2 \frac{\mathbf{p}^2}{q^3} + 24q^{-\frac{1}{3}} [V(\boldsymbol{\beta}) - 1], \\ \dot{\beta}_\pm &= -2 \frac{p_\pm}{q^2}, \quad \dot{p}_\pm = 36q^{\frac{2}{3}} \partial_\pm V(\boldsymbol{\beta}), \end{aligned} \quad (2.57)$$

where  $\partial_\pm := \partial_{\beta_\pm}$ . The above system of dynamical equations admits the following scaling symmetry:

$$\begin{aligned} t' &= \frac{t}{\delta^{1/2}}, \quad q' = \frac{q}{\delta^{3/4}}, \quad p' = \frac{p}{\delta^{1/4}}, \\ \beta'_\pm &= \beta_\pm, \quad p'_\pm = \frac{p_\pm}{\delta}. \end{aligned} \quad (2.58)$$

This scaling symmetry can transform large-universe solutions into small-universe solutions, even into the ones that are smaller than the Planck scale at their possible classical re-collapse ( $p = 0$ ). It is natural to expect this symmetry to be broken at the quantum level that must involve a new scale coming from the nonvanishing Planck constant.

We can express the dynamically most relevant geometric quantities in terms of the phase space variables:

$$H = \frac{p}{8q}, \quad R_{iso} = \frac{3}{2q^{\frac{4}{3}}}, \quad R_{ani} = -\frac{3V(\boldsymbol{\beta})}{2q^{\frac{4}{3}}}, \quad \sigma^2 = \frac{\mathbf{p}^2}{48q^4} \quad (2.59)$$

where  $H$ ,  $R_{iso}$ ,  $R_{ani}$  and  $\sigma^2$  are respectively the Hubble rate, the isotropic intrinsic

<sup>7</sup>The canonical quantization (Dirac) of the Hamiltonian constraint, by promoting it to an operator acting on the universe wave function  $\Psi$ , leads to the well-known Wheeler-DeWitt equation [34]. This equation does not remove the singularity. Therefore, we make use of an alternative quantization method that removes the singularity, that is implemented with the new isotropic variables.

<sup>8</sup>This symmetry group is introduced later at the end of section 2.4.1, since it plays an essential role in the quantization method of the model.

curvature, the anisotropic intrinsic curvature (potential term of anisotropy) and the shear squared (kinetic term of anisotropy). Upon rewriting the constraint equation in terms of them, we obtain the generalized Friedmann equation for the mixmaster model:

$$H^2 = -\frac{1}{6}R_{iso} + \frac{1}{3}\sigma^2 - \frac{1}{6}R_{ani} + \frac{1}{6}\rho_r, \quad (2.60)$$

where we added the matter component to the model in the last term, since we assume that at some stage in the early evolution of the universe the expansion was driven by matter fields. We chose radiation to be the matter component with  $\rho_r = M_r/q^{\frac{8}{3}}$  being the energy density and  $M_r$  is a constant<sup>9</sup>.

The classical mixmaster, as a homogeneous model of the early universe, was originally proposed by Misner [36]. In this model the universe undergoes the BKL scenario previously described: an oscillatory and chaotic epoch close to the initial cosmological singularity. The name "mixmaster" is due to the fact that, in this scenario, the universe is thought to behave like a three-dimensional mixer, acting on spatial directions, squeezing and blowing up each repeatedly and randomly, while the overall volume is shrinking. The mixmaster is similar to the closed FLRW universe, in the sense that spatial slices are positively curved and are topologically three-spheres  $S^3$ . Nevertheless, in the FLRW universe there is only one dynamical variable, the scale factor  $a(t)$ , that parameterises the overall size of the  $S^3$ , which can only contract or expand. In the Mixmaster, the spatial  $S^3$  slices can contract and expand (parameterised by  $\Omega$  or  $q$ ) but also get distorted anisotropically (parameterised by the shape parameters  $\beta_{\pm}$ ). By studying the motion of the fictitious point-particle inside the mixmaster potential (2.53), Misner showed that the physical universe would exhibit a repeated pattern of contraction in some directions and expansion in others, with the directions of contraction and expansion changing periodically. Since the potential is roughly triangular and concave, Misner suggested that the evolution is chaotic. Because the spatial slices evolve differently in each direction, homogeneity is preserved but not isotropy.

The dynamics of the mixmaster is very hard. Before collapsing into the singularity in a finite proper time, infinitely many oscillations take place. Its classical asymptotic dynamics is usually approximated by an infinite sequence of epochs of the so-called Kasner universe. Each epoch is a vacuum solution to the homogeneous spacetime model of Bianchi type I ( $m^i = 0$ ). The transitions between epochs are the effect of non-negligible spatial curvature, which arises quickly and vanishes after a relatively short period of time. These transitions are commonly given by solutions to the Bianchi type II model ( $m^1 = 1, m^{2,3} = 0$ ). The universe becomes dominated by the gravitational energy (with the matter energy negligible) and undergoes an infinite number of chaotic transitions and eventually collapses into a singularity. Misner failed to resolve the singularity. He initiated studies on the quantum dynamics of the mixmaster with such objective, but his analysis was based on simplistic approximations of the anisotropic potential and the dynamics. It appears that there have not been any significant advancements in the field since then. However, very recently, a novel approach to quantization and analysis of the quantum model started to be developed [37–42]. In the work presented in this thesis (chapter 6), based on in the direction of such previous studies, we propose a quantum model of the mixmaster universe replacing the classical singularity with a quantum bounce. Approximating

<sup>9</sup>The expression of the radiation term is derived from the fluid constraint (2.14) ( $w = 1/3$  for radiation) by means of the appropriate choice of the value of  $K = w(w+1)^{-\frac{1+w}{w}}$ , and  $M_r$  is assumed to be a constant related to the momentum of the fluid  $M_r = (p^\phi)^{1+w}$ .

the description of quantum dynamics provides fresh insights into the new intricate physics of the bounce and its interplay with anisotropy. The main goal is to use such model to investigate the possibility of the quantum mixmaster universe undergoing an spontaneous inflationary phase.

In order to quantise the mixmaster, integral covariant methods of quantization, based on coherent states, are applied to the canonical coordinates. The same method is applied as well for the quantization of the Hamiltonian (2.34) obtained for the isotropic background in the previous section. Therefore, the section 2.4.2 of the present chapter is devoted to coherent states and quantization methods based on them.

## 2.3 The standard model of cosmological Inflation

Since the work presented in this thesis lies in the domain of alternative models of quantum cosmology to the most accepted inflation scenario, we shall present here some basis of the standard inflationary scenario, its postulates and most important predictions of the early universe regarding the actual available observational data. We put the focus on the ones that are more relevant to compare with the presented study. This allows us to understand clearly the source of the difference between the results obtained in our models and in the inflation model.

The Standard Cosmological Inflation Model proposes a solution to some of the deep-rooted problems of the Big Bang theory, such as horizon, flatness or monopole problems among others, by introducing a period of exponential accelerated expansion in the early universe. The standard model of inflation assumes that the dynamics is driven by a scalar field called the inflaton ( $\phi$ ) [43]. The scalar field is thought to have dominated the energy density of the universe during inflation, and the rapid expansion caused by the inflaton field is responsible for smoothing out any initial irregularities of the universe, explaining its isotropic and homogeneous state, and producing the seeds for the large-scale structure we observe today.

There exist a wide range of inflationary models, going from the simplest standard one of chaotic inflation where the scalar field follows a quadratic potential  $V(\phi) = \frac{1}{2}m^2\phi^2$ , where  $m$  is the mass of the inflaton, to extensions in which the potential can be any polynomial or power law function of one or even multiple scalar fields, that can be coupled like in the case of hybrid inflation [44]. In most models, it is usually assumed that at the beginning of the inflationary period, the scalar field was in a state of high energy and subject to random quantum fluctuations [45]. As the universe stretched out, the field settled into a lower state and released energy that drove the rapid exponential expansion. According to the theory, the inflationary period came to an end through a phase transition where the scalar field decayed, causing the universe to be reheated and leading to the production of particles and radiation. Inflation has led to the remarkable result of establishing a connection between the primordial density perturbations (amplified during the rapid accelerated expansion) that led to the Universe's large-scale structure and the inflaton's initial quantum vacuum fluctuations.

The inflation model assumes a classical background, whose dynamics is driven by the inflaton field according to the classical equations of motion. The background spacetime is assumed isotropic and homogeneous. The scalar field is split into the homogeneous background and small inhomogeneous perturbations. The perturbation modes are canonically quantized and set initially to be in the vacuum state.

The cosmological horizon is defined as the maximum distance from which light could have travelled to the observer in the age of the universe [46]. Therefore, it measures the distance from which we could possibly retrieve information. The Hubble horizon at a given moment  $t$  is the distance that light can travel in the Hubble time value at that moment ( $H(t)^{-1}$ ), that is, the time in which the size of the universe doubles. Scales larger than the Hubble horizon remain out of casual contact. During inflation, the comoving Hubble horizon size decreases rapidly, then the quantum fluctuations are stretched to cosmological scales and modes of perturbations that were initially inside the horizon become larger than the horizon (see Fig. 2.2 from [47]). The exiting of the horizon of the relevant modes leaves imprints on the large-scale structure of the universe, that can be observed on the cosmic microwave background radiation for the modes (or scales) that re-entered the cosmological horizon. The amplitude and spectral tilt of these fluctuations are determined by the details of the inflationary model.

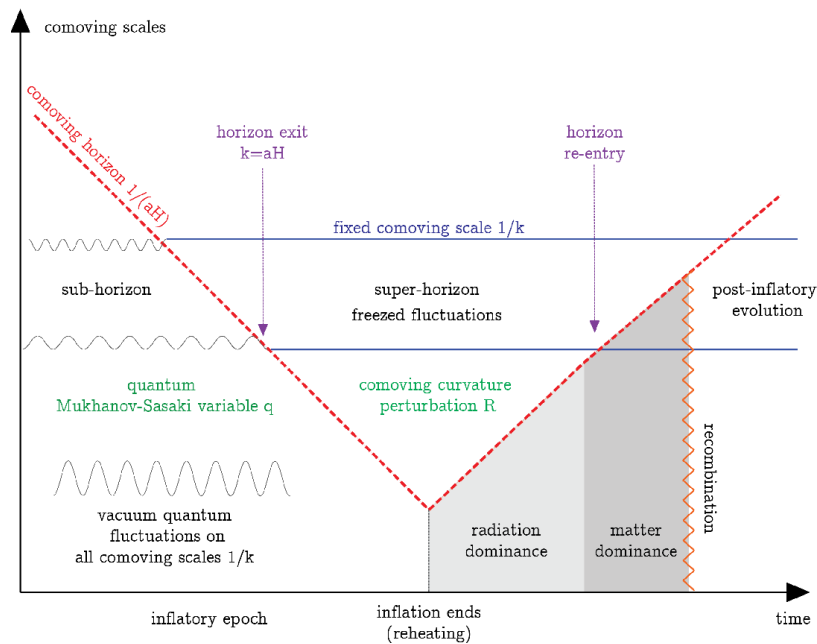


FIGURE 2.2: An illustrative representation of how the perturbations for the different modes (or scales) evolve during the inflationary period, taken from [47]. In chapters 4 and 5 we analyse some details of this picture in the framework of quantum bouncing cosmology, such as how the perturbations are amplified from vacuum and the super-horizon constancy of curvature perturbations.

Inflation models are usually classified by the values of the so-called slow-roll parameters they assume. Slow-roll inflation refers to the situation in which the inflaton is assumed to roll down the sufficiently high potential hill ( $\dot{\phi} \ll V(\phi)$ ) very slowly in comparison to the expansion of the Universe ( $|\ddot{\phi}| \ll |3H\dot{\phi}|$ ). One can use the Friedmann equation and the equations of motion of the scalar field to write such conditions in terms the slow roll parameters [26], defined as:

$$\epsilon := \frac{1}{3\kappa} \left( \frac{V_{,\phi}}{V} \right)^2 \ll 1, \quad |\eta| := \frac{1}{3\kappa} \left| \frac{V_{,\phi\phi}}{V} \right| \ll 1. \quad (2.61)$$

The parameters represent represents the nearly flat slope ( $\epsilon$ ) and curvature ( $\eta$ ) of the potential, ensuring inflation to happen for sufficiently long time. The minimally

coupled inflaton field can be described by means of its effective cosmological fluid pressure and energy density:  $\rho_\phi = \dot{\phi}^2/2 + V(\phi)$  and  $p_\phi = \dot{\phi}^2/2 - V(\phi)$ . By means of Friedmann equation as well, it can be shown [47] that the accelerated expansion phase can occur for fluids with barotropic index  $w < -1/3$ . The slow roll regime in inflation generally yields to the assumption  $H \simeq \text{constant}$ , leading to  $w \approx -1$ , that clearly satisfies the above condition. The predictions of the inflationary model for the power spectrum of scalar curvature perturbations in the large wavelengths limit can be expressed at 1<sup>st</sup> order in terms of the slow-roll parameters [26]:

$$\mathcal{P}_\zeta(k) \propto k^{n_s-1} = k^{2\eta-4\epsilon} \quad (2.62)$$

Inflation is successful in predicting an almost scale invariant power spectrum for scalar perturbations, with  $n_s \lesssim 1$ . It is very useful to express the formula of the spectral index of scalar perturbations in terms of the slow-roll parameters  $n_s = 1 - 2\eta - 4\epsilon$  because it clearly manifest the freedom in the fine-tuning of the scalar field potential that the standard inflationary model posses. Such freedom translates into the capability of inflation for obtaining some flexible range of values of the slow-roll parameters, allowing them to be constrained by observations in order to reproduce the value of the spectral index given by the power spectrum of the Cosmic Microwave Background:  $n_s = 0.9649 \pm 0.004$  [48]. The fact that the CMB data gives  $n_s \lesssim 1$  for the scalar spectral index make us refer to it as a slightly *red-tilted* spectrum, because it is slightly stronger on larger angular scales than on the smaller ones. The opposite situation,  $n_s \gtrsim 1$ , is referred as a slightly *blue-tilted* spectrum.

Nonetheless, in spite of its impressive success in explaining the genesis of the large scale structures, the inflationary paradigm does not address some other issues of the Big Bang theory [49]. Among those, the one that mainly concern us for the future chapters is the ingrained initial singularity problem.

## 2.4 Coherent states

Coherent states are a class of quantum states that closely exhibit a classical behaviour. They are frequently employed to depict a group of states that possess minimum uncertainty and, in a way, are most akin to a classical portrayal of the underlying phenomenon. The original coherent states were introduced by Erwin Schrödinger in 1926 [50] as a generalization of the classical harmonic oscillator. These states are known as Schrödinger or canonical coherent states, its probability density is Gaussian and its peak follows the sinusoidal trajectory of a classical particle. The coherent state are referred to as "displaced" ground states since their probability density differs from that of the ground state only due to its time-varying shift in the position of the peak. Let us summarise some of the basic properties of the Schrödinger coherent states:

- The canonical pair of the quantum harmonic oscillator annihilation  $\hat{a}$  and creation  $\hat{a}^\dagger$  satisfy the commutation relation:  $[\hat{a}, \hat{a}^\dagger] = \mathbb{I}$ . The coherent states are created by the action of an unitary operator, the displacement operator, on the harmonic oscillator vacuum state  $|0\rangle$ , that plays the role of fiducial state:

$$|\alpha\rangle = e^{-\bar{\alpha}\hat{a} + \alpha\hat{a}^\dagger} |0\rangle, \quad \alpha \in \mathbb{C}. \quad (2.63)$$

The vacuum state vanishes under the action of the annihilation operator  $\hat{a}|0\rangle = 0$ . The displacement operator is undetermined to an arbitrary imaginary additive constant (global phase).

- They are the eigenstates of the annihilation operator of a harmonic oscillator:  $\hat{a}|\alpha\rangle = \alpha|\alpha\rangle$ .
- They lie in the middle of the minimum uncertainty curve, meaning they minimise the Heisenberg uncertainty principle:  $\Delta_{\hat{Q}}|\alpha\rangle\Delta_{\hat{P}}|\alpha\rangle = \frac{1}{2}$ , where  $\Delta_{\hat{A}}|\alpha\rangle = \sqrt{\langle\alpha|\hat{A}^2|\alpha\rangle - \langle\alpha|\hat{A}|\alpha\rangle^2}$ . More technically, the general solutions to the last condition are called squeezed-coherent states, essentially because the uncertainty can be squeezed from  $\hat{Q}$  into  $\hat{P}$  and vice-versa by introducing the squeezing operator  $S(\zeta) = e^{\frac{1}{2}(-\zeta\hat{a}^2 + \zeta^*\hat{a}^{\dagger 2})}$ , where  $\zeta \in \mathbb{C}$ .
- They are not orthogonal states:  $\langle\beta|\alpha\rangle = e^{-\frac{1}{2}(|\alpha|^2 + |\beta|^2 - 2\alpha\beta^*)} \neq \delta(\alpha - \beta)$ . Therefore, if the oscillator is in the quantum state  $|\alpha\rangle$  it is also with nonzero probability in any quantum state  $|\beta\rangle$ .
- A family of coherent states  $\{|\alpha\rangle\}$  is overcomplete, meaning that, as a consequence of their non-orthogonality and their closure relation, any coherent state can be expanded in terms of all the other coherent states of the family. The closure relation they obey is expressed by the following resolution of the identity:

$$\frac{1}{\pi} \int_{\mathbb{C}} d\Re(\alpha) d\Im(\alpha) |\alpha\rangle\langle\alpha| = \mathbb{I}, \quad (2.64)$$

where  $\Re(\alpha)$  and  $\Im(\alpha)$  are respectively the real and imaginary part of  $\alpha$ . This property is actually the most important one in many applications.

### 2.4.1 Generalized Coherent states (GCS)

In 1954, Senitzky [51] demonstrated that the coherent states can be generalized by displacing any other energy eigenstate in such a way that its probability density oscillates in accordance with the classical dynamics. It was shown that these generalized coherent states are also a solution for the harmonic oscillator. These states were reintroduced by Perelomov [52] in 1972, with a construction based on the use of Lie algebraic methods. Generalized coherent states, are a more general class of states that can be constructed by applying a linear or nonlinear operator, generally an unitary irreducible representation of a symmetry group, on a reference arbitrary state  $|\psi_0\rangle$  (called fiducial vector) in Hilbert space  $\mathcal{H}$ . Hence, Schrödinger coherent states are a special case of generalized coherent states. Generalized coherent states can also be used to construct non-classical states such as squeezed states and displaced Fock states. The only two basic conditions that all GCS must obey are:

- Continuity: The displacement operator shifts the fiducial vector in phase space by a displacement parameter, which labels the GCS:  $|\vec{z}\rangle$  (a vector in  $\mathcal{H}$ ). The parameter belongs to some label space  $\mathcal{Z}$ , and uniquely identifies the state within the set of GCS. By varying this parameter, one can generate a family of states that span a continuous region of the phase space. This means that the mapping  $\vec{x} \rightarrow |\vec{z}\rangle$  is strongly continuous, and for each vector  $|\psi\rangle$  in  $\mathcal{H}$ , the function  $\Psi(\vec{z}) = \langle\vec{z}|\psi\rangle$  is continuous in the topology of  $\mathcal{Z}$ . The continuity of the set of states arises from the fact that the displacement parameter varies smoothly and continuously over this region. Any two states in the set can be smoothly connected to one another by a continuous path. Then, the distance between two states in the Hilbert space with different label parameters tends to zero as one of the parameters approach the value of the other:  $\| |\vec{z}\rangle - |\vec{z}'\rangle \| \rightarrow 0$  as  $\vec{z} \rightarrow \vec{z}'$

- Overcompleteness: The continuity of the label of GCS is closely related to the completeness property of the set of states, explained above. We can generalise the resolution of the identity (2.64) as:

$$\int_{\mathcal{Z}} \frac{d\mu(\vec{z})}{\mathcal{N}} |\vec{z}\rangle\langle\vec{z}| = \mathbb{I}, \quad (2.65)$$

where  $\mathcal{N}$  is the normalization factor coming from the fixed fiducial state. If we take the positive measure  $d\nu$  on  $\mathcal{Z}$  to be  $d\nu(\vec{z}) = d\mu(\vec{z})/\mathcal{N} = d\Re(\alpha)d\Im(\alpha)/\pi$  and  $\mathcal{Z} \equiv \mathbb{C}$ , we recover the definition of canonical coherent states. The continuity ensures the non-orthogonality of the GCS. Hence, overcompleteness property means that any state in the Hilbert space can be expressed as a linear combination of the GCS:

$$|\psi\rangle = \int_{\mathcal{Z}} \Psi(\vec{z}) |\vec{z}\rangle d\nu(\vec{z}). \quad (2.66)$$

This means that there is a one-to-one correspondence between the states in the set and the points in the continuous labelling parameter space. It also means that the set of states forms an overcomplete basis for the Hilbert space.

### Phase space representation

The phase space representation of coherent states provides a useful way of intuitively understanding of the properties of the state. It allows for the visualization of more complicated wave functions. Representing the state in terms of both position and momentum coordinates. We start by introducing, respectively, the position and momentum self-adjoint operators:

$$\hat{Q} = \sqrt{\frac{1}{2k\omega}} (\hat{a}^\dagger + \hat{a}), \quad \hat{P} = i\sqrt{\frac{\omega}{2k}} (\hat{a}^\dagger - \hat{a}), \quad (2.67)$$

By defining the complex label variable  $z = \sqrt{\frac{\omega k}{2}} q + i\sqrt{\frac{k}{\omega}} p$  in terms of the phase space canonical coordinates  $(q, p) \in \mathbb{R}^2$ , the displacement operator is transformed into the Weyl-Heisenberg translator operator:

$$\hat{U}_W = e^{ik(p\hat{Q} - q\hat{P})}. \quad (2.68)$$

Quantum physics sets  $k = \hbar^{-1}$ , and we assume  $\hbar = 1$ . It is referred to as a translation operator because it translates a state in phase space by a  $z = (q, p)$ :

$$\hat{U}_W^\dagger \hat{Q} \hat{U}_W = \hat{Q} + q\mathbb{I}, \quad \hat{U}_W^\dagger \hat{P} \hat{U}_W = \hat{P} + p\mathbb{I}. \quad (2.69)$$

Then the Weyl-Heisenberg translation operator form an irreducible, unitary representation (UIR) of a Lie group called the Weyl-Heisenberg symmetry group, explained below. We write the coherent state as:  $|z\rangle = |q, p\rangle = \hat{U}_W |0\rangle$ . The states  $|q, p\rangle$  generate continuous representation of the canonical phase space. The physical interpretation of the phase space coordinate labels is:

$$q = \langle q, p | \hat{Q} | q, p \rangle, \quad p = \langle q, p | \hat{P} | q, p \rangle. \quad (2.70)$$

The fiducial vector represents the generalization of the reference vacuum state in the canonical coherent states. It is a normalised and (almost) arbitrary fixed state in

the Hilbert space, that determines the whole family of coherent states built from the UIR of chosen group. Since the conditions of GCS don't state anything about the fiducial vector, we can choose it to be any state  $|\psi_0\rangle$  belonging to the Hilbert space  $\mathcal{H}$ . However, it is typically convenient to select  $|\psi_0\rangle$  such that Eq. (2.70) holds, by imposing the following physical centering conditions:

$$\langle\psi_0|\hat{Q}|\psi_0\rangle = 0, \quad \langle\psi_0|\hat{P}|\psi_0\rangle = 0. \quad (2.71)$$

If we choose a different fiducial state, we get a shift of the phase space by their expectation value of the position and momentum operator. Supplementarily, besides the fiducial vector, the most important part of the generalization comes from the choice of operator that acts on it and creates the coherent states, specially from its relation with a symmetry group. As we will now see, they allow to construct a group representative in a Hilbert space.

### Weyl-Heisenberg symmetry group

As we previously mentioned, the Weyl-Heisenberg operators serve as a unitary and irreducible representation of the Weyl-Heisenberg symmetry group, consisting in the group of  $\mathbb{R}^2$  phase space translations on the Hilbert space  $\mathcal{H} = L^2(\mathbb{R}, dx)$  of square-integrable complex valued functions (on a full line).

The regular representation of the translational symmetry is defined as:

$$\mathcal{T} : (\mathcal{T}(q_0, p_0))f(q, p) = f(q - q_0, p - p_0), \quad (2.72)$$

where  $(q_0, p_0)$  represents the origin of the phase space, whose choice is arbitrary since the phase space  $\mathbb{R}^2$  is homogeneous. The fiducial state  $|\psi_0\rangle$  is selected from the Hilbert space  $\mathcal{H}$ , such that the physical centering conditions (2.71) are fulfilled, and the physical interpretation of the labels  $(q, p)$ , following from (2.70), are just the position and momentum respectively, and are usually referred as the "classical" degrees of freedom, whereas any other variable, typically related to the shape of the fiducial quantum state, shall be referred as "quantum" degree of freedom (or parameter).

Besides (2.69), the Weyl-Heisenberg operator also has the following properties:

$$\begin{aligned} U_W(0, 0) &= \mathbb{1}, & \text{Tr}(U_W(q, p)) &= 2\pi\delta(q)\delta(p), \\ \hat{U}_W^{-1}(q, p) &= \hat{U}_W^\dagger(q, p) = \hat{U}_W(-q, -p), \end{aligned} \quad (2.73)$$

From the multiplication law of the Weyl-Heisenberg group we have:

$$U_W(q, p)U_W(q', p') = e^{i\sigma((q, p) \circ (q', p'))} U_W(q + q', p + p'), \quad (2.74)$$

where the real valued parameter  $\zeta$  encodes the non-commutativity of the representation, hence representing a feature of quantization. This means that for the UIR (2.68) the symplectic form reads:  $\sigma((q, p) \circ (q', p')) = -k(q, p) \wedge (q', p') = k(qp' - q'p)$ , where quantum physics fixes  $k = \hbar^{-1}$ . The non-commutativity is given by Weyl-Heisenberg algebra, satisfying the familiar commutation relation:

$$[q, p] = I. \quad (2.75)$$

The above commutation relation is the Lie algebra corresponding to the set of operators:  $I \rightarrow -i\mathbb{1}$ ,  $q \rightarrow i\hat{Q}$ , and  $p \rightarrow i\hat{P}$ , which gives the canonical commutation

relation of quantum mechanics ( $\hbar = 1$ ). The Lie algebra representation (2.68), with  $k = \hbar^{-1} = 1$ , is not just an UIR of the Weyl-Heisenberg group, but it is, besides the trivial choice ( $k = 0$ ), the unique one<sup>10</sup>. This representation is called the Schrödinger representation [54], because the canonical (or Schrödinger) coherent states correspond to elements of the Weyl-Heisenberg group acting on the ground vacuum state through the Schrödinger representation. As mentioned, both position  $\hat{Q}$  and momentum  $\hat{P}$  operators are self-adjoint in the Hilbert space  $\mathcal{H} = L^2(\mathbb{R}, dx)$ . If  $\hat{Q}$  acts on  $\mathcal{H}$  on its spectrum  $\mathbb{R}$  as  $\hat{Q}\psi(x) = x\psi(x)$ , then the momentum acts as  $\hat{P} \rightarrow -i\partial_x$ .

The Weyl-Heisenberg transform of a phase space function into an operator in  $\mathcal{H}$  is defined as:

$$f(q, p) \mapsto \mathcal{W}[f] = \int_{\mathbb{R}^2} U_W(q, p) f(q, p) \frac{dq dp}{\pi} \quad (2.76)$$

From (2.74) we obtain the formula for the trace [55]:

$$\text{Tr}(U_W(q, p)^\dagger U_W(q', p')) = \pi \delta(q - q') \delta(p - p'). \quad (2.77)$$

Using this last formula and (2.73), we can invert the Weyl-Heisenberg transform (2.76):

$$f(q, p) = \text{Tr}(U(-q, -p) \mathcal{W}[f]). \quad (2.78)$$

### Affine group

The construction in terms of symmetry groups, can be used to define coherent states for irreducible, unitary representations of any arbitrary Lie groups, besides the Weyl-Heisenberg coherent states.

The considered cosmological models in this thesis involve isotropic phase space coordinates (2.19) (2.54) that form a half-plane,  $(q, p) \in \mathbb{R}^+ \times \mathbb{R}$ . Such phase space can be associated with the Hilbert space  $\mathcal{H} = L^2(\mathbb{R}^+, dx)$  of square-integrable functions on a half-line. The symmetry of the open half-plane corresponds to the arbitrariness of the choice of the origin, namely 1 for the scaling variable  $q_0 > 0$ , and 0 for its conjugate momentum  $p_0 \in \mathbb{R}$ , since the phase space is still homogeneous. This modification of the position center is expected since on the Hilbert space defined on the positive real line, the position expectation value must be positive definite. The group of canonical transformations of this phase space form the affine group  $\text{Aff}_+(\mathbb{R})$  of the real line, that satisfies the following multiplication law:

$$(q, p) \circ (q', p') = (qq', \frac{p'}{q} + p). \quad (2.79)$$

The regular representation of the affine symmetry is defined via the group inverse as:

$$\mathcal{A} : (\mathcal{A}(q', p')) f(q, p) = f((q', p')^{-1} \circ (q, p)) = f(\frac{q}{q'} \cdot q'(p - p_0)). \quad (2.80)$$

The affine set of transformations of the real line consist in transformations of the form  $x \rightarrow x' = a \cdot x + b$ , where  $a > 0$ ,  $b \in \mathbb{R}$ . The generators of its algebra are  $q$

<sup>10</sup>In general, elements of the Weyl-Heisenberg group are defined by three variables  $(t, q, p)$  with  $t \in \mathbb{R}$ , however, since the coherent states we are interested in are defined only by the phase space coordinates  $(q, p)$  we dropped  $t \rightarrow 0$ . Therefore the general UIR would read  $T(t) \cdot U_W(q, p)$ , where the operator  $\hat{\mathbb{1}}$  lifts to the operator  $T(t) = e^{-i\frac{t}{\hbar} \hat{\mathbb{1}}}$ , which relates to the fact that vectors in  $L^2(\mathbb{R})$  correspond to the same state if they differ only by a phase factor. Thus, the unique UIR (2.68), is actually a Lie algebra representation of the Weyl-Heisenberg algebra, called the Schrödinger representation, where we dropped  $t$  [53].

(position) and  $d = pq$  (dilation):  $\{q, p\} = 1 \rightarrow \{q, d\} = q$ . The idea is to replace the translations in position (due to the barrier at  $q = 0$ ) with dilations. The translations in momentum and the dilations generate the affine group (in a line). The momentum operator is a self-adjoint generator of the UIR of the Lie group of Weyl-Heisenberg on a full line, but in the new Hilbert space for the new Lie group of affine symmetry it becomes a symmetric operator but not self-adjoint because of the boundary at  $x = 0$ . Hence, in the Lie algebra representation of the affine algebra, (when following the canonical prescription  $q \rightarrow i\hat{Q}$ ,  $p \rightarrow i\hat{P}$ ,  $1 \rightarrow -i\mathbb{1}$ ) only the position and the dilation operator, defined as  $d \rightarrow -i\hat{D} = -\frac{1}{2}i(\hat{Q}\hat{P} + \hat{P}\hat{Q})$ , are self-adjoint in the mentioned Hilbert space  $\mathcal{H}$ . Then, we get the canonical commutation of quantum mechanics that gives the resulting affine commutation rule for these two operator,

$$[\hat{Q}, \hat{P}] = i\mathbb{1} \longrightarrow [\hat{Q}, \hat{D}] = i\hat{Q}. \quad (2.81)$$

The so-called affine coherent states (ACS) are defined as being created by the action of the non-trivial UIR<sup>11</sup> of the affine group in terms of these two self-adjoint operators

$$|q, p\rangle = U_A(q, p)|\psi_0\rangle = e^{\frac{i}{\hbar}p\hat{Q}}e^{-\frac{i}{\hbar}\ln(q)\hat{D}}|\psi_0\rangle, \quad (2.82)$$

on the fiducial vector  $|\psi_0\rangle$ , and parametrised by the half-plane  $(q, p) \in \mathbb{R}^+ \times \mathbb{R}$ . Again, we assume  $\hbar = 1$ . As we chose our arbitrary origin to be  $(q, p) = (1, 0)$ , the physical centering conditions (2.71) on the fiducial state used for the expectation values on the half line, are shifted like

$$\langle\psi_0|\hat{Q}|\psi_0\rangle = 1, \quad \langle\psi_0|\hat{P}|\psi_0\rangle = 0. \quad (2.83)$$

The action of the UIR of the affine group on  $\mathcal{H} = L^2(\mathbb{R}^+, dx)$  introduce a continuous family of unit vectors (in the position representation) as follows:

$$\langle x|q, p\rangle := \langle x|U_A(q, p)|\psi_0\rangle = U_A(q, p)\psi_0(x) = \frac{e^{ipx}}{\sqrt{q}}\psi_0\left(\frac{x}{q}\right) \in \mathcal{H}, \quad (2.84)$$

where  $\psi_0(x) = \langle x|\psi_0\rangle \in \mathcal{H}$ . The resolution of identity for ACS is found to read:

$$\int_{\mathbb{R}^+ \times \mathbb{R}} \frac{dqdp}{\mathcal{N}} |q, p\rangle\langle q, p| = \mathbb{1} \quad (2.85)$$

where  $\psi_0(x)$ <sup>12</sup> is a fixed fiducial vector that satisfies the normalization imposed by the affine group [57]:

$$\mathcal{N} = 2\pi \cdot \rho(0) < \infty \quad \text{where} \quad \rho(x) := \int \frac{|\psi_0(x)|^2}{x^{\alpha+1}} dx \quad (2.86)$$

<sup>11</sup>In fact, the affine group has two non-equivalent UIR  $U_{\pm}$  [56], but only the UIR  $U_+$  is concerned in this thesis.

<sup>12</sup>In general, this fiducial vector entering the identity resolution does not need to be the same as the one used for the expectation values (2.83).

<sup>13</sup>The normalization comes from the group integrability (or admissibility) condition, which puts an additional restriction on the fiducial vectors:  $|\psi_0\rangle \in L^2(\mathbb{R}, dx) \cap L^2(\mathbb{R}, dx/x)$ . As it is explained in several works [57, 58], the admissibility condition is necessary because the affine group is non-unimodular, meaning that the measure  $d\mu_{\mathcal{A}}(q, p) = dqdp$  is left-invariant by (2.79) but not right-invariant. In this thesis we assume left regular representations of the symmetry groups (2.72), (2.80), hence we work with left-invariant measures.

Since the momentum operator reads as  $-i\partial_x$  in the position representation, for later purposes, it is also useful to define:

$$\sigma(\alpha) := \int \frac{|\partial_x \psi_0(x)|^2}{x^{\alpha+1}} dx. \quad (2.87)$$

As we show later, utilizing the affine representation to quantize cosmological models produces intriguing and intricate outcomes, all the while maintaining the fundamental paradigm of quantum physics, the canonical commutation rule.

### 2.4.2 Quantization methods based on coherent states

Let us first define what a quantization procedure is [59]: given a classical phase space  $\mathcal{X}$ , and a vector space  $C(\mathcal{X})$  of complex-valued functions  $f(x)$  on  $\mathcal{X}$ , the quantization is a linear map from  $C(\mathcal{X})$  to a vector space  $\mathcal{A}(\mathcal{H})$  of linear operators  $\hat{A}_f$  on some Hilbert space  $\mathcal{H}$ :

$$\mathcal{Q} : f \in C(\mathcal{X}) \mapsto \mathcal{Q}(f) \equiv \hat{A}_f \in \mathcal{A}(\mathcal{H}) \quad (2.88)$$

The map must fulfill the following conditions:

- (1) To  $f = 1$  there corresponds the identity on  $\mathcal{H}$ :  $f = 1 \mapsto \hat{A}_f = \mathbb{I}_{\mathcal{H}}$
- (2) To a real function  $f$  there corresponds an (essentially) self-adjoint operator  $\hat{A}_f$  in  $\mathcal{H}$ .

In addition, physics introduce further conditions. Some natural requirements inspired by canonical quantization rules [60] are postulated:

- (i) The map is linear:  $\hat{A}_{c_1 f + c_2 g} = c_1 \hat{A}_f + c_2 \hat{A}_g$ , where  $c_1, c_2 \in \mathbb{C}$ .
- (ii) Enhancing (2): in the context of physics,  $f$  would be a real observable, to which is assigned a symmetric operator. Moreover, if the observable is semi-bounded, it is promoted to a semi-bounded operator, that is always a self-adjoint extension<sup>14</sup>.
- (iii) The classical limit of the quantum commutator (at the order  $\hbar$ ) corresponds to the Poisson bracket:  $\{f, g\} = h \mapsto [\hat{A}_f, \hat{A}_g] = i\hbar \hat{A}_h$ . (The non-commutativity in operators' algebra is a fundamental property of Quantum Mechanics).
- (iv) Any quantization based on GCS generated by the UIR of a symmetry group must be covariant with respect to the group symmetry, in the same sense that canonical quantisation is covariant with respect to positions and momentum translations.

The resolution of identity (2.65) provides a remarkable property that motivates the use of GCS within the so-called *integral* quantization methods<sup>15</sup>:

$$f \mapsto A_f = \int f(q, p) |q, p\rangle \langle q, p| \frac{d\mu(q, p)}{\mathcal{N}}, \quad (2.89)$$

This integral map is known as the diagonal representation of operators, and it fulfills all the requirements listed above for a quantization map. Furthermore, when

<sup>14</sup>This is called Friedrich extension [61]: The self-adjoint extension of the semi-bounded (from below) symmetric operator  $\hat{A}_f$ , that may fail to be essentially self-adjoint

<sup>15</sup>From now on we drop the hat-notation in  $A_f$  when referring to operators obtained by integral quantization map.

the construction involves the use of a group action, it is possible to insist on the method's covariance aspects. Lie group representation theory provides many possibilities for constructing explicit integral quantization methods [59]. Then, the above map is usually called a phase-space covariant map, since states  $|q, p\rangle$  are chosen to be created by the action of the convenient representation of the phase space symmetry  $\mathcal{G}$ . Therefore the map provides an integral quantization of complex-valued functions  $f_{\mathcal{G}}$  on the Lie group  $G$  of such symmetry:

$$A_f = \int_G f_{\mathcal{G}}(q, p) \mathcal{Q}_{\mathcal{G}}(q, p) \frac{d\mu_{\mathcal{G}}(q, p)}{\mathcal{N}_{\mathcal{G}}}, \quad \text{with } \mathcal{Q}_{\mathcal{G}} := |q, p\rangle_{\mathcal{G}} \langle q, p|_{\mathcal{G}}. \quad (2.90)$$

where  $\mathcal{G} \mapsto U_{\mathcal{G}}$  is a UIR of  $G$  in the Hilbert space, and the quantization is covariant in the sense that  $U_{\mathcal{G}} A_f U_{\mathcal{G}}^{\dagger} = A_{(\mathcal{G})f}$ <sup>16</sup>. The diagonal family of operators  $\mathcal{Q}_{\mathcal{G}}$  is obtained by a  $\mathcal{G}$ -translation as

$$\mathcal{Q}_{\mathcal{G}}(q, p) = U_{\mathcal{G}}(q, p) \mathcal{Q}_0 U_{\mathcal{G}}^{\dagger}(q, p) \quad (2.91)$$

of the chosen unit trace (self-adjoint on  $\mathcal{H}$ ) operator  $\mathcal{Q}_0 = |\psi_0\rangle \langle \psi_0| = \mathcal{N}_{\mathcal{G}} \mathbb{I}$ , where  $\mathcal{N}_{\mathcal{G}} = \int_G d\mu_{\mathcal{G}}(q, p) |\langle \psi_0 | U_{\mathcal{G}} | \psi_0 \rangle|^2 < \infty$  is the normalization factor coming from the fixed unit fiducial vector  $|\psi_0\rangle$  for the group  $G$ <sup>17, 18</sup>.

The proposed quantization approach highlights the important role of phase space symmetry and permits an infinite number of quantization maps, provided that they are covariant with respect to such a symmetry. An advantage of our quantization method is that it describes the ambiguities present in the quantization process with a convenient parametrization. This makes our analysis more robust, as we will see when computing affine quantization of the isotropic variables in our cosmological models.

### 2.4.3 Semiclassical formalism

Integral quantization enables the construction of a natural semi-classical framework. It allows to write down the formula for classical-like expectation value

$$\text{Tr} (P_{\mathcal{G}} A_f) = \int_G f_{\mathcal{G}}(q, p) \text{Tr} (P_{\mathcal{G}} \mathcal{Q}_{\mathcal{G}}(q, p)) \frac{d\mu_{\mathcal{G}}(q, p)}{\mathcal{N}_{\mathcal{G}}}, \quad (2.92)$$

<sup>16</sup>An example of symmetries  $(\mathcal{G})f$  are  $(\mathcal{T})f$  (Eq. (2.72)) and  $(\mathcal{A})f$  (Eq. (2.80)), with  $U_{\mathcal{G}} \rightarrow U_W$  or  $U_A$ , respectively, for the Weyl-Heisenberg group of translations and the Affine symmetry group.

<sup>17</sup>According to the admissibility condition of the operator  $U_{\mathcal{G}}$  imposed by the orthogonality relation of the given group [62]

<sup>18</sup>In the context of quantization using the affine group, it is important to emphasize here that the operators  $\hat{Q}$ ,  $\hat{P}$  and  $\hat{D}$  in (2.81) were obtained from  $q$ ,  $p$  by means of the usual canonical quantization prescription. In this well-known procedure, we get the canonical commutation relation of quantum physics and the classical limit of the obtained commutation relation coincides with the Poisson bracket of the algebra of the generators, what is a requirement of quantization as stated in condition (iii) above. When applying a different method of quantization, it is not trivial that the operators obtained from quantizing the observables  $q \rightarrow A_q$  and  $p \rightarrow A_p$  will satisfy the same commutation relation as the one of the operators obtained by the canonical rule (2.81), that has the proper classical limit. Therefore, if a method of quantization based on GCS is applied, the fiducial vector for quantization must be selected imposing that the commutation relation of the quantum operators is the same as (2.81), in addition to the integrability condition (2.86). However, this might be in conflict with the physical centering imposed by the group (2.83) on the fiducial vector. In that case, there are two options: a) we use two different families of fiducial vector of GCS, one for the quantization method and one for the expectation values (as it was done in the work presented in chapter 3); b) we look for a fiducial vector that fulfills both conditions (as we did in work presented in of chapter 6, where a more general fiducial vector in terms of two parameters controlling the quantum dispersion is introduced).

where  $P_G = |q', p'\rangle_G \langle q', p'|_G$  is in general a different family of unit trace operators of the same group obtained from a different fiducial vector  $P_0 = |\bar{\psi}_0\rangle \langle \bar{\psi}_0|$ . The operators are typically denoted by  $P_G$  due to the fact that the quantity  $\text{Tr}(P_G Q_G) = \langle q, p|_G P_G |q, p\rangle_G = |\langle q, p|q', p'\rangle_G|^2$  acts as a probability distribution for a state  $|q, p\rangle$  to be in the state  $|q', p'\rangle$ , implying uncertainties in the phase space. More generally,  $P_G$  can be seen as a projector describing a quantum system whose wave-function Hilbert space is approximated with the family of coherent states  $|q', p'\rangle_G$ . The expectation value in projectors  $P_G$  for a quantum observable represented by a self-adjoint operator  $A_f$  on  $\mathcal{H}$  is then given by:  $\langle A_f \rangle_{(q', p')_G} = \text{Tr}(P_G A_f)$ . Hence, using the above formula, we can write the so-called lower symbol [63] of the observable  $f \mapsto \check{f}$ , which is viewed as a semiclassical representation of the operator  $A_f$ . In terms of the GCS<sup>19</sup>, it reads:

$$\check{f}(q, p) := \text{Tr}(P_G A_f) = \int_G |\langle q, p|q', p'\rangle_G|^2 f(q', p') \frac{d\mu_G(q', p')}{\mathcal{N}_G} \quad (2.93)$$

The above formula provides a semiclassical version of the observable  $f$ , which can be interpreted as the classical limit of its quantum corrected version. This formula combines the quantization by GCS of the group  $G$ , with the semiclassical portrait of the operators issued from the same GCS group.

Equivalently, the full procedure could be split in two steps, the first to obtain the quantum operator  $A_f$  that correspond to the observable  $f$  and, the second to evaluate its expectation value with a different family of coherent states of the same group yielding its semiclassical portrait<sup>20</sup>:

$$\check{f}(q, p) = \langle q, p|_G A_f |q, p\rangle_G. \quad (2.94)$$

In addition, there exists an alternative formula for integral quantization that might be more practical to utilize in some situations. The latter is obtained using the so-called symplectic Fourier transform of  $f(q, p)$  over a group:

$$\mathcal{F}[f](q, p) = \int_G e^{i\sigma((q, p) \circ (q', p'))} f(q', p') \frac{d\mu_G(q', p')}{\mathcal{N}_G} \quad (2.95)$$

Therefore, by defining a weight function via the corresponding group transform

$$\Pi_G(q, p) := \text{Tr}(U_G(q, p) \mathcal{Q}_0) \implies \mathcal{Q}_0 = \int_G U_G(q, p) \Pi_G(q, p) \frac{d\mu_G(q, p)}{\mathcal{N}_G} \quad (2.96)$$

and substituting (2.91) in (2.90), it can be shown that one obtains the equivalent form of  $G$ -group integral quantization [55]:

$$A_f = \int_G U_G(q, p) \mathcal{F}[f](-q, -p) \Pi_G(q, p) \frac{d\mu_G(q, p)}{\mathcal{N}_G} \quad (2.97)$$

<sup>19</sup>Changing labels for simplicity  $q \leftrightarrow q', p \leftrightarrow p'$

<sup>20</sup>The first procedure was the one employed for the Mixmaster background of the work presented in chapter 3, whereas the second option was performed in the Friedmann background of the work in chapter 6

together with corresponding lower symbol:

$$\check{f}(q, p) = \int_{\mathcal{G}} \mathcal{F}[\Pi(q, p)] * \mathcal{F}[\check{\Pi}] f(q' - q, p' - p) f(q', p') \frac{d\mu_{\mathcal{G}}(q', p')}{\mathcal{N}_{\mathcal{G}}^2} \quad (2.98)$$

where  $\check{\Pi}(q, p) = \Pi(-q, -p)$ . This alternative formulation is sometimes convenient, since more tractable formulas can be obtained when the weight function instead of the family of operators  $\mathcal{Q}_{\mathcal{G}}(q, p)$  (or the defining  $\mathcal{Q}_0$ ) is used<sup>21</sup>.

### Semiclassical and semiquantum trajectories

The coherent state semiclassical description constitutes a tool that allows to obtain an approximation to the exact quantum dynamics of systems that undergo evolution in both the classical and quantum regimes. In this formalism, the dynamics of the quantum states just describes the propagation of fixed reference states, in a way such that the mean position and momentum obey the evolution of the labels  $q(t)$ ,  $p(t)$  of their phase space representation. During the motion, the shape of the wavefunction is kept fixed. The evolution of the phase space semiclassical trajectories include corrections from the quantum evolution. When the quantum effects are visible, then the quantum uncertainty cannot be neglected. Therefore, sometimes these trajectories are named as "semiquantum" instead of semiclassical, in order to emphasize their quantum nature. This in particular implies that the expectation values of compound operators are not, in general, simple functions of the expectation values of basic operators. The name "semiclassical" is usually restricted to trajectories of classical variables that, don't follow the classical equations of motion, but retain all the properties the classical trajectories have. That means, functions of these variables are those that would be obtained if they were actually classical; with quantum uncertainties assumed negligible<sup>22</sup>.

#### 2.4.4 Application of GCS methods to Quantum Cosmology

We apply the presented quantization methods and semiclassical formalism based on GCS to the background variables of our cosmological models explained in the previous sections. For the isotropic variables, since we cannot apply canonical quantization because they are defined on the half-plane  $(q, p) \in \mathbb{R}_+ \times \mathbb{R}$  (as one can observe in (2.19) and (2.54)), it is necessary to employ the affine group integral quantization. For the anisotropic background variables of the mixmaster-model, defined in the full-plane  $(\beta_{\pm}, p_{\pm}) \in \mathbb{R}^2$ , we use the Weyl-Heisenberg integral quantization and semiclassical portrait.

In general, as we shall prove, the affine semiclassical formalism for the isotropic variables supplements the kinetic term  $\propto p^2$  of the background Hamiltonian with a term of the form  $+K/q^2$ , where  $K > 0$ . Thus, with affine quantization we arrive to

<sup>21</sup>We employ this quantization approach for the anisotropic background variables by making the replacement  $(q, p) \rightarrow (\beta_{\pm}, p_{\pm})$  in section 6.1.2.

<sup>22</sup>Here I provide an intuitive example of when the term semiquantum applies for the trajectories: when in the context of General Relativity we assume we have a regular 4-dimensional spacetime, seen as a classical object, but now solving quantum corrected equations of motion instead of Einstein equations, the phase space trajectories are commonly understood as semiclassical. If in the same framework we refer to a trajectory as semiquantum, we are meant to point out that such space time is not seen as classical anymore but quantum, and we should focus on the uncertainties of the background, that may produce ambiguous predictions on quantum observables over that semiquantum background phase space.

a quantum model in which the appearance of the term  $K/q^2$ , with form of a repulsive potential, generates a "quantum force" that removes the singularity, since the point  $q = 0$  is never reached. When  $q \rightarrow 0$ , the potential grows unboundedly, creating an impassable barrier that prevents the geometry from collapse. That yields, the contracting universe to rebound off the potential at a value  $q > 0$ , initiating an expansion phase, which is smoothly connected to the contracting one. Later in time, the potential term quickly decreases, since  $q$  increases for the expanding universe, and therefore, far away from the bounce, the dynamics becomes again (at the level of expectation values of the basic variables) classical.

This result unlocks a wide-ranging field for scientific investigations. Within these, our focus is on the inquiry into the possible ambiguities of evolution in the (semi)quantum regime of the big bounce scenario and the potential observational impacts.



# 3

## Unitarily inequivalent quantum cosmological models

**DISCLAIMER:** The material presented in this Chapter was originally published in Phys. Rev. D 105 023522 (2022) (which corresponds to the reference [23]) of which I am a coauthor. Part of it was also included in my contribution to the Proceedings of the 2022 Cosmology session of the 56th Rencontres de Moriond (2022) [arXiv:2203.03924] (Ref. [64]). My contributions to this publication can be summarised as follows: I participated in defining the two parametrizations of the classical model and in solving the classical equations of motion. I verified the derivation of the quantum models and computed the inequivalent potentials stemming from the quantization ambiguity. I participated in the discussion of the obtained results, illustrating them with plots. I participated in the preparation of the paper for publication. I gave talks presenting these results in: "4th PU International Conference on Gravitation and Cosmology" (Lahore, Pakistan in Nov. 2021) and "NCBJ PhD Seminar 2021" (National Centre for Nuclear Research, Poland in Mar. 2021).

The inflationary scenario is currently the most accepted model for the origin of primordial perturbations, from which present cosmological structure evolved. This means that primordial perturbations are usually studied in the framework of inflation, which assumes a classical homogeneous background spacetime, while only the small inhomogeneous perturbations are quantized [26]. Quantizing the perturbations is crucial for making accurate predictions of the temperature anisotropies in the Cosmic Microwave Background (CMB). Due to its success, inflation provides compelling evidence for the quantum nature of the gravitational field and motivates further exploration of potential quantum effects in the evolution of the cosmological background. This opens up the possibility of alternative cosmological scenarios that, although using the same mechanism of parametric amplification in generating primordial structures, rely on quantum background evolution instead of a classical inflationary phase. In this chapter, we introduce such a scenario, which is based on the (semi)quantum dynamics of scalar perturbations in a quantum FLRW universe, where a contracting phase and a quantum bounce play the role of the amplifier of vacuum fluctuations. We postpone the detailed analysis of the dynamics to the next chapter 4, focusing in the present chapter on a fundamental ambiguity in definitions of quantum bouncing models with perturbations.

Most bouncing models are either based on a classical (or semiclassical) background [65, 66]. The purpose of this chapter is to show that there might be some important caveat that should be taken into account as an unsolved ambiguity, not to be mistaken with that due to operator ordering (also present but fixed independently), can emerge in a quantum bouncing scenario. It is worth mentioning that already in classical backgrounds, the notion of the initial vacuum state depends on the choice of perturbation variables for quantization as discussed e.g., in [67]. This physical ambiguity becomes worse, and concerns the dynamics of perturbations as well, once the background is quantized. A similar point was considered in recent works [68] for an inflationary background, leading to a vanishingly small effect. Since the quantum character of the background is emphasized, we shall call the  $\hbar$ -corrected background trajectories of our system *semiquantum* and not semiclassical, as explained at the end of section 2.4.3.

In what follows, we examine a simple model of a perturbed FLRW universe filled with a perfect fluid. The classical physical Hamiltonian that generates the dynamics of such model with respect to the internal clock  $\tau$  was given in (2.34):

$$\mathbf{H} = \mathbf{H}^0 - \sum_k \mathbf{H}^{(2)}, \quad \text{with} \quad (3.1)$$

$$\mathbf{H}^{(0)} = 2\kappa_0 p^2, \quad \mathbf{H}_k^{(2)} = \frac{1}{2} |\pi_{\phi,k}|^2 + \frac{1}{2} w(1+w)^2 \left( \frac{q}{\gamma} \right)^{\frac{4(3w-1)}{3(1-w)}} k^2 |\phi_k|^2.$$

As we showed in (2.28), this model is classically singular, all trajectories either expand from a singularity (vanishing scale factor) or contract toward one. However, as anticipated in 2.4.4, the quantized dynamics of the background sews the contracting and expanding phases, with a Big Bounce.

Before proceeding to the quantization, it is convenient to introduce a conformal time  $\eta$  for our system, defined in terms of the internal time as  $Nd\tau = ad\eta$ , and given by

$$d\eta = Z^2 d\tau = (1+w) \left( \frac{q}{\gamma} \right)^{\frac{2(3w-1)}{3(1-w)}} d\tau, \quad (3.2)$$

where we made use of Eq. (2.19) and we have defined the function

$$Z(\tau) \equiv \sqrt{1+w} \left( \frac{q}{\gamma} \right)^{\frac{3w-1}{3(1-w)}}. \quad (3.3)$$

The singularity is also assumed to happen for  $\eta \rightarrow 0$ . One then finds the ‘‘classical’’ conformal time to read

$$\eta = \frac{1+w}{r_1+r_2} \left( \frac{q_B \omega}{\gamma} \right)^{2r_1} \tau^{r_1+r_2}, \quad (3.4)$$

which is straightforwardly inverted to yield  $\tau(\eta)$ , and finally

$$q(\eta) = q_B \omega \left[ \frac{r_1+r_2}{1+w} \left( \frac{q_B \omega}{\gamma} \right)^{-2r_1} \eta \right]^{1/(r_1+r_2)} \propto \eta^{\frac{3(1-w)}{1+3w}}, \quad (3.5)$$

where we have set

$$r_1 = \frac{3w-1}{3(1-w)} \quad \text{and} \quad r_2 = r_1 + 1 = \frac{2}{3(1-w)} \quad (3.6)$$

(the reason for introducing  $r_1$  and  $r_2$  will become clearer later).

### 3.1 A quantum background

We proceed now to describe our approach to quantization of the background, which resolves the classical singularity with a bounce. Instead of using the Wheeler-De Witt equation [69], we use the semiclassical approximation introduced in section 2.4.4 leading to regular, bouncing behaviour.

The phase space for the cosmological background  $(q(\tau), p(\tau))$  is the half-plane rather than the full plane and hence the usual canonical quantization rules seem to be inadequate. Therefore, we apply a general quantization scheme of section 2.4.2, which respects the symmetries of the phase space and which takes care of the factor ordering ambiguity. This method provides all factor orderings in a convenient parametrization, that is, they are encoded in (yet) unknown parameters that enter into the symmetrized operator  $A_f$  version of the classical  $c$ -numbers-valued function of the phase space  $f$ . We introduce then a family of quantum models, described by a set of free parameters that can be computed in the framework of GCS quantization using the affine group of 2.4.1 for the half-plane. The affine quantization has already been proposed before for a consistent quantum gravity program [70, 71].

#### 3.1.1 Affine quantization of the background

Since the background phase space is the half plane, we use the covariant integral quantization method based on the unitary, irreducible and square-integrable representation of the affine group in the Hilbert space  $\mathcal{H} = L^2(\mathbb{R}^+, dx)$ , introduced in Eq. (2.84). The affine coherent states are generated by the action of such representation on a fiducial vector state, denoted here by  $|\psi_0\rangle$ :

$$\mathbb{R}^+ \times \mathbb{R} \ni (q, p) \mapsto |q, p\rangle := U_A(q, p)|\psi_0\rangle \in \mathcal{H}, \quad (3.7)$$

where, for the purpose of quantization, we choose the following family of fiducial states:

$$\psi_{0\nu}(x) = \left(\frac{\nu}{\pi}\right)^{\frac{1}{4}} \frac{1}{\sqrt{x}} \exp\left[-\frac{\nu}{2} \left(\ln x - \frac{3}{4\nu}\right)^2\right], \quad (3.8)$$

for the parameter  $\nu > 0$  controlling the quantum uncertainty, such that the condition of Eq. (2.86) is satisfied, and for which the coefficients introduced in that equation and Eq. (2.87) read:

$$\begin{aligned} \rho_\nu(\alpha) &= \exp\left[\frac{(\alpha-2)(\alpha+1)}{4\nu}\right], \\ \sigma_\nu(\alpha) &= \left[\frac{\nu}{2} + \left(\frac{\alpha+2}{2}\right)^2\right] \exp\left[\frac{\alpha(\alpha+3)}{4\nu}\right], \end{aligned} \quad (3.9)$$

and are positive definite. Once the above are known, we can apply the quantization map (2.90), using (2.84), to find the affine coherent state quantization of the following observables (a detailed example of the explicit computations can be found in, e.g.,

Appendix of [72]):

$$A_1 = \mathbb{1}, \quad (3.10a)$$

$$A_{q^\alpha} = \mathfrak{a}(\alpha) \hat{Q}^\alpha, \quad (3.10b)$$

$$A_p = \hat{P}, \quad (3.10c)$$

$$A_{q^\alpha p^2} = \mathfrak{a}(\alpha) \hat{Q}^\alpha \hat{P}^2 - i\alpha\hbar\mathfrak{a}(\alpha) \hat{Q}^{\alpha-1} \hat{P} + \mathfrak{c}(\alpha) \hbar^2 \hat{Q}^{\alpha-2}, \quad (3.10d)$$

where  $\hat{Q}$  and  $\hat{P}$  are the "position" and "momentum" operators on the half-line: meaning Eqs. (3.10b) and (3.10c) are to be understood as  $\langle x|A_{q^\alpha}|\phi\rangle = \mathfrak{a}(\alpha)x^\alpha\phi(x)$  and  $\langle x|A_p|\phi\rangle = -i\hbar d\phi/dx$ , where  $\phi(x) := \langle x|\phi\rangle$ . They satisfy the usual commutation relation  $[\hat{Q}, \hat{P}] = i\hbar$ , and therefore  $[\hat{Q}^\alpha, \hat{P}] = i\hbar\alpha\hat{Q}^{\alpha-1}$ , so that the symmetric operator (3.10d) can be written as:

$$q^\alpha p^2 \mapsto \mathfrak{a}(\alpha) \hat{P} \hat{Q}^\alpha \hat{P} + \hbar^2 \mathfrak{c}(\alpha) \hat{Q}^{\alpha-2}; \quad (3.11)$$

The parameters

$$\mathfrak{a}(\alpha) = \frac{\rho(\alpha)}{\rho(0)}, \quad \text{and} \quad \mathfrak{c}(\alpha) = \frac{1}{2}\alpha(1-\alpha)\mathfrak{a}(\alpha) + \frac{\sigma(\alpha-2)}{\rho(0)} \quad (3.12)$$

are calculable for the real fiducial vector  $\psi_{0_\nu}(x)$ . This family of fiducial vectors was chosen on purpose such that  $\mathfrak{a}(1) = 1$ , i.e.  $\rho_\nu(1) = \rho_\nu(0) = e^{-1/(\nu)}$ , as needed to ensure the usual commutation relation of Quantum Mechanics between the position variable and its associated canonical momentum  $[A_q, A_p] = i\mathfrak{a}(1)\hbar = [\hat{Q}, \hat{P}] = i\hbar$ . Hence, numerous quantum models are obtained (depending on  $\nu$ ) from a particular classical model. However, this arbitrariness does not result in qualitatively distinct quantum dynamics. Instead, it permits one to freely set numerical parameters in the quantum Hamiltonian in accordance with the physical intuition or, optimally, available observational data. We consider this aspect an advantage of the presented approach over different quantization methods in which one obtains a single quantum model that is totally determined by theory and not adjustable to observational data.

Thus, the existing ambiguity due to the usual factor ordering when going from classical to quantum is fully taken care of in this framework by providing actual numbers for the gothic-style parameters appearing in Eqs. (3.10b) and (3.10d) by setting some value to  $\nu$ . Assuming knowledge of these (e.g., by comparison with some relevant experimental result), one expects the ensuing predictions to be unambiguous from the point of view of factor ordering; whatever remaining ambiguity, as the one detailed below, cannot follow from it. Hence, one might think about the coherent state quantization based on the fiducial vector as a convenient method for parametrizing natural ordering ambiguities

From the above mappings, it follows that the application of the affine quantization to the background Hamiltonian yields

$$\mathbf{H}^{(0)} \mapsto \hat{\mathbf{H}}^{(0)} = 2\kappa_0 \left( \hat{P}^2 + \hbar^2 \mathfrak{c}_0 \hat{Q}^{-2} \right), \quad (3.13)$$

with the free parameter being  $\mathfrak{c}_0 = \mathfrak{c}(0) = \sigma(-2)/\rho(0) = \nu/2$ . The value  $\mathfrak{c}_0 = 0$ , would correspond to the "canonical quantization" case. However, for the present method of affine quantization we have  $\mathfrak{c}_0 > 0$ , yielding the repulsive potential

$\propto \hat{Q}^{-2}$ , of quantum geometric origin, to naturally prevent the universe from reaching the singular point  $q = 0$  by reversing its motion from contraction to expansion. If  $\nu > 3/2 \rightarrow c_0 \geq \frac{3}{4}$ , then  $\hat{H}^{(0)}$  is essentially self-adjoint and no boundary condition for the evolution of the wave-function of the universe needs be imposed at  $\hat{Q} = 0$  to ensure a unique and unitary dynamics (see, e.g., Ref. [73] and references therein). The only way to determine the right value of the parameter  $c_0$  (and then  $\nu$ ) is, as suggested above, to compare the predictions of the model with the actual observations of the Universe.

### 3.1.2 Phase space semiquantum approximation

We now introduce a semiquantum approximation (as suggested in 2.4.3) to the quantum dynamics of the background geometry. It should be noted that any ambiguous effect such as the one we obtain here at a semiquantum level may only be enhanced if a fully quantum description of the background were to be used. We carefully construct the semiquantum trajectory description with the use of affine coherent states.

First we construct wave functions evolving in accordance with (3.13):  $|\psi_B(\tau)\rangle$ , that correspond to various energies and have various spreads in  $\hat{Q}$  and  $\hat{P}$ . One can find a wide class of solutions by approximating the Hilbert space with a family of coherent states, given by state vectors  $(q, p) \mapsto |q, p\rangle$  in one-to-one correspondence with the phase space. The quantum dynamics of the background can be approximated by confining the quantum motion to a family of the affine coherent states that we construct with another fiducial vector,  $|\tilde{\psi}_0\rangle$ . Then, one builds the affine coherent state for the semiquantum portrait by means of Eq. (2.82):

$$|q(\tau), p(\tau)\rangle = e^{ip(\tau)\hat{Q}/\hbar} e^{-i\ln q(\tau)\hat{D}/\hbar} |\tilde{\psi}_0\rangle, \quad (3.14)$$

The expectation values of  $\hat{Q}$  and  $\hat{P}$  in  $|q(\tau), p(\tau)\rangle$  are respectively  $q(\tau)$  and  $p(\tau)$ . In order for the latter statement to be fulfilled, the physical centering conditions (2.83) of the affine group must be satisfied by the new fiducial state:  $\langle \tilde{\psi}_0 | \hat{Q} | \tilde{\psi}_0 \rangle = 1$  (recall  $q$ , and therefore  $\hat{Q}$ , is dimensionless) and  $\langle \tilde{\psi}_0 | \hat{P} | \tilde{\psi}_0 \rangle = 0$ . It can be shown that the fiducial vector  $\psi_{0\nu}(x)$  used for quantization does not satisfy these conditions:  $\langle \psi_0 | \hat{Q} | \psi_0 \rangle = \rho_\nu(-2) = e^{3/(2\nu)} \neq 1$ . That is precisely the reason why we introduce the second family of fiducial vector states for the semiquantum approximation, that yields the expectation values for the momentum and position operators in any coherent state, aligned with the phase space point to which a given coherent state is assigned:

$$\tilde{\psi}_{0\mu}(x) = \left(\frac{\mu}{\pi}\right)^{\frac{1}{4}} \frac{1}{\sqrt{x}} \exp\left[-\frac{\mu}{2} \left(\ln x + \frac{1}{4\mu}\right)^2\right], \quad (3.15)$$

where now  $\mu > 0$  is assumed. In addition, this new family must also satisfy the integrability condition of the affine coherent states (2.86), for the new fiducial state  $|\tilde{\psi}_0\rangle$ . The corresponding coefficients for this new family of fiducial vectors are:

$$\begin{aligned} \tilde{\rho}_\mu(\alpha) &= \exp\left[\frac{(\alpha+1)(\alpha+2)}{4\mu}\right], \\ \tilde{\sigma}_\mu(\alpha) &= \left[\frac{\mu}{2} + \left(\frac{\alpha+2}{2}\right)^2\right] \exp\left[\frac{(\alpha+3)(\alpha+4)}{4\mu}\right]. \end{aligned} \quad (3.16)$$

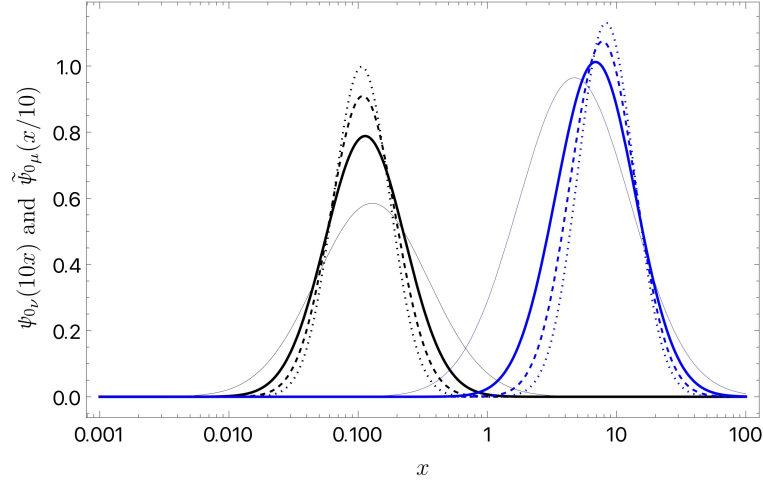


FIGURE 3.1: Fiducial functions  $\psi_{0_\nu}(10x)$  and  $\tilde{\psi}_{0_\mu}(x/10)$  (blue), for  $\nu, \mu = 1$  (thin line), 2 (full), 3 (dashed) and 4 (dotted). For better readability of the figure, the functions have been shifted so that  $\psi_{0_\nu}$  appears centered around 0.1 and  $\tilde{\psi}_{0_\mu}$  around 10. As functions of  $x$ , they should all be centered around  $x = 1$ .

These are also positive definite as expected. It is now clear that  $\tilde{\rho}_\mu(-2) = 1$ , as expected for this description to satisfy the centering condition. However, as expected, this family of fiducial states, being different from the one employed for quantization, does not satisfy the canonical commutation rule (on the half-line):  $\tilde{\rho}(1) = e^{3/(2\mu)} \neq e^{1/(2\mu)} = \tilde{\rho}(0)$ . Some example fiducial functions  $\psi_{0_\nu}(x)$  and  $\tilde{\psi}_{0_\mu}(x)$  are displayed in Fig. 3.1. In some cases, it is possible to select a more general unique family of fiducial states, typically by assuming it depends on more than just one quantization parameter ( $\mu$  or  $\nu$  here), that satisfy both the commutation rule and the physical centering conditions.

The evaluation of the expectation value of the Hamiltonian can be obtained by computing:

$$\begin{aligned} \langle q, p | \hat{Q}^\alpha \hat{P}^2 | q, p \rangle &= \tilde{\rho}(-\alpha - 1) q^\alpha p^2 + i\alpha \tilde{\rho}(-\alpha) q^{\alpha-1} p \\ &+ \left[ \tilde{\sigma}(-\alpha - 1) + \frac{\alpha(1-\alpha)}{2} \tilde{\rho}(-\alpha + 1) \right] q^{\alpha-2}, \end{aligned} \quad (3.17a)$$

$$\langle q, p | \hat{Q}^\alpha \hat{P} | q, p \rangle = \tilde{\rho}(-\alpha - 1) q^\alpha p + i \frac{\alpha}{2} \tilde{\rho}(-\alpha) q^{\alpha-1}, \quad (3.17b)$$

$$\langle q, p | \hat{Q}^\alpha | q, p \rangle = \tilde{\rho}(-\alpha - 1) q^\alpha. \quad (3.17c)$$

### Semiquantum background trajectories

The dynamics of the background confined to the vectors  $|q(\tau), p(\tau)\rangle$  can be deduced from the quantum action

$$\mathcal{S}_B = \int \langle q(\tau), p(\tau) | \left( i\hbar \frac{\partial}{\partial \tau} - \hat{\mathbf{H}}^{(0)} \right) | q(\tau), p(\tau) \rangle d\tau, \quad (3.18)$$

which, upon using the properties of the state (3.14), can be transformed into

$$\mathcal{S}_B = \int \{ \dot{q}(\tau) p(\tau) - H_{\text{sem}} [q(\tau), p(\tau)] \} d\tau, \quad (3.19)$$

with the semiquantum Hamiltonian given by

$$H_{\text{sem}} = \langle q, p | \hat{\mathbf{H}}^{(0)} | q, p \rangle, \quad (3.20)$$

from which one derives the usual Hamilton equations

$$\dot{q} = \frac{\partial H_{\text{sem}}}{\partial p} \quad \text{and} \quad \dot{p} = -\frac{\partial H_{\text{sem}}}{\partial q}. \quad (3.21)$$

Given the quantum Hamiltonian (3.13), we find that the semiquantum background Hamiltonian reads:

$$H_{\text{sem}} = 2\kappa_0 \left( p^2 + \frac{\hbar^2 \mathfrak{K}}{q^2} \right), \quad (3.22)$$

where the actual value of the new constant  $\mathfrak{K} > 0$  depends on the choice of the family of coherent states:  $\mathfrak{K} = \mathfrak{c}_0 \tilde{\rho}(1) + \tilde{\sigma}(-2) = \left( \frac{\nu}{2} + \frac{2\mu+1}{4} \right) \exp\left(\frac{3}{2\mu}\right)$ , whose minimum value  $\mathfrak{K}_{\text{min}}$  is reached for  $\nu = 0$  and  $\mu_{\text{min}} = (3 + \sqrt{21})/4 \approx 1.89$ , at which point one has  $\mathfrak{K}_{\text{min}} \approx 2.64$ . Thus,  $\mathfrak{K} > 0$  is positive irrespective of whether  $\mathfrak{c}_0 = 0$  or  $\mathfrak{c}_0 > 0$ .

We find the solution to (3.21) to read

$$q = q_{\text{B}} \sqrt{1 + (\omega\tau)^2}, \quad (3.23a)$$

$$p = \frac{q_{\text{B}} \omega^2}{4\kappa_0} \frac{\tau}{\sqrt{1 + (\omega\tau)^2}}, \quad (3.23b)$$

where  $q_{\text{B}}^2 = 2\kappa_0 \hbar^2 \mathfrak{K} / H_{\text{sem}}$  then represents the minimum scale factor volume and  $\omega = 2H_{\text{sem}} / (\hbar \sqrt{\mathfrak{K}})$  the acceleration at the bounce. We display in Fig. 3.2 a few trajectories in the phase space illustrating these solutions and comparing them with their classical counterparts (2.28).

With this semiquantum solution, one can also integrate (3.2) to obtain the conformal time  $\eta$ , as a function of  $\tau$

$$\eta = (1+w)\tau \left( \frac{q_{\text{B}}}{\gamma} \right)^{2r_1} \mathcal{F} \left[ \frac{1}{2}, -r_1; \frac{3}{2}; -(\omega\tau)^2 \right], \quad (3.24)$$

where  $\mathcal{F}(a, b; c; z)$  is the hypergeometric function (see Sec. 15 of Ref. [74]). As expected, one recovers the classical power law (3.4) in the late-time limit  $\tau \gg \omega^{-1}$ , up to a constant depending on the barotropic index  $w$  and vanishing for  $w = \frac{1}{3}$ . Figure 3.3 shows the classical and semiquantum relations  $\eta(\tau)$ .

## 3.2 Classical perturbations

We have explained our quantization of the background spacetime and its semiquantum evolution. In what follows, we discuss the classical and quantum dynamics of the perturbations to the background spacetime. We restrict our attention in this section to classical perturbations over the classical background, following the terminology previously introduced.

The reduced phase space is a pair of basic perturbation variables  $(\phi_k, \pi_{\phi,k})$  equipped with the second-order classical Hamiltonian  $\mathbf{H}_k^2$  of Eq. (3.1). There is, however, no preferred (from the physical point of view) choice of basic variables, and one is free to perform any canonical transformation in the reduced phase space prior to quantization. All these classical formulations are physically equivalent. We

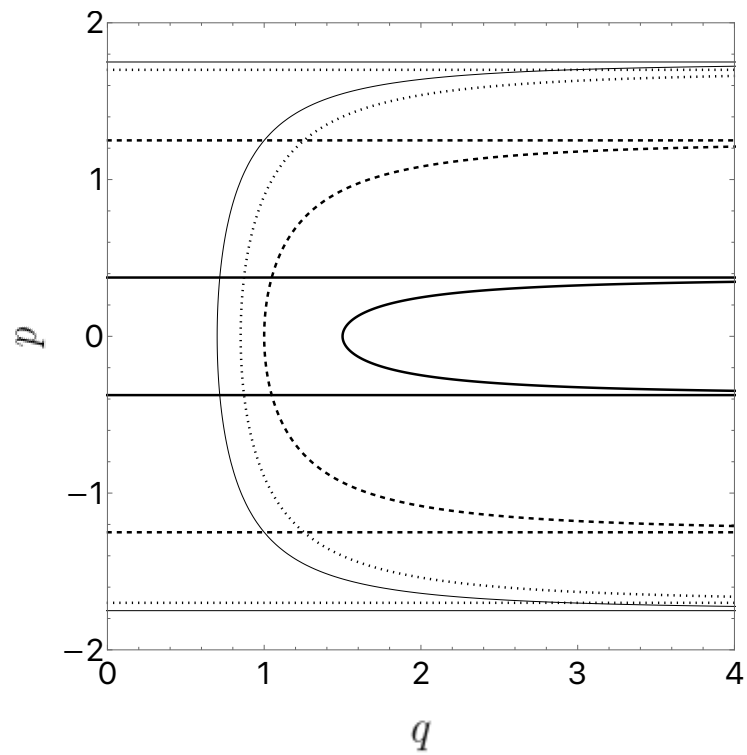


FIGURE 3.2: Background phase space evolutions for different values of  $q_B$  and  $\omega$ : the straight lines represent Eqs. (2.28), either going to or emerging from a singularity ( $q \rightarrow 0$ ), while the curves are the solutions (3.23) leading to the same asymptotic classical lines. The semi-quantum solution are seen to consist of a bounce smoothly joining expanding ( $p > 0$ ) and contracting ( $p < 0$ ) classical universes.

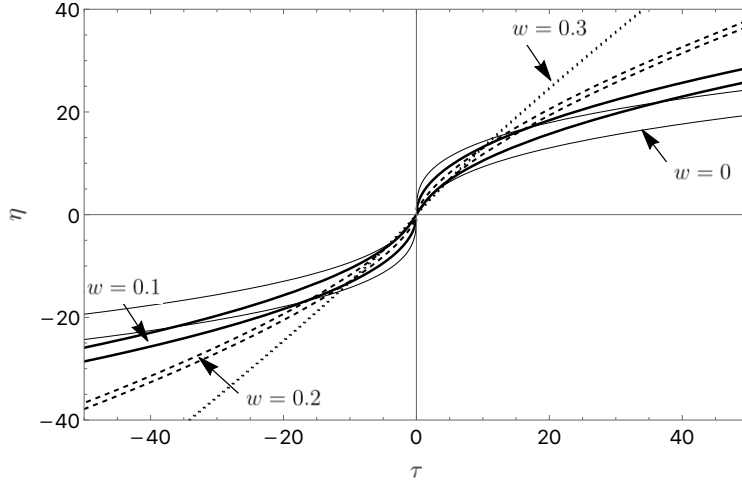


FIGURE 3.3: Conformal time  $\eta$  as a function of  $\tau$ , for the classical (3.4) and semiquantum (3.24) solutions for  $w = 0$  (thin line),  $w = 0.1$  (thick),  $w = 0.2$  (dashed) and  $w = 0.3$  (dotted). The quantum conformal time tends to the classical one up to a constant factor, which vanishes for  $w = \frac{1}{3}$ .

consider two examples of them to analyse the potential different results that may arise from the quantization of these classically equivalent theories.

### 3.2.1 Fluid parametrization

We name (2.34) the *Fluid*-parametrization of the second-order Hamiltonian:

$$\mathbf{H}_k^{(2)} = \frac{1}{2} |\pi_{\phi,k}|^2 + \frac{1}{2} w(1+w)^2 \left(\frac{q}{\gamma}\right)^{4r_1} k^2 |\phi_k|^2, \quad (3.25)$$

with  $r_1$  defined in (3.6). We call it the fluid-parametrization as for the fluid time  $\tau$  the Hamiltonian (3.25) takes a simple form in which its kinetic term is canonical. The Fourier component  $\phi_k$  of the perturbation field is a combination of the fluid perturbation<sup>1</sup>  $\delta\phi_k$  and the intrinsic curvature perturbation  $\delta R_k$ , that can be seen in (2.36). The angular mode wavenumber  $k \equiv |k|$  is the amplitude of the wave vector; recall that since the FLRW background (2.16) is isotropic, as usual, the initial conditions, and therefore the solutions of the perturbation evolution equation depend only on the amplitude  $k$  and not on its direction  $k/k$ . Given our conventions, the physical dimensions are  $[\phi_k] = \sqrt{ML}$  and  $[\pi_{\phi,k}] = \sqrt{M}$ . The Poisson bracket reads  $\{\phi_{k_1}, \pi_{\phi,-k_2}\} = \delta_{k_1,k_2}$ . From the Hamilton equations for the perturbation pair, the equation of motion expressed in the internal time is found to read

$$\ddot{\phi}_k + \left(\frac{q}{\gamma}\right)^{4r_1} w(1+w)^2 k^2 \phi_k = 0. \quad (3.26)$$

It shows that for radiation, i.e. for  $w = \frac{1}{3}$ , which implies  $r_1 = 0$ , the dynamics of  $\phi_k$  becomes decoupled from the dynamical background.

<sup>1</sup>The background fluid time  $\tau$  is actually a combination of the fluid background variable and its canonical momentum,  $(1+w)\tau = \bar{\phi}|\bar{p}^\phi|^{-1/w}$ , as it was defined in Eq. (2.23).

### 3.2.2 Conformal perturbations

Another example of canonical fields is provided by the pair  $(v, \pi_v)$ , that is commonly used for solving the dynamics of scalar perturbations in inflationary models. It is defined by the canonical transformation

$$v_k = Z\phi_k, \quad (3.27a)$$

$$\pi_{v,k} = Z^{-1}\pi_{\phi,k} + \frac{\dot{Z}}{Z^2}\phi_k, \quad (3.27b)$$

where the function  $Z$  is defined in (3.3) above.

It can be noted that in the comoving gauge, one has  $\delta\phi_k = 0$ , and thus  $v_k = -\sqrt{\frac{3(1+w)}{w\kappa_0}}a\mathcal{R}_k$ , where  $\mathcal{R}_k$  is the comoving curvature perturbation (see Eq. (2.37)), and  $v_k$  represents the Mukhanov-Sasaki variable for the given mode  $k$  [75].

We obtain the second-order Hamiltonian  $\mathbf{H}_k^{(2)}$  in terms of  $(v, \pi_v)$ , namely

$$\mathbf{H}_k^{(2)} = \frac{1}{2}Z^2 \left\{ |\pi_{v,k}|^2 + [wk^2 - \mathcal{V}_{\text{cl}}(\tau)] |v_k|^2 \right\}, \quad (3.28)$$

with the potential  $\mathcal{V}_{\text{cl}}$  defined through

$$\mathcal{V}_{\text{cl}} = \frac{1}{Z^4} \left[ \frac{\ddot{Z}}{Z} - 2 \left( \frac{\dot{Z}}{Z} \right)^2 \right] \quad (3.29)$$

which can be written explicitly in terms of the background canonical variables  $q$  and  $p$  as

$$\mathbf{H}_k^{(2)} = \frac{1}{2}(1+w) \left( \frac{q}{\gamma} \right)^{2r_1} \left\{ |\pi_{v,k}|^2 + \left[ wk^2 - \frac{8}{9q^2} \left( \frac{q}{\gamma} \right)^{-4r_1} \frac{(2\kappa_0)^2(1-3w)p^2}{(1+w)^2(1-w)^2} \right] |v_k|^2 \right\}, \quad (3.30)$$

where we used the background equations of motion.

The coefficient in front of the Hamiltonian (3.30) can be removed by switching to the internal conformal time  $\eta$  (3.2) [76], in terms of which the potential (3.29) takes the simpler and usual form  $\mathcal{V}_{\text{cl}} = Z''/Z$  (which is the familiar form of the gravitational potential in the Mukhanov-Sasaki equation), where a prime means a derivative with respect to the conformal time  $\eta$ : ( $Z' \equiv dZ/d\eta$ ). The double derivative with respect to the conformal time can be expressed in terms of the internal time as:

$$\frac{d^2}{d\eta^2} = Z^{-4} \left[ \frac{d^2}{d\tau^2} - 4r_1 \frac{p}{q} \frac{d}{d\tau} \right] \quad (3.31)$$

The second-order Hamiltonian  $Z^{-2}\mathbf{H}_k^{(2)}$  is then found to generate

$$v_k'' + \left[ wk^2 - \frac{8}{9q^2Z^4} \frac{(2\kappa_0)^2(1-3w)}{(1-w)^2} p^2 \right] v_k = 0, \quad (3.32)$$

which can be written in the usual Mukhanov-Sasaki form

$$v_k'' + [wk^2 - \mathcal{V}_{\text{cl}}(\eta)] v_k = v_k'' + \left( wk^2 - \frac{z''}{z} \right) v_k = 0, \quad (3.33)$$

thereby identifying the classical potential

$$\mathcal{V}_{\text{cl}}(\eta) = \frac{8}{9q^2 Z^4} \frac{(2\kappa_0)^2 (1-3w)}{(1-w)^2} p^2 = \frac{z''}{z}, \quad (3.34)$$

where the last equality is obtained by applying the classical Hamilton equations of motion for the background  $dq/d\tau = 4\kappa_0 p$ ,  $dp/d\tau = 0$ , and there are in fact two different and equivalent choices that can be made for the function  $z$ , being these  $z_1 = q^{r_1}$  and  $z_2 = q^{r_2}$ , namely

$$\mathcal{V}_{\text{cl}} = \frac{(q^{r_1})''}{q^{r_1}} = \frac{(q^{r_2})''}{q^{r_2}} = \frac{2(1-3w)}{(1+3w)^2 \eta^2}, \quad (3.35)$$

as usual for a background dominated by a perfect fluid with constant equation of state. These two power laws stem from the fact that although what enters into (3.28) is  $Z''/Z$ , with  $Z \propto z_1$ , one can then just as well choose the second solution of  $z''/z = Z''/Z$ , namely  $z_2 \propto Z \int d\eta/Z^2 = Z \int d\tau = Z\tau$  which, taking the background solution  $q \propto \tau$  [see Eq. (2.28)] yields  $z_2 \propto Zq = z_1 q = q^{r_1+1}$ , as indeed one has  $r_2 = r_1 + 1$ .

The internal conformal time provides a convenient form of the equation of motion for perturbations. We shall, however, quantize the dynamics of both the background and the perturbations reduced with respect to a unique internal time, the internal fluid time. The term  $z''/z$  is usually referred to as the potential for the perturbations, as Eq. (3.33) is mathematically identical to a time-independent Schrödinger equation in such a potential [77]. As

$$\mathcal{V}_{\text{cl}} = \frac{z''}{z} = \frac{1-3w}{2} \mathcal{H}^2 \quad (3.36)$$

has the clear physical meaning of the conformal Hubble rate  $\mathcal{H}$  squared ( $w < \frac{1}{3}$ ), the conformal Hubble rate determines the coordinate scale at which the amplification of perturbations starts to take place.

We shall call the set of variables  $(v_k, \pi_{v,k})$  the conformal parametrization, as it involves naturally the conformal time. It differs from the fluid parametrization (3.25) by the nontrivial coefficient standing in front of the entire expression as well as the frequency that now depends on both background variables,  $q$  and  $p$ .

### 3.2.3 Solutions for classical perturbations

The two parametrizations described above,  $(\phi, \pi_\phi)$  and  $(v, \pi_v)$ , being related by a canonical transformation, are physically equivalent and therefore it is sufficient to solve the equations of motion for just one of them, e.g., the conformal one, in order to determine the dynamics of perturbations. It is also true at the quantum level [78] provided the background evolution is described by classical trajectories<sup>2</sup>.

Using the definition (3.2) to derive the power-law behavior of  $q(\eta)$  in (2.28), the potential  $z''/z$  in Eq. (3.33) is found to yield the specific form (3.35) (independently of the choice  $z = q^{r_1}$  or  $z = q^{r_2}$ ), so that the classical evolution of perturbation modes is

$$\frac{d^2 v_k}{d\eta^2} + \left[ w k^2 - \frac{2(1-3w)}{(1+3w)^2 \eta^2} \right] v_k = 0. \quad (3.37)$$

<sup>2</sup>Or semiclassical trajectories, understood as the ones described at the end of section 2.4.3 (the ones neglecting the quantum uncertainties), whereas the neologism semiquantum applies to the trajectories obtained here (without neglecting the quantum uncertainties) by the semiclassical methods described. We stress the quantum nature of the latter.

Clearly, the potential  $\mathcal{V}_{\text{cl}} \propto \eta^{-2}$  is singular at the singularity  $\eta \rightarrow 0$ . The solution can be expressed in terms of Hankel functions, namely

$$v_k(\eta) = \sqrt{\eta} \left[ c_1(\mathbf{k}) H_\nu^{(1)}(\sqrt{w}k\eta) + c_2(\mathbf{k}) H_\nu^{(2)}(\sqrt{w}k\eta) \right], \quad (3.38)$$

where  $\nu = \frac{3(1-w)}{2(3w+1)}$  and  $c_1(\mathbf{k}), c_2(\mathbf{k})$  are constants depending on the comoving wave vector  $\mathbf{k}$  through the initial conditions; for quantum vacuum fluctuations in isotropic spacetime set as initial conditions, they can depend only on the amplitude  $k$  and not on the direction  $\mathbf{k}/k$ . The solution is finite but discontinuous at  $\eta = 0$ . Therefore, the comoving curvature  $\Psi_k \propto v_k/a$  in general blows up at  $\eta = 0$  where the scale factor reaches the singularity  $a \rightarrow 0$ ; see Ref. [79] for a full treatment of the relevant cases.

### 3.3 Quantum perturbations

In the present section, we quantize the physically equivalent Hamiltonians (3.25) and (3.30). Next we apply some approximations in order to integrate the dynamics.

#### 3.3.1 Quantization of fluid parametrization

The canonical perturbation variables of the fluid parametrization satisfy the reality condition  $\phi_k^* = \phi_{-k}$  and  $\pi_{\phi,k}^* = \pi_{\phi,-k}$  and it is possible to promote their real and imaginary parts to canonical operators in  $L^2(\mathbb{R}^2, \frac{i}{2}d\phi_k d\phi_k^*)$  for each direction  $k$ . It is, however, more convenient to work with the Fock representation [80],

$$\phi_k \mapsto \hat{\phi}_k = \sqrt{\frac{\hbar}{2}} \left[ a_k \phi_k^*(\tau) + a_{-k}^\dagger \phi_k(\tau) \right], \quad (3.39)$$

where the time-dependent mode functions  $\phi_k(\eta)$  are assumed to be isotropic and  $a_k$  and  $a_k^\dagger$  are fixed annihilation and creation operators that satisfy  $[a_{k_1}, a_{k_2}^\dagger] = \delta_{k_1, k_2}$  (we assume the compactness of space, implying discrete eigenvalues  $k$ )<sup>3</sup>. As shown later, it follows that the mode functions must satisfy a suitable normalization condition. Note that the whole evolution of the operators  $\hat{\phi}_k$  and  $\hat{\pi}_{\phi,k}$  in the Heisenberg picture is encoded into the mode functions.

Combining the background affine quantization (3.10) with the quantization of perturbations above, using the definition (3.6) of the classical power laws, yields the quantized version of Hamiltonian (3.25) in the fluid parametrization (henceforth dubbed F-parametrization)

$$\hat{\mathbf{H}}_k^{(2)} = \frac{1}{2} |\hat{\pi}_{\phi,k}|^2 + \frac{\mathfrak{L}_Q}{2} w(1+w)^2 \left( \frac{\hat{Q}}{\gamma} \right)^{4r_1} k^2 |\hat{\phi}_k|^2, \quad (3.40)$$

where  $\mathfrak{L}_Q = \alpha(4r_1) = \rho(4r_1)/\rho(0)$  [see Eqs. (3.10b) and (3.12)] is a free parameter of the quantization.

<sup>3</sup>We apply conventional canonical quantization to the perturbation degrees of freedom in Fock representation, as it is done in the standard framework of inflation. This is due to the fact that we want to focus on the potential effects resulting from the quantization of the background, for which we decide to use the enhanced methods of quantization both, because the canonical quantization is problematic due to the boundary  $q = 0$ , and because it provides a convenient way to parameterise all the ambiguities. Then, we are able to clearly observe new effects on the propagation of perturbations quantized canonically, in comparison to the standard inflationary theory with perturbations promoted in the same way, but in classical background.

### 3.3.2 Quantization of conformal parametrization

We repeat the same quantization for the conformal parametrization (C-parametrization in what follows),

$$v_k \mapsto \hat{v}_k = \sqrt{\frac{\hbar}{2}} \left[ a_k \bar{v}_k(\tau) + a_{-k}^\dagger v_k(\tau) \right], \quad (3.41)$$

and obtain the quantum Hamiltonian derived from (3.30) as

$$\hat{\mathbf{H}}_k^{(2)} = \frac{1}{2}(1+w) \left( \frac{\hat{Q}}{\gamma} \right)^{2r_1} \mathfrak{M}_Q \mathbf{H}_{k,\text{eff}}^{(2)} \quad (3.42)$$

with

$$\begin{aligned} \hat{\mathbf{H}}_{k,\text{eff}}^{(2)} = & |\hat{\pi}_{v,k}|^2 + \left[ wk^2 - \right. \\ & \left. - \frac{8\mathfrak{M}_Q^{-1}}{9\hat{Q}^2} \frac{(2\kappa_0)^2(1-3w)}{(1-w)^2(1+w)^2} \left( \frac{\hat{Q}}{\gamma} \right)^{-4r_1} \left( \mathfrak{N}_Q \hat{P}^2 + i\hbar \mathfrak{N}_Q \hat{Q}^{-1} \hat{P} + \hbar^2 \mathfrak{T}_Q \hat{Q}^{-2} \right) \right] |\hat{v}_k|^2, \end{aligned} \quad (3.43)$$

where  $\mathfrak{M}_Q = \mathfrak{a}(2r_1) = \rho(2r_1)/\rho(0)$ ,  $\mathfrak{N}_Q = \mathfrak{a}(-2r_2) = \rho(-2r_2)/\rho(0)$ ,  $\mathfrak{R}_Q = 2r_2 \mathfrak{a}(-2r_2) = 2r_2 \mathfrak{N}_Q$  and  $\mathfrak{T}_Q = \mathfrak{c}(-2r_2) = -r_2(1+2r_2)\mathfrak{N}_Q + \sigma(-2r_2-2)/\rho(0)$  are free parameters in the quantization map [see Eqs. (3.10)]. Obviously, these parameters are to a large extent free as the affine quantization depends on the fiducial vector  $\psi_{0_v}(x)$ . Note that there are more free parameters and hence more quantization ambiguities in the C-parametrization (3.43) than in the F-parametrization (3.40).

## 3.4 Semiquantum perturbations

A general approach to solving the dynamics of quantum perturbations in quantum bouncing spacetime was recently given in [27]. In what follows, we assume the full state vector to be a product of background and perturbation states, i.e.,

$$|\psi(\tau)\rangle = |\psi_B(\tau)\rangle \cdot |\psi_P(\tau)\rangle \in \mathcal{H}_B \otimes \mathcal{H}_{\text{pert}}, \quad (3.44)$$

where  $\mathcal{H}_B$  is the Hilbert space of the homogeneous background  $L^2(\mathbb{R}^+, dx)$  and  $\mathcal{H}_{\text{pert}}$  is the Hilbert space of the inhomogeneous perturbations  $L^2(\mathbb{R}^2, \frac{i}{2} d\phi_k d\phi_k^*)$ . The canonical formalism for cosmological perturbations has been developed under the assumption that the perturbations do not backreact on the background spacetime, and there is no entanglement between the background and the perturbations. Therefore, the dynamics of  $|\psi_B(\tau)\rangle$  should be determined independently of the state  $|\psi_P(\tau)\rangle$ . This decomposition of the wave-function is called the cosmological Born-Oppenheimer approximation, in analogy to one with the same name in the field of molecular physics, employed to simplify the interaction between the nuclei and the electrons. Its validity for quantum cosmologies is currently debated [81–83].

Such assumption invalidates the use of Schrödinger equation, and instead, a different law for quantum dynamics needs to be derived through the application of variational principle on the quantum action. Given that the dynamics of the background state is fixed by  $|\psi_B\rangle$ , the dynamics of the perturbation state  $|\psi_P(\tau)\rangle$  can be

deduced from such quantum action at second order  $\mathcal{S}^{(0)+(2)} = \mathcal{S}_B + \mathcal{S}_P$

$$\mathcal{S}^{(0)+(2)} = \int \langle \psi(\tau) | \left( i\hbar \frac{\partial}{\partial \tau} - \hat{\mathbf{H}}^{(0)} + \sum_k \hat{\mathbf{H}}_k^{(2)} \right) | \psi(\tau) \rangle d\tau, \quad (3.45)$$

with the state vector  $|\psi(\tau)\rangle$  given by (3.44). We extract the zeroth order action  $\mathcal{S}_B$  that gives (3.18), yielding to the dynamical law,

$$i\hbar \frac{\partial}{\partial \tau} |\psi_B(\tau)\rangle = \hat{\mathbf{H}}^{(0)} |\psi_B(\tau)\rangle, \quad (3.46)$$

hence assuming, as usual, the Hamiltonian of perturbations to be much smaller than the one of the background. For the perturbations one finds:

$$\mathcal{S}_P = \int \langle \psi_P | \left( i\hbar \frac{\partial}{\partial \tau} + \sum_k \hat{\mathbf{H}}_k^{(2)} \right) | \psi_P \rangle d\tau, \quad (3.47)$$

and setting  $|\psi_P\rangle = \prod_k |\psi_k\rangle$  with  $\langle \psi_{k_1} | \psi_{k_2} \rangle = \delta_{k_1, k_2}$ , one gets the associated Schrödinger equation for each Fourier mode  $|\psi_k\rangle$  (up to an irrelevant phase factor), namely

$$i\hbar \frac{\partial}{\partial \tau} |\psi_k\rangle = \tilde{\mathbf{H}}_k |\psi_k\rangle, \quad (3.48)$$

where the operator  $\tilde{\mathbf{H}}_k \equiv -\langle \psi_B | \hat{\mathbf{H}}_k^{(2)} | \psi_B \rangle$  is obtained from either (3.40) or (3.42) depending on the choice of parametrization, by evaluating the second-order Hamiltonians inside the second family of coherent states  $|\psi_B\rangle \rightarrow |q(\tau), p(\tau)\rangle$  obtained from  $\tilde{\psi}_{0,\mu}(x)$ , as we did for the semiquantum portrait of the background. We discuss those in turn below.

### 3.4.1 Fluid modes

Within the semiquantum approximation, one can then proceed to evaluating the behaviour of perturbations. In the F-parametrization case, the second-order Hamiltonian generating the dynamics of perturbations is obtained from (3.40), reading

$$\langle q, p | \hat{\mathbf{H}}_k^{(2)} | q, p \rangle = \frac{1}{2} |\hat{\pi}_{\phi, k}|^2 + \frac{\mathcal{L}_S}{2} w(1+w)^2 \left( \frac{q}{\gamma} \right)^{4r_1} k^2 |\hat{\phi}_k|^2, \quad (3.49)$$

where the value of  $\mathcal{L}_S = \mathcal{L}_Q \tilde{\rho}(-4r_1 - 1)$ , depends on the value of  $\mathcal{L}_Q$  from quantization and on the family of coherent states used to approximate the background dynamics (see Eq. (3.17c)).

The Heisenberg equations of motion are

$$\frac{d}{d\tau} \hat{\phi}_k = -\hat{\pi}_{\phi, k}, \quad (3.50a)$$

$$\frac{d}{d\tau} \hat{\pi}_{\phi, k} = \mathcal{L}_S w(1+w)^2 \left( \frac{q}{\gamma} \right)^{4r_1} k^2 \hat{\phi}_k, \quad (3.50b)$$

and it follows from (3.50a) that

$$\hat{\pi}_{\phi, k} = \sqrt{\frac{\hbar}{2}} \left[ a_k \dot{\phi}_k^*(\tau) + a_{-k}^\dagger \dot{\phi}_k(\tau) \right], \quad (3.51)$$

and hence the canonical commutation rule, namely  $[\hat{\phi}_{-k}, \hat{\pi}_{\phi,k}] = i\hbar$ , implies the normalization condition on the mode functions  $\dot{\phi}_k \phi_k^* - \phi_k \dot{\phi}_k^* = 2i$ . By combining the above equations, we may obtain the second-order dynamical equation for  $\hat{\phi}_k$ , which must also be obeyed by the mode function  $\phi_k$ . We switch to the internal conformal clock given by Eq. (3.2) and rescale the mode functions,  $v_k^F = Z\phi_k$ , to make it coincide with the Mukhanov-Sasaki variable  $v_k^F$ , already present in the C-parametrization before the quantization. The superscript ‘‘F’’ indicates that its dynamics is generated by the fluid Hamiltonian. More specifically, we find that the dynamics of  $v_k^F$  generated by the Hamiltonian (3.49) reads

$$\frac{d^2 v_k^F}{d\eta^2} + [k_F^2 - \mathcal{V}_F(\eta)] v_k^F = 0, \quad (3.52)$$

with the effective wave number  $k_F \equiv \sqrt{\mathcal{L}_s \omega k}$ , and the fluid potential given by

$$\mathcal{V}_F = \frac{8}{9q^2 Z^4} \frac{(2\kappa_0)^2 (1-3w)}{(1-w)^2} \left[ p^2 - \frac{3(1-w)\mathfrak{R}}{2q^2} \right]. \quad (3.53)$$

Note that for large  $q$ , i.e. away from the bounce, the quantum correction becomes negligible so that the semiquantum potential (3.52) approaches the classical one (3.30). Indeed, using  $\dot{Z}/Z = r_1 \dot{q}/q$  and  $q' = \dot{q}/Z^2$ , one finds

$$\frac{Z''}{Z} = \frac{r_1}{Z^4} \left[ \frac{\ddot{q}}{q} - (1+r_1) \left( \frac{\dot{q}}{q} \right)^2 \right], \quad (3.54)$$

and replacing the function  $q(\tau)$  by the solution (3.23) for the background semiquantum trajectory, it is straightforward to check that, for all times, the potential  $\mathcal{V}_F$  can be given the familiar form:

$$\mathcal{V}_F = \frac{Z''}{Z} = \frac{(q^{r_1})''}{q^{r_1}}. \quad (3.55)$$

Since the semiquantum trajectory (3.23) is asymptotic to the classical one (2.28) for  $\omega\tau \rightarrow \infty$ , i.e. for  $\eta \rightarrow \infty$ , the fluid potential satisfies

$$\mathcal{V}_F(\eta) \simeq \mathcal{V}_{\text{cl}}(\eta) \quad \text{for } \omega\tau \gg 1, \quad \text{i.e. } \frac{q}{q_B} \gg 1, \quad (3.56)$$

where  $\mathcal{V}_{\text{cl}}$  is given by (3.35); it is illustrated in Fig. 3.4.

### 3.4.2 Conformal modes

The same procedure applied to the conformal parametrization yields

$$\langle q, p | \hat{\mathbf{H}}_k^{(2)} | q, p \rangle = \frac{1}{2} Z^2 \mathfrak{M}_s (|\hat{\pi}_{v,k}|^2 + \Omega_v^2 |\hat{v}_k|^2), \quad (3.57)$$

with

$$\Omega_v^2 = \omega k^2 - \frac{8\mathfrak{M}_s^{-1} (2\kappa_0)^2 (1-3w)}{9q^2 Z^4} \left( \mathfrak{N}_s p^2 + \frac{\hbar^2 \mathfrak{T}_s}{q^2} \right), \quad (3.58)$$

where the free semiquantum parameters are  $\mathfrak{M}_s = \mathfrak{M}_Q \tilde{\rho} (-2r_1 - 1)$ ,  $\mathfrak{N}_s = \mathfrak{N}_Q \tilde{\rho} (2r_2 - 1)$ ,  $\mathfrak{T}_s = \mathfrak{N}_Q \tilde{\sigma} (2r_2 - 1) + \mathfrak{T}_Q \tilde{\rho} (2r_2 + 1)$ , dependent also on the family

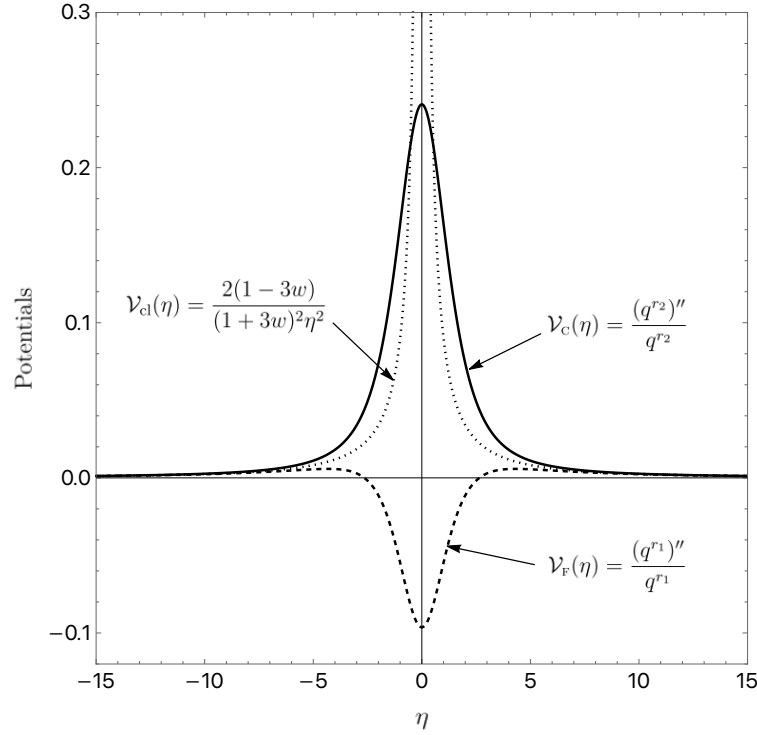


FIGURE 3.4: The gravitational potentials  $V_C$  (full line), from (3.60), and  $V_F$  (dashed line), from (3.52), as functions of the conformal time  $\eta$ ; the parameter values are chosen as  $q_B \rightarrow 1$ ,  $\omega \rightarrow 1$ ,  $\kappa_0 \rightarrow 1$  and  $w = 0.2$  for the purpose of illustration. These potentials are deduced from the quantum fluid (3.49) and conformal (3.57) Hamiltonians and the classical Hamiltonian. They all asymptotically decay as  $\eta^{-2}$  far from the bounce where they are well-approximated by their classical counterpart given by  $V_{cl} = \frac{2(1-3w)}{(1+3w)^2 \eta^2}$  (dotted line) [cf. Eq. (4.11)].

of coherent states used to approximate the background dynamics and on the values of the quantization parameters (see Eq. (3.17)). The canonical commutation rule implies the normalization condition on the mode functions

$$\dot{v}_k v_k^* - v_k \dot{v}_k^* = 2i(1+w) \left(\frac{q}{\gamma}\right)^{-2r_1} \mathfrak{M}_s = 2iZ^2 \mathfrak{M}_s. \quad (3.59)$$

After switching to the internal conformal clock, the normalization condition reads  $v_k' v_k'^* - v_k v_k'^* = 2i\mathfrak{M}_s$  and the Hamiltonian (3.57) is found to generate the following dynamics of the mode function  $v_k^c$  (the subscript “C” now indicating that its dynamics is generated by the conformal Hamiltonian)

$$\frac{d^2 v_k^c}{d\eta^2} + [\mathfrak{M}_s^2 w k^2 - \mathfrak{M}_s \mathfrak{N}_s \mathcal{V}_C(\eta)] v_k^c = 0, \quad (3.60)$$

where the potential reads

$$\mathcal{V}_C = \frac{8}{9q^2 Z^4} \frac{(2\kappa_0)^2 (1-3w)}{(1-w)^2} \left( p^2 + \frac{\hbar^2 \mathfrak{I}_s / \mathfrak{M}_s}{q^2} \right), \quad (3.61)$$

whose limit for large  $q$  yields back the classical case (3.34). This potential is shown in Fig. 4.1 for different numerical values of the relevant parameter  $\chi$  defined as  $\mathfrak{I}_s / \mathfrak{M}_s =$

$\chi\mathfrak{K}$  for later convenience. The usual Mukhanov-Sasaki equation is recovered from (3.60) provided one defines a rescaled conformal time  $\zeta$  through  $\zeta = \sqrt{\mathfrak{M}_s \mathfrak{N}_s} \eta$ , leading to

$$\frac{d^2 v_k^c}{d\zeta^2} + [k_C^2 - \mathcal{V}_c(\zeta)] v_k^c = 0, \quad (3.62)$$

as expected; in Eq. (3.62), the effective wave number is  $k_C \equiv k \sqrt{w \mathfrak{M}_s / \mathfrak{N}_s}$ .

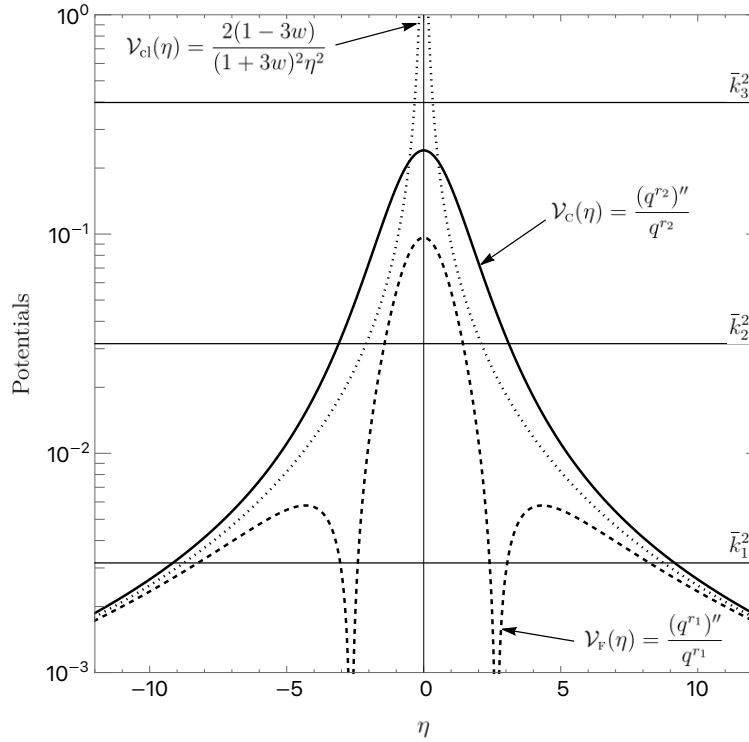


FIGURE 3.5: Same as Fig. 3.4 in logarithmic scale for the potentials, with different wave numbers  $\bar{k}$  standing for either  $k_F$  or  $k_C$  depending on the case at hand), illustrating the various possible predictions. For  $\bar{k} \sim \bar{k}_3$ , the quantum potentials is not felt by the perturbations, and only the classical potential induce a nontrivial spectrum. In the region of wavelengths around  $\bar{k} \sim \bar{k}_2$ , the perturbations enter the potentials at different points, but the characteristic behavior is more or less comparable; one would expect in this regime to have different amplitudes and even perhaps power indices, but an overall similar shape. For  $\bar{k} \sim \bar{k}_1$  on the other hand, the number of entries and exits of the perturbation in and out of the potentials  $V_F$  and  $V_C$  being different, predictions between the two models could radically differ, e.g. with superimposed oscillations changing the shape of the primordial power spectrum. A more detailed study is presented in the next chapter 4

We have seen above that  $\mathcal{V}_F = (q^{r_1})''/q^{r_1}$ . Let us see under what conditions the potential  $\mathcal{V}_C$  can also be put in a similar form  $X''/X = (q^r)''/q^r$  for a given function

$X(\eta) = q^r$  with a power  $r$  to be determined. Straightforward calculation yields

$$\begin{aligned} \frac{X''}{X} &= \frac{r}{Z^4} \left[ \frac{\ddot{q}}{q} + (r - 2r_1 - 1) \left( \frac{\dot{q}}{q} \right)^2 \right] \\ &= \frac{4(2\kappa_0)^2}{Z^4 q^2} r(r - 2r_1 - 1) \left[ p^2 + \frac{\mathfrak{K}}{(r - 2r_1 - 1)q^2} \right], \end{aligned}$$

where in the second equality we have made use of the semiquantum solution (3.23). In order to recover the classical limit (3.32), the power  $r$  should satisfy  $r(r - 2r_1 + 1) = \frac{2}{9}(1 - 3w)/(1 - w)^2$ , whose two roots happen to coincide with  $r_1$  and  $r_2$ . Setting  $r = r_1$  yields (3.53), with a negative coefficient in the  $q^{-2}$  term (we assume  $0 < w < 1$ ), as could have been anticipated. The second root  $r = r_2$  yields instead a positive coefficient in the  $q^{-2}$  term, and reproduces (3.61) only if we demand that  $w < \frac{1}{3}$  and

$$\frac{\mathfrak{T}_s}{\mathfrak{N}_s} = \frac{3\mathfrak{K}(1 - w)}{1 - 3w} \implies \mathcal{V}_C \rightarrow \frac{(q^{r_2})''}{q^{r_2}}. \quad (3.63)$$

Both conformal and fluid potentials in such familiar form are shown in Figs. 3.4 and 3.5. The above combination of semiquantum parameters (3.63) can be expressed in terms of the parameters of the family of fiducial vectors  $\mu$ , and  $\nu$  as:

$$\frac{\mathfrak{T}_s}{\mathfrak{N}_s} = \left( \frac{1}{4} + \frac{\mu + \nu}{2} \right) \exp \left[ \frac{17 - 9w}{6\mu(1 - w)} \right], \quad (3.64)$$

so that the conformal potential can be cast into the usual  $(q^{r_2})''/q^{r_2}$  form if the equation (using the expression for  $\mathfrak{K}$  below Eq. (3.22))

$$\left( \mu + \nu + \frac{1}{2} \right) \exp \left[ \frac{17 - 9w}{6\mu(1 - w)} \right] = \frac{3(1 - w)}{1 - 3w} \left[ \nu + \left( \mu + \frac{1}{2} \right) \exp \left( \frac{3}{2\mu} \right) \right] \quad (3.65)$$

has non trivial solutions for  $\mu, \nu > 0$ , which indeed it has for  $w < 1/3$  (see Appendix of [23]).

### Difference between both semiquantum perturbation theories

It is clear from (3.53) and (3.61) that the two equivalent parametrizations of the classical model induce two inequivalent quantum theories, as is clear from Figs. 3.4 and 3.5 showing a comparison of the respective gravitational potentials. The difference is perhaps even clearer when the gravitational potentials are given in the familiar form based in the configuration space and the semiclassical variable  $q$  is raised to two distinct powers, i.e.  $r_1 = \frac{3w-1}{3(1-w)}$  and  $r_2 = \frac{2}{3(1-w)}$ . In some sense these two parametrizations are exhaustive in regard to the quantization ambiguity as these are the only powers possible for theories that satisfy the classical limit, as follows from our discussion below (3.33).

The source of the ambiguity is the nonlinearity of the theory of gravity. Since the quantization concerns both the linear perturbations and the background variables, the transformation of the perturbation variables (3.27) is nonlinear (i.e., at the quantum level the transformations do not enjoy a unique unitary representation consistent with Dirac's canonical quantization rule of basic variables, that only works for simplest observables), contrary to the situation of Ref. [78], and therefore, it leads to unitarily inequivalent theories.

In our framework, the non-equivalence is responsible for the discrepancy between the two semiquantum F-potential (3.53) and C-potential (3.61). The formula

(3.40) that is used to derive the F-potential, through the Heisenberg equations of motion, is a function of  $\hat{Q}$  only. On the other hand, the C-potential comes from the expectation value of a compound observable, involving both  $\hat{Q}$  and  $\hat{P}$ , and given in (3.43). These two potentials cannot coincide because the classical relations between basic and compound observables do not apply to the expectation values of the respective operators due to the quantum uncertainty ( $\langle \mathcal{V}(\hat{Q}, \hat{P}) \rangle \neq \mathcal{V}(\langle \hat{Q} \rangle, \langle \hat{P} \rangle)$ ).

### 3.5 Brief discussion of results

In this chapter we have derived a compact cosmological model in which quantum gravitational effects play a crucial role, resolving the classical singularity to a bouncing scenario. Our model consists in general relativity coupled to a perfect fluid with constant equation of state  $p = w\rho$ . Classically, the FLRW solution starts out of or contracts to a singularity at which the scale factor  $a$  vanishes. The perturbations around such a background also generally diverge at the singularity.

By quantizing the background, factor ordering ambiguities permit to add a repulsive potential term to the zeroth order Hamiltonian, whose strength remains to be determined. Choosing the canonical ordering removes it altogether, while choosing any other ordering fixes the potential. The fact that the trajectories are nonsingular results from our definition of these trajectories as expectation values. For coherent states, that leads to Eq. (3.23). The ordering ambiguity also translates into the fact that the coefficients appearing in this equation, i.e. the minimum scale factor  $q_{\text{B}}$  and its acceleration  $\omega$  at the bounce, are free parameters which cannot be calculated from first principles, but should be constrained, ideally, from observations. In that sense, the ordering ambiguity is always present in our model and, at the perturbation level, is conveniently encoded in the free parameters  $\mathcal{L}_{\text{Q}}$ ,  $\mathcal{M}_{\text{Q}}$ ,  $\mathcal{N}_{\text{Q}}$ ,  $\mathcal{R}_{\text{Q}}$  and  $\mathcal{T}_{\text{Q}}$ .

Assuming a coherent state to describe the evolution in terms of an actual space-time, i.e. a trajectory  $a(\tau)$  for the scale factor, one can then calculate a phase space trajectory which, thanks to the quantum effective potential in the background Hamiltonian, smoothly connects the contracting and expanding solutions, avoiding the singularity in the process. Most model-building approaches would then identify these bouncing trajectories as what is commonly understood by semiclassical, and would then go on to quantize the perturbations on top, without accounting for the uncertainties of the background introduced in (3.40) or (3.43) and encoded in the quantization parameters. For instance, in the framework of cosmological perturbation theory based on inflation, plugging such a semiclassical solution into the perturbation action does not lead to any ambiguity as one then merely quantizes the perturbation modes, keeping their classical and quantum canonical transformations equivalent<sup>4</sup>. By doing so, one would then be allowed whatever canonical transformation on the perturbation variables, leading to classically and quantum mechanically indistinguishable theories<sup>5</sup>. Here however, we take seriously the quantum nature of the background time development and show that the classically harmless canonical transformations lead to unitarily inequivalent theories with potentially different physical predictions: the bouncing trajectories are semiquantum and not the typical semiclassical.

<sup>4</sup>In the sense that the transformations are kept linear, enjoying a unique unitary representation consistent with the Dirac's rule of quantization: "Poisson bracket  $\rightarrow$  Commutator", which does not apply in our theory by the quantum nature of background variables inside the compound function  $Z$  in (3.27), obstructing the quantum equivalence of the basic perturbation variables.

<sup>5</sup>The calculations we showed concern the scalar part of the perturbation, but is not restricted to it, the tensor component being also presumably affected by a similar ambiguity.

Summarizing, we found that upon quantizing the background to regularize the classical singularity, one finds two qualitatively different perturbation theories. It is important to note that had the background dynamics been given by a classical or semiclassical trajectory, singular or nonsingular, the relation between the two quantum perturbation theories would be unitary as the change of perturbation variables would be given by a linear (time-dependent) canonical transformation. However, the introduction of a background wave function and the subsequent replacement of the background variables with the respective expectation values is not equivalent to the background following an actual trajectory. One should not be misled by the existence of semiclassical trajectories in Fig. 3.2, representing in such plot expectation values of  $q = \langle \hat{Q} \rangle$  and  $p = \langle \hat{P} \rangle$  only; they cannot be assumed to provide a semiclassical dynamics, meaning that they cannot be used to determine the other expectation values that are involved in the transformation (3.27) between the two sets of perturbation variables.

To explicate the matter further, in this instance, the notion of a classical or even semiclassical spacetime in which quantum perturbations evolve needs to be replaced by a more general notion of "quantum spacetime" that violates the properties of classical geometry. The perturbation fields do not propagate in a fixed spacetime anymore, and the discrepancies between the evolutions of different perturbation variables reflect the quantumness of spacetime.

In conclusion, we showed that there exists an ambiguity in the choice of relevant basic perturbation variables over a quantum background, that might potentially lead to incompatible observational physical predictions.

# 4

## Ambiguous power spectrum in a quantum bounce

**DISCLAIMER:** The material presented in this Chapter is originally included in a paper submitted for publication in *Phys. Rev. D* (which corresponds to the reference [84]) of which I am a coauthor. Part of it was also included in my contribution to the Proceedings of the 2022 Cosmology session of the 56th Rencontres de Moriond (2022) [arXiv:2203.03924] (Ref. [64]). My contributions to this publication can be summarised as follows: I solved both analytically and numerically the dynamics of the perturbations in both parametrizations, and obtained the final amplitude spectra. I also solved the dynamics in the simplifying ansatz that involved the Dirac delta as a part of the gravitational potential in order to explain the origin of the dynamical ambiguity. I produced the plots showing the dynamics of the modes and the spectral dependence of the primordial perturbation amplitude. I participated in the discussion of the obtained results. I participated in the preparation of the paper for publication. I gave talks presenting these results (and the ones from the previous chapter) in: "56th Rencontres de Moriond 2022 – Cosmology" (La Thuile, Italy in Jan. 2022) and "NCBJ PhD Seminar 2022" (National Centre for Nuclear Research, Poland in Mar. 2022).

As found in the previous chapter, simple re-scalings of the curvature perturbation, in a Friedmann universe, by powers of the scale factor prior to quantization produce different gravitational potentials in the Mukhanov-Sasaki equation, thereby making the dynamics of the perturbation depend on the choice of the field variable employed in its quantization. This ambiguity stems from the non-classical nature of the background evolution. In the present chapter we begin the study of the physical consequences of this ambiguity, trying to identify all possible and inequivalent predictions for primordial power spectrum from a quantum bounce<sup>1</sup> [84]. If the infinitely many gravitational potentials found (depending on infinite possible values of the different semiquantum parameters) actually lead to infinitely many different physical predictions, then the theory could be considered unphysical.

---

<sup>1</sup>We find relevant to note here that we view our framework of quantum perturbation fields in quantum spacetime as a truncation (better or worse) of a full theory of quantum gravity. In order for a truncation to be consistent, it should make use of a unique internal time variable (in which the dynamics of the full theory is assumed to be naturally expressed) for quantizing and describing all dynamical variables, both for the background and the perturbations. We emphasize that our framework satisfies this requirement. Nevertheless, even if many internal time variables are available, the particular choice one makes does not seem to be crucial for the physical predictions of quantum gravity (since this is not a topic of this thesis, we refer the interested reader to some works devoted to this issue [85–88]).

We explore whether the primordial power spectrum described previously in the literature [13, 14, 27, 77] constitutes the only possible solution in a bouncing cosmology. We find it important to seek other possibilities because, according to the present knowledge, the simplest quantum bouncing cosmologies produce blue-tilted power spectrum contrary to inflationary predictions and observational results.

In this context, we pose the natural question of whether the Mukhanov variable remains a preferred choice for describing scalar perturbations in a fuller, more quantum description of the primordial universe or perhaps it should be replaced with another, better-suited, variable. In inflationary models it is convenient to use the Mukhanov variable because it allows to asymptotically define a quantum vacuum in the same way as for flat spacetime. However, it is not the only possible choice for the perturbation variables even in the context of inflation as discussed, e.g., in [67]. In a fully quantum universe, the issue is even less clear as the choice of perturbation variables can influence both the definition of the initial state as well as its dynamics. Similarly, in late universe, with completely classical description, one usually finds it more suitable to employ the Bardeen potential, rather than the Mukhanov variable that actually becomes singular, i.e., it blows up, in a matter-dominated universe.

## 4.1 The ambiguity

The perturbation mode functions of the both semiquantum models presented in the previous chapter (3.4.1 and 3.4.2) follow a dynamical law in the form of Mukhanov-Sasaki equation (for the generic label  $s = F$  or  $C$ ):

$$\frac{d\tilde{\sigma}_k^s}{d\eta^2} + (k_s^2 - \mathcal{V}_s) \tilde{\sigma}_k^s = 0, \quad (4.1)$$

up to redefinitions of time and wavenumber, the latter taking as possible values:  $k_F = \sqrt{w}\mathfrak{L}_s k$  and  $k_C = \sqrt{w}\mathfrak{M}_s\mathfrak{N}_s k$ . The two potentials for each semiquantum theory read (assuming  $\hbar = 1$ ):

$$\mathcal{V}_F = \frac{8(2\kappa_0)^2(1-3w)}{9(1-w^2)^2q^2} \left(\frac{q}{\gamma}\right)^{-4r_1} \left(p^2 - \frac{3(1-w)\mathfrak{K}}{2q^2}\right), \quad (4.2a)$$

$$\mathcal{V}_C = \frac{8(2\kappa_0)^2(1-3w)}{9(1-w^2)^2q^2} \left(\frac{q}{\gamma}\right)^{-4r_1} \left(p^2 + \frac{\mathfrak{T}_s/\mathfrak{N}_s}{q^2}\right), \quad (4.2b)$$

They differ in the numerical coefficient of the last term  $\propto q^{-2}$ , namely  $\mathfrak{T}_s/\mathfrak{N}_s$  in (4.2b) and  $-\frac{3}{2}(1-w)\mathfrak{K}$  in (4.2a) with  $\mathfrak{K} > 0$ . Setting the coefficient of conformal parametrization to  $\chi\mathfrak{K}$  defines the (free) ambiguity parameter:

$$\chi = \frac{\mathfrak{T}_s}{\mathfrak{N}_s\mathfrak{K}}, \quad (4.3)$$

and the Fluid parametrization results when the combination of the free semiquantum parameters defining  $\chi$  takes the exact value:

$$\chi_F := -\frac{3}{2}(1-w) \quad (4.4)$$

which is always negative as  $w < 1$ . Then, we write the generic potential as

$$\mathcal{V}_\chi = \frac{8(2\kappa_0)^2(1-3w)}{9(1-w^2)^2q^2} \left(\frac{q}{\gamma}\right)^{-4r_1} \left(p^2 + \frac{\chi\mathfrak{K}}{q^2}\right), \quad (4.5)$$

which, upon using the background solution (3.23) and expressing  $\mathfrak{K}$  and  $H_{\text{sem}}$  in terms of  $q_B$ ,  $\omega$  and  $\kappa_0$ , namely

$$\mathfrak{K} = \frac{q_B^4\omega^2}{16\kappa_0^2} \quad \text{and} \quad H_{\text{sem}} = \frac{q_B^2\omega^2}{8\kappa_0}, \quad (4.6)$$

becomes

$$\mathcal{V}_\chi = \frac{2\omega^2}{9Z^4} \frac{1-3w}{(1-w)^2} \frac{\chi + (\omega\tau)^2}{[1 + (\omega\tau)^2]^2}, \quad (4.7)$$

with (recalling Eq. (3.3))

$$Z = \sqrt{1+w} \left(\frac{q}{\gamma}\right)^{r_1}, \quad (4.8)$$

As it was previously shown, there are two special values for  $\chi$ , namely  $\chi = \chi_F$  for which the potential is  $\mathcal{V}_F = (q^{r_F})''/q^{r_F}$ , and

$$\chi = \chi_C := \frac{3(1-w)}{(1-3w)}, \quad (4.9)$$

leading to  $\mathcal{V}_C = (q^{r_C})''/q^{r_C}$ , where now, due to the power law in the familiar form of the potential for each parametrization (3.55) (3.63), we rename such power laws (3.6) as:

$$r_F = r_1 = \frac{3w-1}{3(1-w)}, \quad \text{and} \quad r_C = r_2 = 1 + r_F = \frac{2}{3(1-w)}. \quad (4.10)$$

implying  $\frac{2}{3} \leq r_C \leq 1$  with  $0 \leq w \leq \frac{1}{3}$ . From now on, the latter will be the range of the barotropic index we are concerned with. It can be argued that these values, naturally reproducing the degenerate classical case

$$\mathcal{V}_{\text{cl}} = \frac{(q_{\text{cl}}^{r_F})''}{q_{\text{cl}}^{r_F}} = \frac{(q_{\text{cl}}^{r_C})''}{q_{\text{cl}}^{r_C}} = \frac{2(1-3w)}{(1+3w)^2\eta^2}, \quad (4.11)$$

with  $q_{\text{cl}}$  and  $p_{\text{cl}}$  the classical solutions (2.28), are the only physically acceptable ones. This argument is reinforced by the fact that  $\chi_F$  and  $\chi_C$  imply the potential to depend only on the background quantities  $w$  and  $\mathfrak{K}$ , in agreement with the idea of perturbation theory. We shall however in what follows assume that  $\chi$  is an arbitrary real parameter and restrict attention to these particular cases whenever necessary. Fig 4.1 shows such possible cases, including the situations  $\chi < \chi_F = -1/r_C$  and  $\chi > \chi_C = -1/r_F$ , illustrating that these extreme points do not lead to anything particular in the shape of the potential apart from the fact that they permit a simple writing of it. In fact, in the large time limit  $\omega\tau \gg 1$ , the term in  $\chi$  in (4.7) is in any way negligible and it can be checked explicitly that the classical case (4.11) is also recovered for any value of  $\chi$ .

One can also note that the potential  $\mathcal{V}_\chi$  in (4.7) can be given a simple form for an arbitrary  $\chi$ , namely

$$\mathcal{V}_\chi = \alpha_\chi^2 \frac{(q^{r_\chi})''}{q^{r_\chi}}, \quad (4.12)$$



which is entirely fixed once the barotropic index of the equation of state  $w$  and the background solution (3.23) are known. On the other hand, the conformal case depends on  $\chi = \mathfrak{T}_s/(\mathfrak{N}_s\mathfrak{K})$ , which is not fixed by the background but rather by the quantization procedure, with the special case  $\chi = \chi_c = \frac{3(1-w)}{1-3w} > 0$  again fixed by the equation of state. Therefore, the first question to address concerns the sign of  $\chi$  and its numerical value.

## 4.2 Spectral indices of the semiquantum models

After having described the ambiguity in the equation of motion, let us now solve the quantum dynamics of the perturbation modes, which we do first numerically and then analytically. We investigate the amplitude of the perturbations as a function of time for various wavenumbers  $k$ , and focus on its dependency on the free parameter of the conformal parametrization  $\chi$ , with the generic form of the potential (4.5).

We shall work in the Heisenberg picture of dynamics and assume the perturbations to be in a fixed vacuum state that is the ground state that minimizes the quantum Hamiltonian (3.49) or (3.57) for all modes of interest in the large contracting universe ( $\eta \rightarrow -\infty$ ). It can be shown [80] that in order for the vacuum state to be the ground state of the quantum Hamiltonians in the infinite past  $\tau, \eta \rightarrow -\infty$ , the mode functions have to satisfy (up to irrelevant phase), respectively

$$v_k^\chi|_{\eta_{\text{ini}}} = \frac{1}{\sqrt{2k_\chi}} \quad \text{and} \quad \frac{dv_k^\chi}{d\eta}|_{\eta_{\text{ini}}} = i\sqrt{\frac{k_\chi}{2}}, \quad (4.13)$$

where we used the vanishing of the gravitational potential in the infinite past<sup>2</sup>. Equipped with the initial conditions (4.13), we now proceed to solve the mode equation (4.1) only for the two special cases  $r_\chi = r_c$  ( $\chi = \chi_c$ ) and  $r_\chi = r_F$  ( $\chi = \chi_F$ ). In following sections we complement such solution with an analysis for an arbitrary value of  $\chi$ .

### 4.2.1 Numerical integration

Since the potential  $\mathcal{V}_\chi$  is known explicitly as a function of the internal time  $\tau$  as shown in Eq. (4.7), it turns out to be technically more tractable to switch back to  $\tau$  to solve Eq. (4.1), even though, for the sake of clarity, we plot the results in terms of the conformal time, substituting the numerical value for  $\tau(\eta)$  in the solution. Given the relationship (3.2) between both times, we have  $d/d\eta = Z^{-2}d/d\tau$  and therefore

$$\frac{d^2}{d\eta^2} = \frac{1}{Z^4} \frac{d^2}{d\tau^2} - \frac{1}{Z^6} \frac{dZ^2}{d\tau} \frac{d}{d\tau}, \quad (4.14)$$

<sup>2</sup>The initial conditions of Eq. (4.13), are, strictly speaking, approximate in the general situation. In the fluid parameterization for instance, the time derivative should read

$$\frac{dv_k^F}{d\eta} = i\sqrt{\frac{k_F}{2}} - \frac{1}{(1+w)\sqrt{2k_F}} \frac{1}{q^{-r_F}} \frac{d(q^{-r_F})}{d\eta},$$

the second term originating from the fact that it is the field  $\phi$  rather than  $v$  that is quantized in this case. As initial conditions are set for  $|\tau| \gg 1$ , one can there use the asymptotic behaviors  $\dot{q}/q \sim \tau^{-1}$  and  $\eta \sim \tau^{r_F+r_c}$ , (see Ref. [23]) to write the extra term in the time derivative of  $v_k^F$  as  $(3w-1)/[(1+w)(1+3w)\sqrt{k_F}\eta]$ : setting initial conditions sufficiently deep into the contracting phase ( $\eta < 0$  and  $|\eta| \gg 1$ ) then permits to neglect such a term for all parameterizations.

so that the perturbation equation of motion for the Mukhanov-Sasaki variable, namely

$$\frac{d^2 v_k^\chi}{d\eta^2} + [k^2 - \mathcal{V}_\chi(\eta)] v_k^\chi = 0, \quad (4.15)$$

reads, plugging the semiquantum solution (3.23) for the generic  $\chi$ -parametrization (with  $\chi = \text{F}$  or  $\text{C}$ ).

$$\frac{d^2 v_k^\chi}{dx^2} - \frac{2r_{\text{F}\chi}}{1+x^2} \frac{dv_k^\chi}{dx} + \left[ \left( \frac{q_{\text{B}}}{\gamma} \sqrt{1+x^2} \right)^{4r_{\text{F}}} (1+w)^2 \tilde{k}_\chi^2 - \frac{2\omega^2(1-3w)}{9(1-w)^2} \frac{\chi+x^2}{(1+x^2)^2} \right] v_k^\chi = 0, \quad (4.16)$$

where  $k_\chi$  denote the wavenumber in the respective parametrizations, and we set  $\tilde{k}_\chi := k_\chi/\omega$  as well as  $x := \omega\tau$ . This solution is valid for any arbitrary value of  $\chi$ , however in this section we show the results only for the two special cases  $\chi = \{\chi_{\text{F}}, \chi_{\text{C}}\}$ , since the later presented analytical solution is only available for such values. In what follows, we drop the index  $\chi$  both for the mode function and the wavenumber as there is no risk of confusion; we will restore the index when we specify the calculation for the fluid or conformal parametrization (with  $\chi = \chi_{\text{C}}$  only in the latter).

Once the initial conditions (4.13) are similarly expressed in terms of the fluid time  $\tau$ , the numerical integration of the above equations allows to follow the dynamics of the amplitude of curvature perturbations (we follow the convention of Ref. [89], up to a normalisation factor  $= \sqrt{\mathcal{V}_0}/(2\pi)$  which we merely set to unity),

$$\delta[k, \tau(\eta)] = \frac{|v_k|}{a} k^{3/2} = k^{3/2} |v_k| \left( \frac{q}{\gamma} \right)^{-r_{\text{C}}}, \quad (4.17)$$

where we made use of the definition (2.19) of the scale factor  $a$  in terms of the variable  $q$ . We focus in this section to the special cases  $\chi = \chi_{\text{F}}$  and  $\chi = \chi_{\text{C}}$ .

Although the amplitude is dynamical, it reaches a plateau right after the bounce when the perturbations have been amplified, and thus remains roughly constant for a significant fraction of its period; this corresponds to the constant (or growing) mode when the perturbation is dominated by the potential. This is illustrated in Fig. 4.2, where the dynamics of the amplitude of a selected mode in both parametrizations and for three different barotropic indices  $w$ . This constant value of the amplitude right after the bounce is called the primordial amplitude, and we shall study its dependence on the wavenumber  $k$ .

We have solved the perturbation equations for many values of  $k$ , both and calculated their primordial amplitude at the time of potential-crossing (also called ‘exit’ time)  $\eta_{\text{cross}}$  (or simply  $\eta_{\text{C}}$ ) at which the mode exits the potential, i.e. for which  $\mathcal{V}(\eta_{\text{C}}) = k^2$ . The mode evolution shown in Fig. 4.2 yields the full spectrum, plotted in Fig. 4.3. One finds two different power laws for the two different parametrizations, as expected, thereby emphasizing the ambiguity at the physical prediction level. Our analytic estimates below for the spectral indices represent very accurate fits for the numerics.

## 4.2.2 Analytical Integration

We now follow the calculation made in [13] for the case of tensor perturbations, transcribed to the scalar modes, consisting in setting a piecewise approximation to

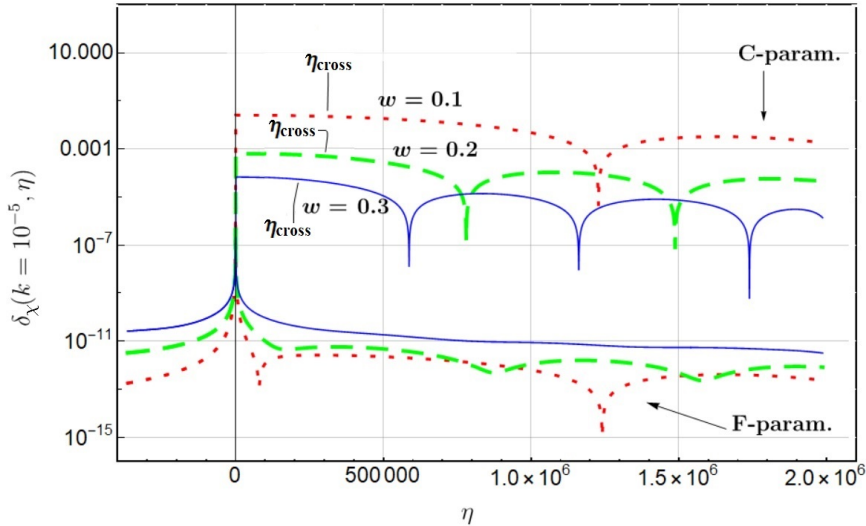


FIGURE 4.2: Conformal time development of the perturbation amplitude (4.17) for the mode  $k = 10^{-5}$  and three different barotropic indices, namely  $w = 0.1$  (dotted),  $w = 0.2$  (dashed), and  $w = 0.3$  (solid). Both parametrizations, fluid (bottom,  $\chi = \chi_F$ ) and conformal (top, for  $\chi = \chi_C$ ), are shown. Also indicated is the time  $\eta_{\text{cross}}$  at which the mode exits the potential, i.e. for which  $\mathcal{V}(\eta_{\text{cross}}) = k^2$ . Here and in the following figures, the background parameters used are fixed by setting  $\kappa_0 \rightarrow 1$ ,  $H_{\text{sem}} = 2^{1+w}$  and  $\mathfrak{R} = 100$  in (3.23).

the solution of our general differential equation

$$\frac{d^2 v_k}{d\eta^2} + \left[ k^2 - \frac{(q^r)''}{q^r} \right] v_k = 0, \quad (4.18)$$

where we set  $\alpha^2 \rightarrow 1$  as we are only interested in the solution for  $r = r_F$  and  $r = r_C$ . We begin by noticing that long before the bounce, at times for which the modes propagate freely, i.e. when  $k^2 \gg |\mathcal{V}|$ , the potential is well approximated by its classical counterpart (4.11). In this regime, the modes are given by

$$v_k(\eta) = \sqrt{-\eta} \left[ c_1 H_\nu^{(1)}(-k\eta) + c_2 H_\nu^{(2)}(-k\eta) \right], \quad (4.19)$$

where  $\nu = \frac{3(1-w)}{2(1+3w)}$  and  $H_\nu^{(1,2)}$  are the Hankel functions of the first and second kinds; the minus signs appearing in (4.19) account for the fact that  $\eta < 0$  in the contracting phase. Since, for  $(-k\eta) \gg 1$ , one has the asymptotic relations  $H_\nu^{(1)}(-k\eta) \sim \sqrt{\frac{-2}{k\eta\pi}} e^{-i[k\eta + (\nu + \frac{1}{2})]}$  and  $H_\nu^{(2)}(-k\eta) \sim \sqrt{\frac{-2}{k\eta\pi}} e^{i[k\eta + (\nu + \frac{1}{2})]}$ , the initial conditions (4.13) that impose the Bunch-Davies vacuum yield  $c_1 = 0$  and  $c_2 = \sqrt{\pi/2} e^{-i\frac{\pi}{2}(\nu + \frac{1}{2})}$ . This implies that at the time  $\eta_{\text{ini}} = -\eta_{\text{cross}}$  of the potential crossing  $k^2 = \mathcal{V}(\eta_{\text{cross}})$ , namely

$$\eta_{\text{cross}} = \frac{\sqrt{2(1-3w)}}{(1+3w)k} =: \frac{x_w}{k}, \quad (4.20)$$

thereby defining the dimensionless variable  $x_w$  depending only on the barotropic index  $w$ , the initial conditions for the following potential domination era read

$$v_k(\eta_{\text{in}}) = \frac{C}{\sqrt{k}} \quad \text{and} \quad v'_k(\eta_{\text{in}}) = D\sqrt{k}, \quad (4.21)$$

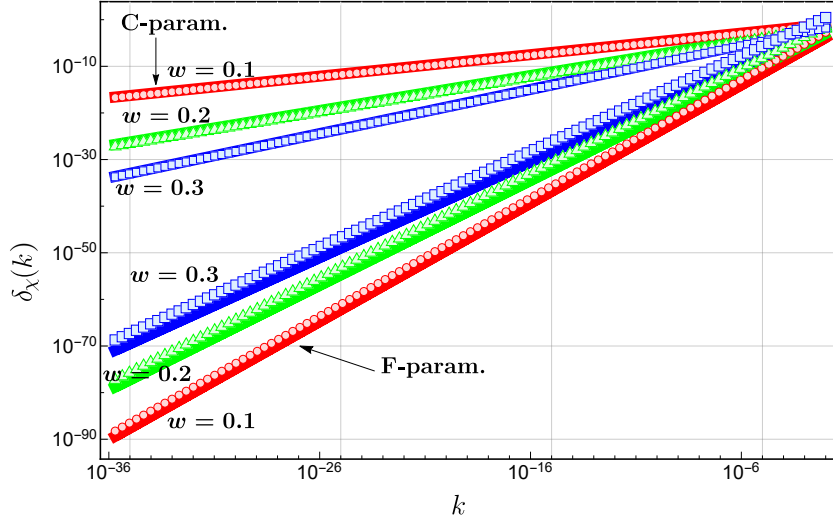


FIGURE 4.3: Primordial density fluctuation power spectrum  $\delta[k, \tau(\eta_{\text{cross}})]$  measured at the crossing time  $\eta_{\text{cross}}$  defined in (4.20) and shown in Fig. 4.2. Both the fluid F–(bottom) and the conformal (for  $\chi = \chi_C$ ) C–(top) parametrizations are displayed for three different fluids as in Fig. 4.2, namely  $w = 0.1$  (circles),  $w = 0.2$  (triangles) and  $w = 0.3$  (squares). The approximate analytical solutions [Eqs. (4.38) and (4.37) below] are shown as superimposed solid lines for each numerical calculation, exemplifying the validity of the approximation.

where

$$C = c_2 \sqrt{x_w} H_v^{(2)}(x_w) \quad (4.22)$$

and

$$D = \frac{c_2}{2} \left\{ \frac{H_v^{(2)}(x_w)}{\sqrt{x_w}} + \sqrt{x_w} \left[ H_{v-1}^{(2)}(x_w) - H_{v+1}^{(2)}(x_w) \right] \right\}. \quad (4.23)$$

From the potential crossing conformal time  $\eta_{\text{cross}}$ , one can derive the fluid time  $\tau_{\text{cross}}$ , which depends on the wavenumber  $k$  of a given mode. In the classical approximation, i.e. assuming this crossing takes place in a regime for which the potential is well approximated by the classical potential (4.11), one finds

$$x_{\text{cross}} = \omega \tau_{\text{cross}} = \left( \frac{q_B}{\gamma} \right)^{\frac{2(1-3w)}{1+3w}} \left[ \frac{k}{\omega f(w)} \right]^{-\frac{3(1-w)}{1+3w}}, \quad (4.24)$$

where  $f(w) = \sqrt{2(1-3w)}/[3(1-w^2)]$ .

Once a given mode crosses the potential, we assume the potential to instantaneously take over the dynamics of the perturbations, so that (4.18) becomes (zeroth-order in  $k$ ):

$$\frac{d^2 v_k}{d\eta^2} - \frac{(q^r)''}{q^r} v_k = 0, \quad (4.25)$$

whose general solution is found to be

$$v_k = [q(\eta)]^r \left\{ A^\chi + B^\chi \int^\eta d\tilde{\eta} [q(\tilde{\eta})]^{-2r} \right\}, \quad (4.26)$$

where  $A^\chi$  and  $B^\chi$  are integration constants, later to depend on  $k$  because of the matching with initial conditions.

In order to use the solution (4.26), one needs to express the background motion  $q$  given by (3.23) as a function of the conformal time  $\eta$ . It turns out that Eq. (3.2) can be integrated to yield

$$\eta = (1+w) \left( \frac{q_B}{\gamma} \right)^{2r_F} \tau \mathcal{F} \left[ \frac{1}{2}, -r_F; \frac{3}{2}; -(\omega\tau)^2 \right],$$

with  $\mathcal{F}$  an hypergeometric function (see Ref. [23] for details). We can perform the integrals in fluid time using the relation (3.2) and obtain the solutions in terms of  $\tau$ , absorbing the choice of the initial time  $\eta_0$  into the constants

$$v_k = \left( \frac{q}{\gamma} \right)^r \left\{ A_k^\chi + \omega\tau \mathcal{F} \left[ \frac{1}{2}, r - r_F; \frac{3}{2}; -(\omega\tau)^2 \right] B_k^\chi \right\}, \quad (4.27)$$

where

$$A_k^\chi = A^\chi \quad \text{and} \quad B_k^\chi = \frac{B^\chi}{\omega(1+w)} \left( \frac{q_B}{\gamma} \right)^{2(r-r_F)}$$

are unknown functions of the wavenumber  $k$ .

The solution (4.27) is valid for the special cases of both the above parametrizations and, setting  $r \rightarrow r_F$  (recovering fluid) or  $r \rightarrow r_C = 1 + r_F$  (within conformal) yields

$$v_k^F = \left( \frac{q}{\gamma} \right)^{r_F} (A_k^F + B_k^F \tau) \quad (4.28)$$

and

$$v_k^C = \left( \frac{q}{\gamma} \right)^{r_C} [A_k^C + B_k^C \arctan(\omega\tau)]. \quad (4.29)$$

Given the form (4.17) of the amplitude of curvature perturbations, one needs to evaluate  $(q/\gamma)^{-r_C} |v_k|$  in the large time limit  $|\tau| \gg 1$ , which yields

$$\begin{aligned} \delta \propto & \left[ A_k^\chi \pm \frac{\sqrt{\pi} \Gamma(r - r_F - \frac{1}{2})}{2 \Gamma(r - r_F)} B_k^\chi \right] |\omega\tau|^{r-r_C} \\ & + B_k^\chi \frac{e^{-2i\pi(r-r_F)}}{1 - 2(r - r_F)} |\omega\tau|^{r_F-r}, \end{aligned} \quad (4.30)$$

in which the  $\pm$  sign in the first line corresponds to the sign of  $\tau$ . One notes that for the values of interest  $r = r_F$  and  $r = r_C$ , this amplitude reads (recall  $r_C - r_F = 1$ )

$$\delta_F = \delta(r_F) \propto \frac{A_k^F}{|\omega\tau|} + B_k^F, \quad (4.31)$$

and

$$\delta_C = \delta(r_C) \propto \left( A_k^C \pm \frac{\pi}{2} B_k^C \right) - \frac{B_k^C}{|\omega\tau|}. \quad (4.32)$$

These two distinct solutions both exhibit a constant mode and a decaying one, and therefore provide a constant amplitude for the primordial spectrum.

As we assume  $w < 1/3$ , the potential (4.7) is positive definite for  $\chi > 0$  with a maximum at  $\eta = 0$ . For  $\chi < 0$  on the other hand, this potential has two positive maxima and a negative minimum at  $\eta = 0$ , so that the modes cross the potential at

four different times (see Fig. 4.1). Given the symmetry of  $V_\chi(\eta)$ , the relevant modes enter the potential for the first time at  $\eta_{\text{in}} = -\eta_c$  and exit for the last time at  $\eta_{\text{out}} = \eta_c$  in regions where it behaves classically (i.e. for  $|\omega\tau| \ll 1$ ). Fig. 4.1 also shows that for a range of values of  $r$ , including in particular the fluid parametrization, the modes also exit and re-enter the potential another time between those points, when quantum corrections cannot be neglected. Due to the shape of the potential, there exist short periods of time during which the value of  $k$  dominates over the value of  $V_\chi(\eta)$ , i.e. in the neighbourhoods of  $\pm\eta_0$  defined by  $V_\chi(\pm\eta_0) = 0$ . It turns out the potential is rather steep close to those points, with a high negative slope when the modes exit and a high positive slope when they re-enter later. For the large wavelengths relevant to the cosmological framework, this time interval is sufficiently small that the approximation, assumed in what follows, of neglecting it altogether, holds. It should be mentioned however that in that case, the potential becoming negative, the behaviors of the modes may be quite different; we shall see below how this should be taken care of.

Combining the matching conditions (4.21) at the time (4.24) with the potential-domination solutions (4.28) and (4.29) yields the coefficients  $A^F$ ,  $A^C$ ,  $B^F$ , and  $B^C$  as functions of  $k$ . To leading order in  $k \ll 1$ , one gets

$$A_k^F = \left( \frac{q_B \omega f}{\gamma} \right)^{\frac{1-3w}{1+3w}} [r_C C + (1+w)fD] k^{-\frac{3(1-w)}{2(1+3w)}} \quad (4.33)$$

and

$$B_k^F = f \left( \frac{q_B \omega f}{\gamma} \right)^{-\frac{1-3w}{1+3w}} [r_F C + (1+w)fD] k^{\frac{3(1-w)}{2(1+3w)}} \quad (4.34)$$

We note that  $A_k^F$  and  $B_k^F$  have inverse  $k$  dependence, so that, in the large wavelength limit,  $A_k^F \gg B_k^F$ . For the conformal case, one finds

$$A_k^C = \frac{\pi}{2} B_k^C + C \left( \frac{q_B}{\gamma} \right)^{-\frac{2}{1+3w}} k^{\frac{3(1-w)}{2(1+3w)}} \quad (4.35)$$

and  $B_k^C = \gamma A_k^F / q_B$ , relations that can also be obtained just by equating (4.28) and (4.29) and their derivatives at the matching point; we kept the subdominant term in  $B_k^C$  in (4.35) for further convenience.

The last step consists in substituting the above expressions into the primordial amplitude spectrum (4.17), keeping the highest order terms in  $k \ll 1$ , assuming  $0 \leq w \leq \frac{1}{3}$ . This yields

$$\delta_\chi(k) = A(w, \chi) \omega f \left( \frac{k}{\omega f} \right)^{n(w, \chi)} \quad (4.36)$$

where the amplitudes

$$A(w, \chi_F) = \left( \frac{q_B}{\gamma} \right)^{-\frac{2}{1+3w}} |(r_F + r_C) C + 2(1+w)fD| \quad (4.37)$$

and

$$A(w, \chi_C) = \pi \left( \frac{q_B}{\gamma} \right)^{-\frac{6w}{1+3w}} |r_C C + (1+w)fD| \quad (4.38)$$

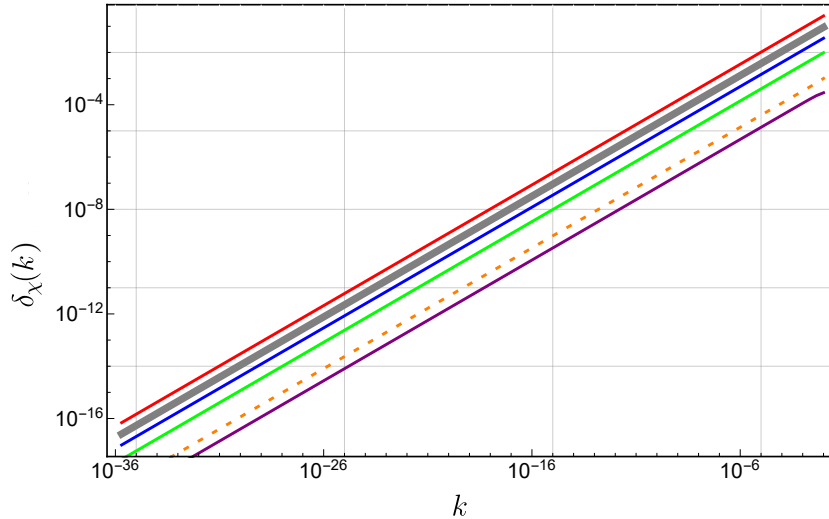


FIGURE 4.4: Numerical primordial amplitude power spectrum at the crossing point for  $w = 0.1$  and various values of  $\chi$ ; in that case,  $\chi_F = -1.35$  and  $\chi_C \simeq 3.86$ . From top to bottom:  $\chi = 9$ ,  $\chi = \chi_C$  (thick line),  $\chi = 2$ ,  $\chi = -0.1$ ,  $\chi = -1.5$  (dashed), and  $\chi = -1.3$ . This illustrates the fact that although the amplitude depends on  $\chi$ , the index remains given by (4.40) provided  $\chi \neq \chi_F$  (not shown). For  $\chi > \chi_F$ , the conformal amplitude is seen to decrease as  $\chi \rightarrow \chi_F$ . It increases again for  $\chi < \chi_F$  (the dashed line).

as well as the spectral indices

$$n(w, \chi_F) = \frac{3(1+w)}{1+3w}, \quad (4.39)$$

and

$$n(w, \chi_C) = \frac{6w}{1+3w}, \quad (4.40)$$

differ to yield effectively distinguishable predictions: the power spectrum being the square of the fractional energy density, i.e.  $\mathcal{P}_S(k) = \delta_\chi^2 \propto k^{n_S-1}$ , one finds two different power indices, namely that given by the fluid parametrization  $n_S^F - 1 = 6(1+w_F)/(1+3w_F)$  (i.e.  $w_F \sim -0.988$  to agree with the CMB Planck data [48]), and  $n_S^C - 1 = 12w_C/(1+3w_C)$  for the conformal one (i.e.  $w_C \sim -2.9 \times 10^{-3}$ ); it is the latter expression which is usually assumed [14]. Fig. 4.3 shows, for various values of the equation of state parameter  $w$ , by superimposing the results, that the predicted spectra (4.37) and (4.38), agree with the numerical calculation.

### 4.3 A tale of two indices

Solving Eq. (4.15) analytically for arbitrary values of  $\chi$  is not possible because of the parameter  $\alpha_\chi$  in (4.12), as it is only for  $\alpha_\chi = 1$ , i.e. for  $\chi \in \{\chi_F, \chi_C\}$ , that the analytic solutions (4.26) are valid. Given that this parameter comes from the quantization process and is thus seemingly arbitrary, one may reasonably worry that the spectral index of scalar perturbations might depend on its exact value, the theory therefore losing its predictive power. Indeed, for the two values for which one can solve the

mode equation, one already obtains an ambiguity as the two spectral indices (4.39) and (4.40) are both possible predictions.

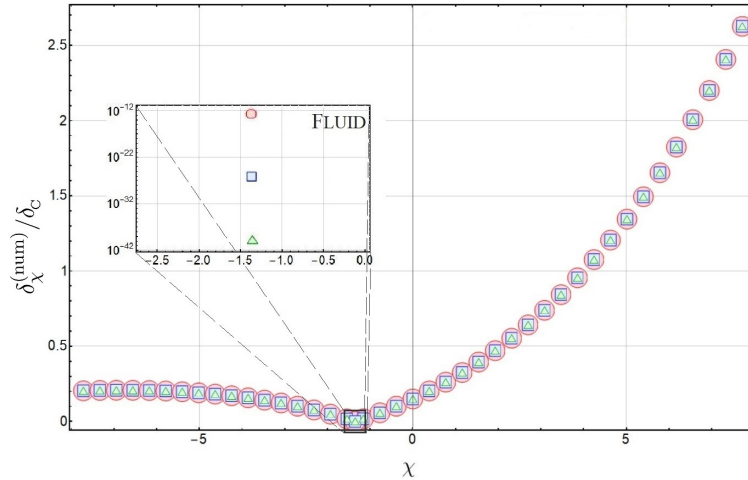


FIGURE 4.5: Ratio  $\delta_\chi^{(\text{num})}/\delta_C$  between the numerical primordial amplitude power spectrum with its analytic counterpart of the conformal parametrization given by Eq. (4.36) for  $\chi = \chi_C$ , as a function of  $\chi$  for  $w = 0.1$  and three different modes, namely  $k_C = 10^{-15}$  (circles),  $k_C = 10^{-25}$  (squares) and  $k = 10^{-35}$  (triangles). The coincidence of the three curves for all values of  $\chi$  expect  $\chi_F$  indicates that the spectral index is indeed  $n_S^C$  given by (4.40) and independent of  $\chi$ . At  $\chi = \chi_F = -1.35$ , the zoom shows three distinct points, exhibiting that the spectral index differs, being then given by (4.39).

### 4.3.1 Numerical facts

Fig. 4.4 shows the fluctuation  $\delta$  as a function of the wavenumber  $k$  for various values of  $\chi$ . One immediately notices that although the amplitude depends on  $\chi$ , decreasing with  $\chi$  until  $\chi_F$  and then increasing again for  $\chi < \chi_F$ , we obtain the same power law for the spectral index that in the special case  $\chi = \chi_C$  (4.40) for all the possible values that  $\chi$  can take within the conformal parametrization in its generic form (4.5). In order to clarify this point, we plot, in Fig. 4.5, the ratio between the numerical spectrum obtained from (4.16) for whatever value of  $\chi$  the generic parametrization can take and that provided by our analytical approximation (4.36) for  $\chi = \chi_C$ . This plot is but an example for a given value of  $w$ , we recovered the same generic image for all values we investigated.

What is also seen in Fig. 4.5 is a generalisation of Fig. 4.4, namely that the spectral index of scalar perturbations is generically given by (4.40) expect in the case of  $\chi = \chi_F$ . That is a very curious situation given the fact that this value, as explained before and seen in Fig. 4.1, do not lead to anything particular in the shape of the potential compared to other values  $\chi < 0$ . The fluid parametrization thus corresponds to the minimum amplitude possible and a different scalar index. In fact, we find that it is understood as the situation in which the conformal amplitude merely vanishes, leading to the subdominant fluid amplitude being the only one, thereby dominating the full spectrum.

We tested this hypothesis by calculating the spectrum as a function of the wavenumber for various values of  $\chi$  close to the fluid case  $\chi_F$ . The result is illustrated in Fig. 4.6 in which the power spectrum is calculated numerically for a value

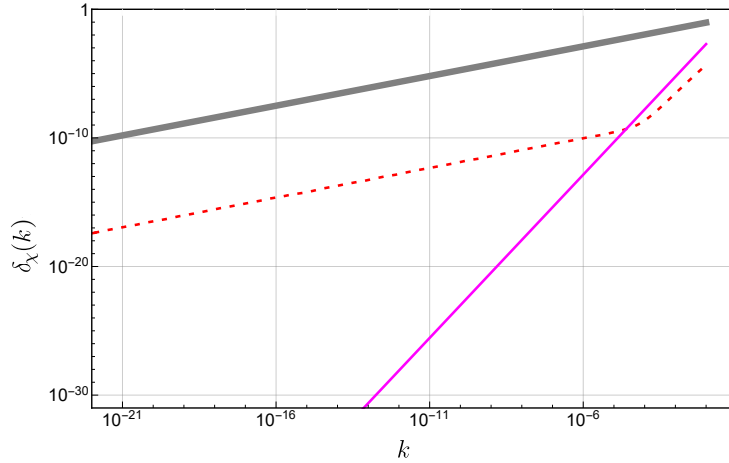


FIGURE 4.6: Primordial density fluctuation spectrum for  $w = 0.1$ : the conformal param. for the case (4.38)  $\chi = \chi_C = 3.86$  is shown as the thick line above, and the fluid case  $\chi = \chi_F$  as the thin bottom line. The dashed line represents a case close to the Fluid case with  $\chi = \chi_F - 10^{-6}$ .

of the parameter  $\chi$  very close to  $\chi_F$ , superimposed with the analytic solutions for the conformal and the fluid cases. It can be seen that the full spectrum somehow interpolates between both cases, following the fluid power law for large wavenumbers and the conformal power law for smaller wavenumbers. This suggests that the full spectrum contains both power law terms, the amplitude depending on  $(\chi - \chi_F)$  for (4.40): as both power laws are positive, when  $k$  decreases, the contribution due to  $n_S^F$  becomes smaller compared to that due to  $n_S^C$ , so the latter finally dominates entirely for very small wavenumbers.

### 4.3.2 A sharp transition

A better understanding of the numerical results of the previous section can be achieved by investigating more closely the potential (4.7) seen as a function of time and  $\chi$ .

Let us first assume that the reference value for  $\chi$  is given by the conformal one in the special case  $\chi_C$ . The potential for any value of  $\chi$  can be written as  $V_\chi = V_C + \delta V$ , where

$$\delta V = \frac{2\omega^2}{9Z^4} \frac{1-3w}{(1-w)^2} \delta\chi \left[1 + (\omega\tau)^2\right]^{-2} \quad (4.41)$$

and  $\delta\chi = \chi - \chi_C$ . Plugging the definition of  $Z$  and looking at the large time limit of the full potential, one finds that  $\delta V|_{\omega\tau \gg 1} \ll V_\chi|_{\omega\tau \gg 1}$ , so that the main contribution of  $\delta V$  is around the bounce time, namely around  $\tau = 0$ . As a function of  $\tau$ , one indeed finds

$$\delta V = \frac{2\omega^2}{9(1+w)^2} \left(\frac{q_B}{\gamma}\right)^{-4r_F} \frac{1-3w}{(1-w)^2} \delta\chi \left[1 + (\omega\tau)^2\right]^{-2r_C}. \quad (4.42)$$

Since we focus on the cases  $0 \leq w \leq \frac{1}{3}$ , one has  $\frac{2}{3} \leq r_C \leq 1$ , so that, compared to  $V_C$ , one can approximate  $\delta V$  as though its contribution is localized entirely at the bounce, i.e. we replace  $\delta V$  by

$$\delta V_{\text{approx}} = Y\delta(\eta), \quad (4.43)$$

where we assume the coefficient  $Y$  takes the form

$$Y = \omega \int_{-\infty}^{\infty} \delta V d\eta,$$

with  $\omega = \omega(w)$  parametrizing the fixed "depth" of the approximate delta that should be of order unity (we shall evaluate it below) to preserve  $V_\chi \simeq V_C + V_{\text{approx}}$ . The integral can be calculated to yield

$$Y = \frac{2\sqrt{\pi}\omega(1-3w)}{9(1+w)(1-w)^2} \left(\frac{q_B}{\gamma}\right)^{-2r_F} \frac{\Gamma(r_C + \frac{1}{2})}{\Gamma(r_C + 1)} \omega(w)\delta\chi, \quad (4.44)$$

transforming Eq. (4.25) into

$$\frac{d^2 v_k}{d\eta^2} - \left[ \frac{(q^{r_C})''}{q^{r_C}} + Y\delta(\eta) \right] v_k = 0, \quad (4.45)$$

whose solution is given by (4.29) on both sides of the bounce  $\eta = 0$ , only with different parameters  $A_k^{C<} = A_k^C$ ,  $B_k^{C<} = B_k^C$  for the contracting phase [given by Eq. (4.35)] and  $A_k^{C>}$ ,  $B_k^{C>}$  for the expanding phases, due to the effect of the delta potential.

Assuming continuity of  $v_\chi$  at  $\eta = 0$  yields  $A_k^{C>} = A_k^C$ , and integrating (4.45) around the bounce provides the discontinuity in the time derivative as

$$v'_k(0^+) - v'_k(0^-) = Yv(0), \quad (4.46)$$

leading to

$$B_k^{C>} = B_k^C - \sqrt{\pi} \frac{\Gamma(r_C + \frac{1}{2})}{\Gamma(r_C + 1)} \frac{\omega\delta\chi}{\chi_F - \chi_C}, \quad (4.47)$$

as can be shown by direct evaluation of  $\chi_F - \chi_C$  as a function of  $w$ .

Plugging the solution after the bounce with the above value of  $B_k^{C>}$  into the definition (4.17) and using the mode solution (4.29), one finds that the power spectrum now consists in two contributions, namely  $\delta = k^{3/2} (D + S)$ , with the dominant term given by:

$$D = \pi |B_k^C| \left[ 1 - \frac{\pi^{3/2} \Gamma(r_C + \frac{1}{2})}{4 \Gamma(r_C + 1)} \frac{\omega\delta\chi}{\chi_F - \chi_C} \right], \quad (4.48)$$

while the subdominant term reads

$$S = S_N |C| \left(\frac{q_B}{\gamma}\right)^{-\frac{2}{1+3w}} k^{\frac{3(1-w)}{2(1+3w)}}, \quad (4.49)$$

with normalisation

$$S_N = \left[ 1 - \frac{\pi^{3/2} \Gamma(r_C + \frac{1}{2})}{2 \Gamma(r_C + 1)} \frac{\omega\delta\chi}{\chi_F - \chi_C} \right]. \quad (4.50)$$

Note that the two modes are obtained only when one keeps the otherwise negligible contribution in (4.35); this is why we kept it in the first place.

Eq. (4.48) shows that, for a fixed unique parameter  $\omega(w)$  of order unity that best approximates  $V_{\text{approx}}$  to  $\delta V$ , there is one and only one value of  $\chi$ , for which the dominant mode vanishes, thereby explaining our numerical findings. Therefore,

one can assume that the best fit is given by

$$\varpi(w) = \frac{4}{\pi^{3/2}} \frac{\Gamma(r_c + 1)}{\Gamma(r_c + \frac{1}{2})}. \quad (4.51)$$

leading the dominant term to only vanish for  $\chi = \chi_F$ , in agreement with the above results. For  $w$  in our range, the "depth" lies between  $\varpi(0) \approx 0.7$  and  $\varpi(1/3) \approx 0.8$ , i.e. a number of order unity as expected.

With the power spectrum (4.48) vanishing, there remains the subdominant piece, which happens to lead to  $\delta \propto k^{n(w, \chi_F)}$  [see Eq. (4.39)]. This reproduces exactly the features observed in the previous section and illustrated in Fig. 4.6, namely that as  $\chi \rightarrow \chi_F$ , the dominant amplitude coefficient with  $n(w, \chi_c)$  becomes smaller and smaller and thus comes to actually dominate over the subdominant one for small wavenumbers. In the limit  $\chi = \chi_F$ , the coefficient exactly vanishes and the subdominant piece, then being the only one, becomes the only relevant spectrum. This also illustrates the fact observed in Fig. 4.5, that only for a specific "depth" of the minimum of the potential when  $\chi < 0$ , we obtain a different spectral index, being that value  $\chi = \chi_F$  (even if its shape resembles nothing peculiar in comparison to other values  $\chi < 0$  as shown in Fig. 4.1).

## 4.4 Brief discussion of results

In this chapter we performed a detailed examination of the dynamical ambiguity that naturally arises in models of the primordial universe, in which both the cosmological background and the perturbations are quantized. In chapter 3 we had exposed that quantizing the background and employing a semiquantum trajectory approximation leads to two different potentials for the perturbations, thereby rendering the theory effectively ambiguous and potentially unpredictable. Here, we identified the relevant quantum parameter describing the difference and expand upon the ambiguity by calculating the expected power spectra produced for initial quantum vacuum fluctuations.

The presented model is only academic in the sense that it describe a universe whose dynamics is driven by a fluid at all times and fails at reproducing the CMB data: to do so, it would require either  $w \sim -2.9 \times 10^{-3}$  for the conformal case, and  $w \sim -0.988$  in the fluid case. Both being negative, the corresponding models are plagued with incurable instabilities; the model we have discussed here assume  $0 \leq w \leq \frac{1}{3}$  so as to avoid such instabilities. Thus, taking into account the quantum nature of the background in a highly rigorous manner, the spectral index solution still experiences the common issue of a blue-tilted spectrum found in the literature of quantum bouncing cosmological models. However, it serves as an illustration of the ambiguity and its resolution: one can expect that the same techniques using a (the most accepted) scalar field as matter component should lead to similar results.

At the classical level, it is possible to build an infinite number of acceptable and equivalent (i.e. related by canonical transformations) perturbation variables which, upon quantization, lead to a priori different quantum theories: obtaining the Mukhanov-Sasaki variable through performing the canonical transformation either before quantization or after the semiquantum trajectory is obtained yield to inequivalent potentials and, therefore, one would have guessed, to different predictions for the expected spectrum. We found the astonishing result that despite the presence of a continuous parameter describing the various possible potentials, there are only two possible predictions for the spectral index.

The usual spectrum with  $n_s^C$  is reproduced for the conformal parametrization, the amplitude depending on the parameters of the semiclassical trajectory. There exists, because of the ambiguity, another possible spectral index, stemming from using the fluid parametrization. However, we found this prediction to be very special: within our family of potentials depending on one parameter  $\chi$ , we found that all values of  $\chi$  predict the same (conformal) spectrum, except when  $\chi \rightarrow \chi_F$  exactly, in which case one gets a different spectrum with no parameter and a single well-defined minimum amplitude. The fluid case can be explained as leading to the subdominant contribution in the spectrum, the amplitude of the dominant term vanishing for the special value  $\chi \rightarrow \chi_F$ . In that sense, it represents a set of measure zero in the general  $\chi \in \mathbb{R}$ , so that one can interpret that the fluid case is so peculiar that the conformal case is the generic, and therefore deduce that the latter represents the correct prediction. Therefore, within such situation one could argue that the ambiguity is solved.

Ultimately: in quantum bounce models, the Mukhanov variable belongs to the class of variables that yield the generic prediction for primordial amplitude spectrum. In this sense, its use in semi-classical theories like inflation can be given a deeper justification. However, on the other hand, it is not the only one in that class. Moreover, which is the most convenient choice of variable it depends on the choice of internal time employed in quantization. Hence, the Mukhanov variable constitutes a valid but not necessarily a preferred choice in quantum bounce models, specially if not first fixed at the classical level as basic variable to quantize.

# 5

## Physical predictions and final state of perturbations in quantum bouncing cosmology

**DISCLAIMER:** The material presented in this Chapter is to be included in a paper currently in preparation (Ref. [90]) of which I am a coauthor. Certain progress on the content of this chapter was also included in my contribution to the Proceedings of the 2022 Cosmology session of the 56th Rencontres de Moriond (2022) [arXiv:2203.03924] (Ref. [64]). My contributions to this publication can be summarised as follows: I computed both analytically and numerically the particle distributions and probability distributions in the phase space representation for the final state of the perturbations. I produced the plots showing both results. I performed the calculation of the value of the temporal the phase shift. I participated in the discussion of the obtained results about the different distributions, the phase shift, its origin and its significance. I obtained the final amplitude spectra in terms of physical parameters. I produced the plots constraining the values of the physical parameters after fitting our model to observational data. I am participating in the preparation of the paper for future publication. I gave a talk presenting these results (and the ones from the previous chapter) in: "Szczecin Cosmology Group – Informal cosmology, particles and nuclear physics seminar" (Institute of Physics, University of Szczecin, Poland in Feb. 2023)

In the previous chapters we studied the quantization ambiguity and the ambiguous predictions it leads to. In particular, we have found that the two parametrizations produce primordial amplitude spectra with distinct spectral indices. However, the conformal index was found to be generic while the mainly subdominant fluid index turned out to be very special. The conformal index was already known in the bouncing cosmology community whereas the other case is new. Therefore, in what follows we study further differences and similarities from an enhanced perspective on the respective final states.

In quantum bouncing cosmology, the final state of perturbations refers to the time when the mode is outside the horizon, just after entering the potential becoming amplified with an amplitude that remains constant until they exit the potential (or "re-enter" the horizon). Different models can produce different final states, leading to distinct physical predictions. All properties of the final states of perturbations can have important consequences for the structure formation in the universe. We particularly study the dependence of the found amplitude on other parameters than

the wave vector (or wavelength). Moreover, we investigate the phase shift with which the modes emerge from the bounce. Confronting the predictions with observations allow us to constraint the relevant physical parameters of the cosmological model.

## 5.1 Final states distributions

We study the underlying quantum state, the Bunch-Davies vacuum, which assumes that the universe began in a state with lowest energy fluctuations. We perform the analysis from the point of view of late-time observers, which can be introduced after the mode exits the horizon. This notion can be extended to the so-called instantaneous observers for times the mode is inside the horizon (or outside the potential). The new interpretation is obtained by means of the Bogolyubov transformations.

### Bogolyubov transformations

We start with the mode expansion of the Mukhanov-Sasaki field  $v(x, \eta)$  in terms of the mode functions  $v_k$  written as follows

$$v(x, \eta) = \sum_k \frac{1}{\sqrt{2}} \left( a_k \bar{v}_k(\eta) e^{ikx} + a_k^\dagger v_k(\eta) e^{-ikx} \right), \quad (5.1)$$

where  $k = |k|$ . The mode function  $v_k$  satisfies one of the equations of motion, either for  $v_k^c$  or  $v_k^f$ , with the initial condition (4.13). The annihilation and creation operators,  $a_k$  and  $a_k^\dagger$ , define the Bunch-Davies vacuum. It is useful to introduce another expansion of the field,

$$v(x, \eta) = \sum_k \frac{1}{\sqrt{2}} \left( b_k \bar{u}_k(\eta) e^{ikx} + b_k^\dagger u_k(\eta) e^{-ikx} \right), \quad (5.2)$$

in which the annihilation and creation operators,  $b_k$  and  $b_k^\dagger$ , define the *instantaneous* vacuum at a different time  $\eta$ , i.e., the lowest-energy eigenstate of the instantaneous Hamiltonian  $\hat{\mathbf{H}}_k^{(2)}(\eta)$ <sup>1</sup>. It implies that  $u_k$  satisfies the following condition:

$$u_k(\eta) = \sqrt{\frac{\hbar}{\sqrt{wk}}}, \quad \dot{u}_k(\eta) = i\sqrt{\hbar\sqrt{wk}}. \quad (5.3)$$

It is known (see, e.g. Ref. [80]) that the following relations must hold:

$$\begin{aligned} v_k(\eta) &= \alpha_k(\eta) u_k(\eta) + \beta_k(\eta) \bar{u}_k(\eta), \\ b_k &= a_k \bar{\alpha}_k(\eta) + a_{-k}^\dagger \beta_k(\eta). \end{aligned} \quad (5.4)$$

<sup>1</sup>We have different vacuum states at different times because the Hamiltonian is time dependent and, hence, the ground state energy as well. Then, we require mode functions which describe the minimum vacuum energy at different instants of time, and the same mode function cannot describe the ground state at two different moments. Instead there is a new mode function that minimizes de energy of the ground state at the new time. Therefore, at the beginning our  $a$ -vacuum state is the Bunch-Davies determined by  $(v_k(\eta_{\text{ini}}), \pi_k(\eta_{\text{ini}}))$ , but at the end is the  $b$ -vacuum determined by  $(v_k(\eta), \pi_k(\eta))$  with  $\eta > \eta_{\text{ini}}$ . For more details see chapter 6.3 of Ref. [80]

These are called the Bogolyubov transformations, where

$$\begin{aligned}\alpha_k &= \frac{e^{-i\sqrt{\omega}k\eta}}{2} \sqrt{\frac{\sqrt{\omega}k}{\hbar}} \left( v_k + \frac{\dot{v}_k}{i\sqrt{\omega}k} \right), \\ \beta_k &= \frac{e^{i\sqrt{\omega}k\eta}}{2} \sqrt{\frac{\sqrt{\omega}k}{\hbar}} \left( v_k - \frac{\dot{v}_k}{i\sqrt{\omega}k} \right),\end{aligned}\tag{5.5}$$

are the sought for Bogolyubov coefficients.

### 5.1.1 Particle distributions

For a fixed mode, we can characterize the final states by means of different physical concepts. We start with particle distributions.

The two annihilation operators  $a_k$  and  $b_k$  define the corresponding vacua  $|0_a\rangle$  and  $|0_b\rangle$ . Making use of the Bogolyubov transformation the Bunch-Davis vacuum  $|0_a\rangle$  can be expressed in the  $b$ -representation, i.e., in terms of states built from the instantaneous  $b$ -vacuum state for an observer at a later time,

$$|0_a\rangle = \prod_k \frac{1}{|\alpha_k|^{1/2}} \exp\left(\frac{\beta_k}{2\alpha_k} b_{-k}^\dagger b_k^\dagger\right) |0_b\rangle.\tag{5.6}$$

This state is a linear combination of  $|k_b\rangle \cdot |-k_b\rangle$  a quantum of the left-moving wave and a quantum of the right-moving wave. Hence, it is made of quanta of a standing wave. The quantity

$$\frac{1}{|\alpha_k|^2} \left| \frac{\beta_k}{\alpha_k} \right|^{2n},\tag{5.7}$$

is the occupation number of the  $n$ -particle state of the standing wave. As a function of  $n$  it yields the probability distribution in the number of particles of the standing-wave mode of the perturbation variable at any given moment of time. We refer to it as the "particle distribution". It is plotted for the crossing time  $\eta_c$  in Fig. 5.1 (for  $\omega = 0.28$  and  $k = 10^{-5}$ ).

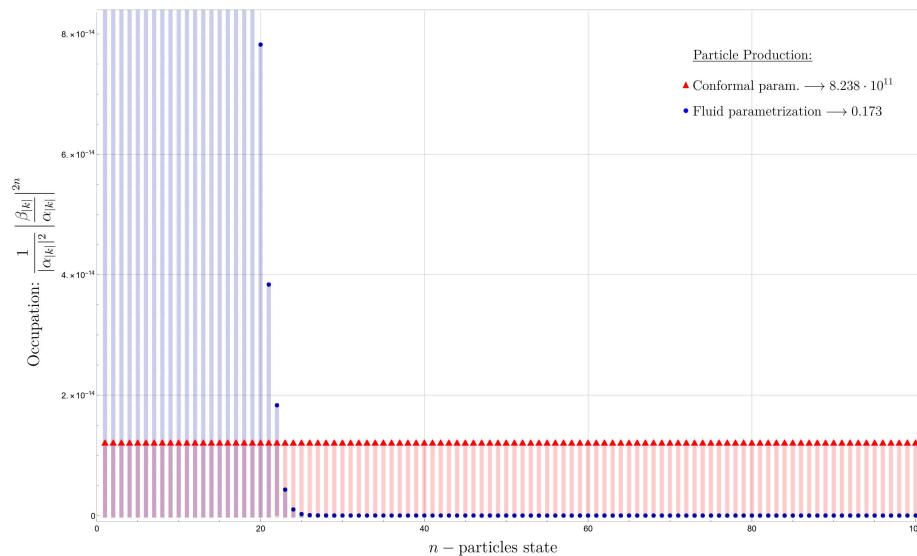


FIGURE 5.1: Particle distribution in states of different  $n$  number of particles for conformal parametrization (blue-circles) and fluid parametrization (red-triangles), for  $\omega = 0.23$  and  $k = 10^{-5}$ .

The plot represents the  $b$ -particle distribution for both parametrizations in the unique Bunch-Davies vacuum. The initial vacuum state turns out to contain on average  $|\beta_k|^2(\eta)$   $b$ -particles at a late-time  $\eta$ . Later we provide a complementary description via probability distributions.

We can observe different particle distributions for both quantum theories. In the Fluid parametrization, we find the occupation numbers to be much larger for states with fewer particles and decaying exponentially as the number of particles in the states  $n$  increases. This reflects a very low particle production in comparison to the conformal case, with only 0.173 particles for the given values of  $w$  and  $k$ .<sup>2</sup> On the other hand, in the conformal parametrization we find a very homogeneous distribution over a vast range of multi-particle states, with the approximately equal occupation numbers for those states. In this parametrization we find the average number of particle to be  $8.238 \times 10^{11}$  for the given mode.

### 5.1.2 Phase space representation

There exist many ways to describe the properties of the final state. In this subsection, we study their probability distributions in the phase space representation, which are obtained with the standard coherent states built from instantaneous vacua.

The Fourier components of the Mukhanov-Sasaki field  $v(x, \eta)$  can be decomposed into its real and imaginary parts,  $v_k = \frac{1}{\sqrt{2}}(v_k^R + iv_k^I)$  and  $v_{-k} = \frac{1}{\sqrt{2}}(v_k^R - iv_k^I)$ , where we used the reality of the field  $v(x, \eta)$ . One may show that  $\{v_k^R, \pi_k^R\} = \{v_k^I, \pi_k^I\} = \frac{1}{2}$ , where  $\pi_k = \dot{v}_k$ . For the Bunch-Davies vacuum the real and imaginary parts describe two "oscillation modes" of the standing wave. At any moment of time the state of each mode expressed in the  $b$ -representation can be cast into the standard (i.e. Schrödinger) coherent state representation. The standard coherent states are obtained by the action of the displacement operator on the  $b$ -vacuum. For the real part of  $v_k$  it reads:

$$D(v_k^R, \pi_k^R) = e^{\frac{2i(\pi_k^R \hat{v}_k^R - v_k^R \hat{\pi}_k^R)}{\hbar}} = e^{-\bar{z} \frac{b_k + b_{-k}}{\sqrt{2}} + z \frac{b_k^\dagger + b_{-k}^\dagger}{\sqrt{2}}}, \quad (5.8)$$

where  $z = i\sqrt{\frac{\sqrt{wk}}{\hbar}} \left( \frac{\pi_k^R}{\sqrt{wk}} - iv_k^R \right)$ . Analogously, for the imaginary part it reads:

$$D(v_k^I, \pi_k^I) = e^{\frac{2i(\pi_k^I \hat{v}_k^I - v_k^I \hat{\pi}_k^I)}{\hbar}} = e^{-\bar{z} \frac{b_k - b_{-k}}{\sqrt{2}} + z \frac{b_k^\dagger - b_{-k}^\dagger}{\sqrt{2}}}, \quad (5.9)$$

where  $z = -\sqrt{\frac{\sqrt{wk}}{\hbar}} \left( \frac{\pi_k^I}{\sqrt{wk}} - iv_k^I \right)$ . The coherent state representations for both modes of the standing wave are given by

$$\langle z | 0_a \rangle = \frac{1}{|\alpha_k|} e^{-\frac{|z|^2}{2}} e^{\frac{z^2}{2} \frac{\beta_k}{\alpha_k}}, \quad (5.10)$$

<sup>2</sup>This does not mean that the absolute number of particles produced is always such small for the fluid case, here being a fraction of a particle. It can be considerably higher for different values of  $w$  and  $k$ . However, in general it is low relatively to the number of particles produced in the conformal parametrization [64]. This is in accordance with the results of the previous chapter, where we showed that the fluid case gives the minimum primordial amplitude within the range of all possible values of  $\chi$  that the conformal case can take.

where the standard coherent states  $|z\rangle$  are defined via the action of the displacement operator  $D(z)$  on the late-time instantaneous vacuum:

$$|z\rangle = D(z)|0_b\rangle. \quad (5.11)$$

Eq. (5.10) represents the transition amplitude between the initial  $a$ -vacuum state and the coherent state  $|z\rangle$  in the frame of the late-observer built from the  $b$ -vacuum at the late-time  $\eta$ . Note that despite that we have a time-dependent notion of the instantaneous vacuum, the state that we represent is the fixed Bunch-Davis  $a$ -vacuum which underlies the evolution in the Heisenberg picture. Therefore, there is no dynamics of coherent states, it is only the  $b$ -vacuum on which we define them that is time-dependent, because at different times we have different instantaneous  $b$ -vacuum states. Nevertheless, as the gravitational potential vanishes the final  $b$ -vacuum sets in at some time  $\eta_c$ , and the "evolution" of the coherent state representations stops.

Then, we compute the normalized phase space probability distribution for the Bunch-Davies vacuum at  $\eta_c$ , reading

$$\rho(z) = \pi^{-1} |\langle z|0_a\rangle|^2 = \frac{e^{-|z|^2} e^{\text{Re}[\frac{\bar{z}^2 \beta_k}{\alpha_k}]} }{\pi |\alpha_k|^2}, \quad (5.12)$$

and is plotted in Fig. 5.2. The probability distribution at the initial time is plotted on the left, which is rotationally invariant and centred at the origin. It represents the vacuum state with no particles, with position and momentum of the perturbation mode functions equally uncertain. Once the system evolves through the bounce, the vacuum gets excited as a number of particles is produced. The corresponding probability distributions for the C- and F-parametrizations, and captured at  $\eta_{\text{cross}}$ , are plotted, respectively, on the center and right images. The final state is the so-called squeezed vacuum state, and the excitation process that leads to it is called "squeezing".

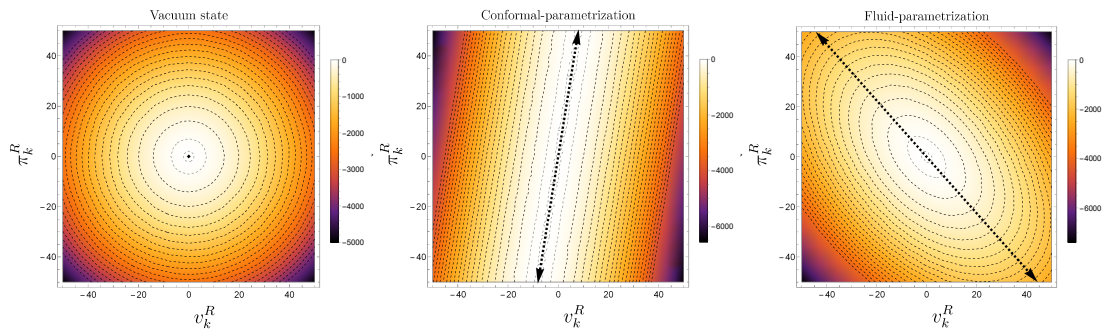


FIGURE 5.2: Phase space probability distribution (5.12) for  $w = 0.23$  and  $k = 10^{-5}$ . *Left*: The initial coherent vacuum state. *Center*: The vacuum squeezed by the Conformal parametrization at  $\eta_c$ . *Right*: The vacuum squeezed by the Fluid param. at  $\eta_c$ . The black dashed line represents the phase shift angle with respect to the  $v_k^R$  axis, and the direction in which the state is squeezed at  $\eta_c$ .

The probability distributions show that the value of the primordial perturbation amplitude is different for each parametrization<sup>3</sup>, and, above all, very quantum and uncertain, and possibly collapsing to a very large value (at least for the conformal case, since we know  $F$ -param. represents a minimum of the amplitude in  $\chi$ ). Although the expectation value of the amplitude (4.17) of the perturbation is zero ( $\langle \delta \rangle \propto \langle v_k \rangle = 0$ ), the square root of the expectation value of the amplitude squared is not ( $\sqrt{\langle \delta^2 \rangle} \propto \sqrt{\langle v_k^2 \rangle} \neq 0$ ), due to this squeezing. Hence, we have pure quantum uncertainty for the amplitude. However, as one can expect, at some remote point a collapse must have occurred in order to observe the current classical universe, with perturbation amplitudes possessing a definite value. In the conformal parametrization, the distribution extends with higher probability over a wider range of the phase space of the perturbations than in the fluid case. This reflects the fact that even very highly excited states are probable and thus, the primordial amplitude can acquire a large value (Fig. 5.2-center). Whereas, in Fluid parametrization (Fig. 5.2-right) we see clearly less elongated elliptical shape of the probability distribution. Then, the conformal parametrization reflects larger amplification, making it more likely to explain the typical transition to reheating after the bounce via enough gravitational particle production [91]. On the other hand, the temporal phase of oscillation with which the amplitude emerges at  $\eta_{\text{cross}}$ , i.e. the direction of squeezing, is very definite and thus classical. The expectation value of the amplitude squared is found to read:

$$\begin{aligned} |v_k|^2 &= |\alpha_k u_k + \beta_k \bar{u}_k|^2 \\ &= |u_k|^2 (1 + 2|\beta_k|^2 + 2|\alpha_k \bar{\beta}_k| \cos[2\sqrt{w}k\eta - 2\theta]), \end{aligned} \quad (5.13)$$

where the phase  $\theta$  is exactly the phase seen in the plots of the probability distributions (Fig. 5.2) represented by the black dotted arrows. The phase  $\theta$  is determined by extremization of the descent of the probability distribution along all the directions around the origin of the phase space. We find:  $\text{Im}(\beta_k/\alpha_k) \cos(2\theta) = \text{Re}(\beta_k/\alpha_k) \sin(2\theta)$ , which under the assumption  $v_k^R \neq 0$  and  $\text{Im}(\beta_k/\alpha_k) \neq 0$  yields:

$$\tan(\theta) = \frac{\pi_k^R}{\sqrt{w}k v_k^R} = \sqrt{1 + \left( \frac{\text{Re}(\frac{\beta_k}{\alpha_k})}{\text{Im}(\frac{\beta_k}{\alpha_k})} \right)^2} - \frac{\text{Re}(\frac{\beta_k}{\alpha_k})}{\text{Im}(\frac{\beta_k}{\alpha_k})}. \quad (5.14)$$

Note that since we work in the Heisenberg picture the phase  $\theta$  is actually the phase shift with which a given perturbation mode emerges from the bounce. We study the evolution of the phase shift in more detail now.

### 5.1.3 Temporal phase shift

It is often said [92] that the primordial cosmological perturbations emerge as a sine wave from the generating phase. For the inflationary model it means that once the inflation is ended, radiation era begins and the gravitational potential becomes negligible, the modes of the Mukhanov-Sasaki field with the wavenumber  $k$  evolve simply as

$$v_k(\eta) \propto \sin(\sqrt{w}k\eta + \theta), \quad (5.15)$$

<sup>3</sup>As explained in chapter 3, this difference occurs because each perturbation field feels the space time in a different form, they are evolving in a different geometry: there is not such thing as a well-defined spacetime anymore, due to the quantum nature of the position and momentum that we assume.

where  $\theta$  is vanishing, or negligible. This is extremely important since, given that the scale factor in the radiation era scales as  $a \propto \eta$ , the sine wave is needed to ensure the constancy of the primordial amplitude of the curvature perturbations (on co-moving hypersurfaces, see around Eq. (2.37)) at super-horizon scales:

$$\mathcal{R}_k \propto \frac{|v_k|}{a} \propto \frac{\sin(\sqrt{w}k\eta)}{\eta} \approx \sqrt{w}k, \quad \eta \lesssim \frac{1}{\sqrt{w}k}. \quad (5.16)$$

Since the inflation did not take place exactly at the big bang singularity but ended at some finite  $\eta_{inf} > 0$ , all the modes must have emerged with a phase shift  $\theta = -\sqrt{w}k\eta_{inf}$ . However, being scale-dependent this phase shift becomes negligible for large cosmological scales  $k \ll 1/\eta_{inf}$  (i.e. super-horizon modes at  $\eta_{inf}$ ).

In the bouncing model we also see the possibility for the phase shift as illustrated in the Fig. 5.3. One part of the phase shift comes from the fact that the amounts of conformal time that have elapsed since the big bang of the classical incomplete theory and the big bounce are different. The difference reads:

$$\Delta\eta = \int_0^\infty \left( \left. \frac{d\eta}{d\tau} \right|_{class} - \left. \frac{d\eta}{d\tau} \right|_{semi} \right) d\tau, \quad (5.17)$$

and causes the shift  $\theta = -\sqrt{w}k\Delta\eta$  that becomes negligible for large cosmological scales  $k \ll 1/\Delta\eta$  in complete analogy to the inflationary phase shift.

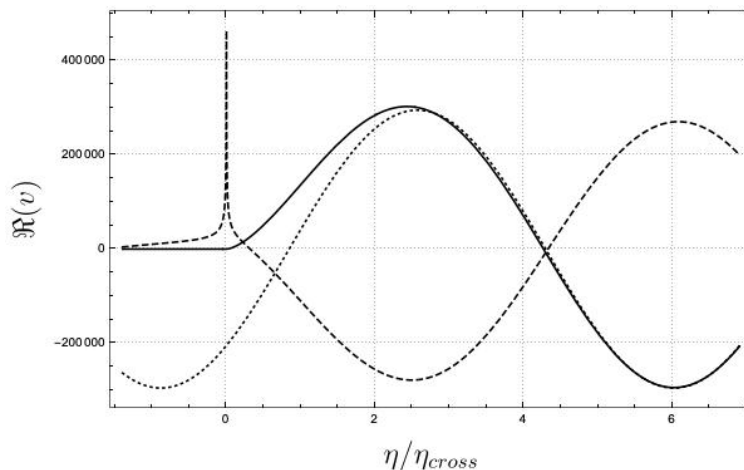


FIGURE 5.3: The dynamics of the real part of perturbation mode  $\Re(v_k)$  for  $k = 0.0001$  in  $\eta_{cross}$  as time units. The solid line takes the form of the sine wave that is gradually shifted in phase and represents  $v_k^C$  (the C-parametrization). The dashed line takes the form of the minus sine wave that is gradually shifted in phase and represents  $v_k^F$  (the F-parametrization). The third, dotted curve is the exact sine wave with a constant shift that is equal to the final phase shift of the Mukhanov-Sasaki variable. We see that  $v_k^C$  ( $v_k^F$ ) eventually becomes the pushed-from-origin (minus) sine wave with the final phase shift as the curves merge.

There is however another source of the temporal phase shift whose final value is not scale-dependent and cannot be ignored when estimating the time at which long-wavelength modes "re-enter" the horizon (or exit the potential) and start to oscillate. It originates in the dynamics of the universe just after the bounce when it is driven by the fluid that in general is not radiation and, in our model, can indeed have  $0 < w \leq \frac{1}{3}$ . This phase shift, if no transition to radiation happens, can actually grow

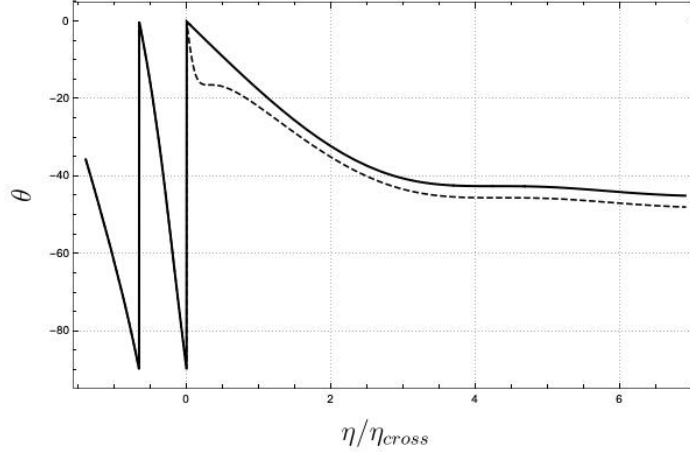


FIGURE 5.4: The evolution of the phase shift  $\theta$  (in angular degrees) for  $k = 0.0001$  in  $\eta_{\text{cross}}$  as time units. The solid line corresponds to  $v_k^{\text{C}}$  (the Conformal parametrization) and the dashed corresponds to  $v_k^{\text{F}}$  (the Fluid parametrization). For smaller wavenumbers  $k$  the two curves tend to merge. We can see that both parametrizations start out at the bounce as sine waves ( $\theta = 0^\circ$ ) and then are gradually shifted by the growing phase shift  $\theta$  that around  $6 - 7$  of  $\eta_{\text{cross}}$  reaches its maximum values and stops growing.

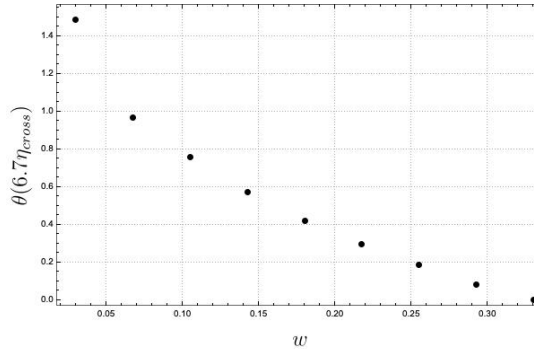


FIGURE 5.5: The maximal value of the phase shift ( $\approx 6.7\eta_{\text{cross}}$ ) in function of the fluid  $w$ . We can see that for radiation there is no phase shift at all and as  $w \rightarrow 0^+$  approaches dust the phase shift grows.

for a few  $\eta_{\text{cross}}$  for each mode until it reaches quite a significant value. Although the final value of the shift is scale-independent, it grows with time at a scale-dependent rate. It turns out that the phase is an unambiguous function of time when expressed the units of  $\eta_{\text{cross}}$  (the time at which each mode exits the potential), the latter being clearly dependent on  $k$ . See the Fig. 5.4.

The transition to radiation era occurs after the relevant modes are amplified to their constant super-horizon amplitude value by entering the potential, but much before the modes of interest "re-enter" the cosmological horizon. In order for the relevant modes to remain approximately constant for sufficient amount of time until their "re-entering", the phase shift must be sufficiently small. This guarantees consistency with the observational data. Then, the growth of the phase shift must be halted upon transition to radiation. That means that the phases cannot be exactly coherent (the same for each  $k$ ), since the growth rate of phase shift is scale-dependent. The incoherence of the modes could lead to spoiling the CMB anisotropy power spectrum for large scales that we observe [93]. We might expect then that the growth has to

be stopped early on when the phase shifts of the relevant modes are still negligible in order to make them sufficiently coherent. We investigate this issue in the next section.

## 5.2 Physical predictions

### 5.2.1 Amplitude and the bounce

The models discussed in the previous sections depend on the background evolution, which is itself dependent on the barotropic index  $w$  and two extra constant numbers, namely the quantum repulsion amplitude  $\mathfrak{R}$  appearing in the semiquantum Hamiltonian (3.22), and the value of  $H_{\text{sem}}$  itself. The latter represents the total energy contained in the entire universe, and (as can be proved using (2.19) and Friedmann equation  $\rho = 3H^2/\kappa$ ) is thus proportional to the energy density  $\rho \propto a^{-3(1+w)} \sim v^{-(1+w)}$ , where  $v$  is the observable volume, as opposed to the total volume  $\mathcal{V}(\eta) = a^3 \mathcal{V}_0$  (with  $\mathcal{V}_0 = 1$  the assumed coordinate volume of the spatial leaf). Setting  $r := \mathcal{V}/v$  the ratio between the observable to the total volume, one then gets  $H_{\text{sem}} \propto r^{1+w}$ .

The relations given below Eqs. (3.23) between the minimum scale factor  $q_{\text{B}}$  and the curvature at the bounce  $\omega^4$  as functions of the above parameters yield

$$q_{\text{B}} \propto \sqrt{\frac{\mathfrak{R}}{r^{1+w}}} \quad \text{and} \quad \omega \propto \frac{r^{1+w}}{\sqrt{\mathfrak{R}}}, \quad (5.18)$$

Once inserted into the Eqs. (4.37) and (4.38), the relations (5.18) permit to evaluate the amplitude of the spectra at the pivot scale  $k_*$ , namely

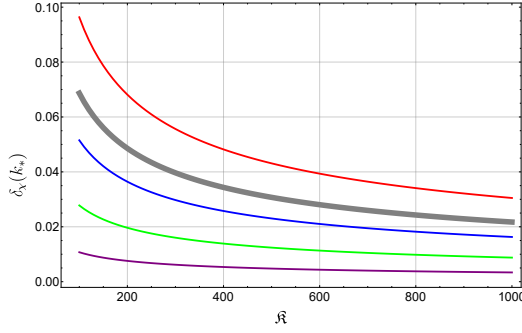
$$\delta_{\text{C}}(k_*) \propto \frac{r}{\sqrt{\mathfrak{R}}}, \quad \text{and} \quad \delta_{\text{F}}(k_*) \propto 1, \quad (5.19)$$

where we assumed  $k_* \propto r^{1/3}$ , a relation stemming from the fact that the larger the entire universe, the larger the conformal wavenumber corresponding to a fixed physical distance.

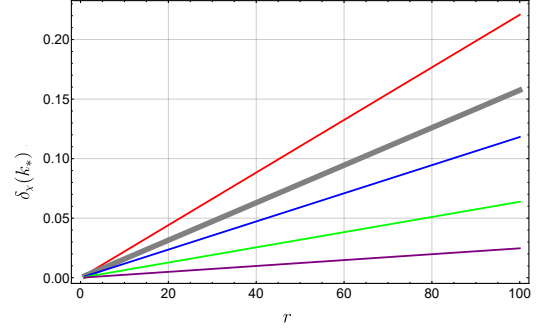
The amplitude  $\delta_{\text{C}}(k_*)$  for the conformal case depends on  $r$  and  $\mathfrak{R}$  in a way that could have been anticipated: the larger the repulsive potential, i.e. the larger  $\mathfrak{R}$ , the sooner the bounce occurs, so the perturbations are less excited, leading to a smaller amplitude. From the geometric point of view, one can argue that the gravitating energy contained in the entire universe increases with its size, implying a deeper bounce and thus a larger amplitude of perturbations. Assuming this relation holds, measuring the local structures in our universe could permit to deduce the size of the entire universe.

It is however quite unexpected to find that, for the fluid case, the spectrum  $\delta_{\text{F}}(k_*)$  depends neither on the size of the universe nor the strength of the quantum repulsion. Indeed, those parameters determine the scale of the bounce and thus should leave an imprint, as discussed in the previous paragraph. Since any change on the physical features of the bounce leaves the amplitude of the Fluid modes unaltered, one could interpret this result as yielding to an unphysical F-solution.

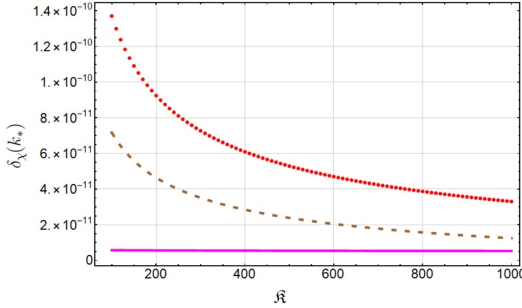
<sup>4</sup>It is called curvature at the bounce because it controls how "steep" (or convex) is the transition between the contraction and expansion phase in the semiquantum trajectories of Fig. 3.2, being less curved for smaller  $\omega$ . It is also called the acceleration at the bounce because it controls how fast the trajectory the scale variable  $q$  increases just after the expansion begins (or decreases just before the bounce).



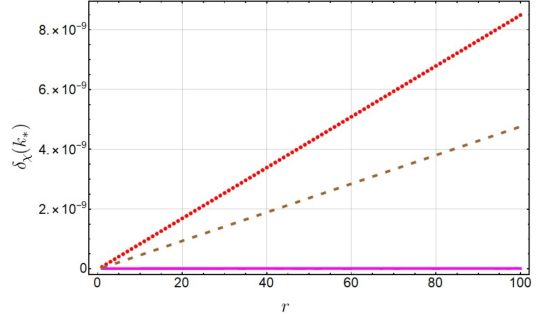
(A) Numerical primordial amplitude power spectrum dependence with respect to  $\tilde{k}$  in conformal parametrization ( $w = 0.1$ ). From top to bottom:  $\chi = 5$ ,  $\chi = \chi_C = 3.86$ ,  $\chi = 3$ ,  $\chi = 1.5$  and  $\chi = 0.001$ , for a scale  $k_* = 10^{-6}$ . We clearly observe that all the curves behave as  $\delta_C(k_*) \propto \sqrt{\tilde{k}}$ .



(B) Numerical primordial amplitude power spectrum dependence with respect to  $r$  in conformal parametrization ( $w = 0.1$ ). From top to bottom:  $\chi = 5$ ,  $\chi = \chi_C = 3.86$ ,  $\chi = 3$ ,  $\chi = 1.5$  and  $\chi = 0.001$ , for a scale  $k_* = 10^{-6}$ . We clearly observe that all of them behave as  $\delta_C(k_*) \propto r$



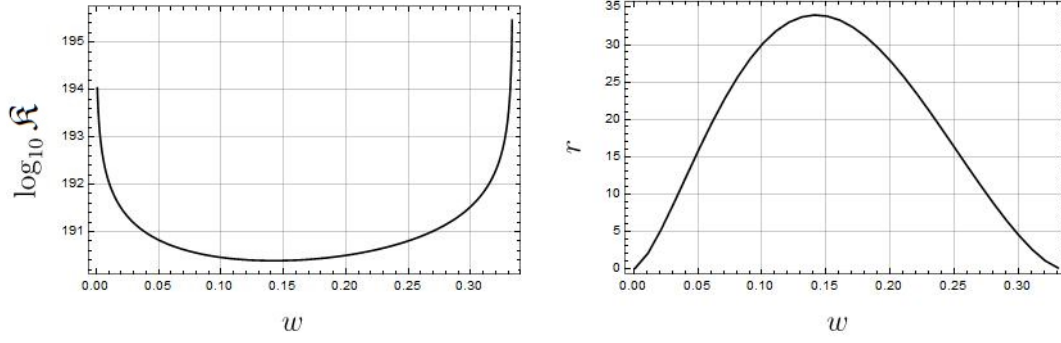
(C) Numerical primordial amplitude power spectrum dependence with respect to  $\tilde{k}$  ( $w = 0.1$ ). For the exact case of Fluid parametrization  $\chi = \chi_F = -1.35$  (solid bottom line) the amplitude is constant in  $\tilde{k}$ , whereas for any very little deviation like  $\chi = \chi_F + 10^{-6}$  (dotted) or  $\chi = \chi_F - 10^{-7}$  (dashed), we recover conformal behaviour  $\delta_C(k_*) \propto \sqrt{\tilde{k}}$



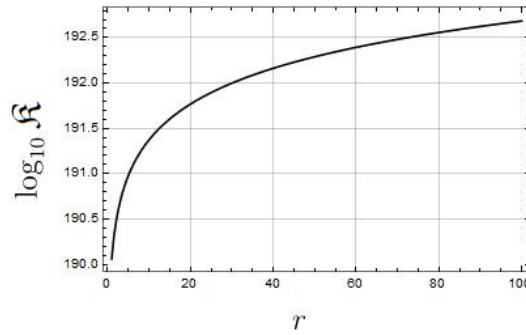
(D) Numerical primordial amplitude power spectrum dependence with respect to  $r$  ( $w = 0.1$ ). For the exact case of Fluid parametrization  $\chi = \chi_F = -1.35$  (bottom solid line) the amplitude is constant in  $r$ , whereas for any very little deviation like  $\chi = \chi_F + 10^{-6}$  (dotted) or  $\chi = \chi_F - 10^{-7}$  (dashed), we recover conformal behaviour  $\delta_C(k_*) \propto r$

Although the relations (5.19) are derived in the analytic approximation obtained in (4.38) and (4.37), we verified them numerically for various values of  $\chi$ : as expected, the conformal behaviour in terms of both parameters holds for all values  $\chi \neq \chi_F$  (see Fig.5.6a and Fig.5.6b), since the quantity appearing in the conformal amplitude formula  $\propto \omega(q_B \omega)^{\frac{-6w}{1+3w}}$ , along with the power spectrum  $k_C^{\frac{6w}{1+3w}}$ , is invariant for any value of the parameter  $\chi$  in the C-parametrization. However, the special fluid case  $\chi = \chi_F$  yields again an extremely unique situation in terms of the ambiguity parameter (see Fig.5.6c and Fig.5.6d) in which no dependence can be observed, as predicted in (5.19).

Let us assume that the amplitude of the power spectrum for the scalar perturbations at the physical pivot scale  $k_{*\text{phys}} = 0.05 \text{ Mpc}^{-1}$  is  $\ln(10^{10} A_s) = 3.044$ , to be consistent with the Planck data [48]. We set the scale  $k_* = k_{*\text{phys}} r^{1/3} \ell_P^{-1} D_{\text{obs}}$  accounting to the part that the pivot scale is of the observable universe, where  $D_{\text{obs}} = 5.44 \cdot 10^{61} l_P$  m is the diameter of the observable universe [27]. This in turn puts constraints on the free parameters  $K$  and  $r$ . In Fig.5.7a, and 5.7b we plot the required values of  $K$  and  $r$  as functions of the barotropic index, and in 5.7c the relation between them.



(A) Admissible values of the parameter  $\mathfrak{K}$  as a function of  $w$  for  $r = 2$ . (B) Admissible values of the parameter  $r$  as a function of  $w$  for  $\mathfrak{K} = 10^{192}$ .



(C) Relation between the two parameters  $\mathfrak{K}$  and  $r$  for the case  $w = 0.1$ .

## 5.2.2 Phase shift

It is usually assumed that all the observable modes of the matter perturbations have started out with coherent phases. As we have showed before, this does not have to be exactly true. Ignoring the phase shift that comes from the discrepancy between classical and semiclassical notions of time, we still obtain the phase shift which is generated prior to the transition of the cosmological fluid to radiation era. Let us denote the dynamical phase shift by  $\theta(w, \frac{\eta}{\eta_{\text{cross}}})$  which is numerically shown to be unique for all the modes, and depends on  $k$  only through  $\eta_{\text{cross}}$ . It is plotted in Fig. 5.4.

Given some finite transition time  $\eta_{tr}$  we are able to estimate the decoherence of the phases by looking at their phase shift variation around a pivot wavenumber  $k_*$ ,

$$\left. \frac{\partial \theta}{\partial k} \right|_{k=k_*, \eta=\eta_{tr}} = \theta' \cdot \left. \frac{\eta}{k \eta_{\text{cross}}} \right|_{k=k_*, \eta=\eta_{tr}}, \quad (5.20)$$

as  $\eta_{\text{cross}} \propto k^{-1}$  and where  $\theta'$  denotes the derivative with respect to the second argument. It is clear that the second factor does not depend on the pivot wavenumber  $k_*$ . Also, given Fig. 5.4 we may safely assume to work in the regime where  $\theta'$  is roughly a constant that can be estimated numerically. That is, after the phase shift starts growing, when the mode is superhorizon. Therefore, the phase shift is not suppressed for large wavenumber, with linear dependence on  $k$ . At the same time it depends linearly on  $\eta_{tr}$  as well.

Let us estimate the phase shift across the observable range of modes. We assume that  $\theta'$  is of order of unity. The difference in  $k$  between the largest and the

shortest mode  $\Delta k = k_{max} - k_{min} \approx k_{max}$  can be set equal to the largest observable wave number. Since the phase shift depends linearly on  $k$ , the decoherence of the phases can be approximated to be the phase shift for the largest  $k_{max}$  as well:  $\Delta\theta = \theta(k_{max}) - \theta(k_{min}) \approx \theta(k_{max})$ . More generally, we could introduce  $\Delta k = k$  for any  $k \gg k_{min}$ . Then the total phase shift of a given mode  $k$  with respect to the largest observables modes reads:

$$\left. \frac{\partial\theta}{\partial k} \Delta k \right|_{\eta=\eta_{tr}} \approx \frac{\eta_{tr}}{\eta_{cross,k}}. \quad (5.21)$$

Let us introduce  $z_{tr}$ , the redshift of the primordial fluid-radiation transition, and recall  $D_{obs}$ , the diameter of the present-day observable universe in the Planck units. Then

$$\frac{\eta_{tr}}{\eta_{cross,k}} = \frac{3(1-w^2)}{\sqrt{2}|1-3w|} \frac{\gamma k}{q_B \omega} (z_{tr}^{-1} D_{obs} r^{\frac{1}{3}})^{\frac{3w+1}{2}}. \quad (5.22)$$

where we used (4.40), (3.35), (3.36), (2.19), (3.22) and  $H_{sem} \approx 10^{120} r^{\frac{4}{3}} (z_{tr}^{-1} D_{obs} r^{\frac{1}{3}})^{3w-1}$  [27], with the redshift being:  $z_\eta \simeq a_0/a(\eta)$ , where  $a_0$  is the present value of the scale factor. Let us assume  $k = 200\pi r^{1/3} l_p^{-1}$  to correspond to one hundredth of the diameter of the observable universe and the transition redshift  $z_{tr} = 10^{28}$ .<sup>5</sup> We obtain a rough estimate of the decoherence of the phases:

$$\Delta\theta \approx \frac{1}{r^{\frac{1+w}{2}}} 10^{-118+50(1-w)}, \quad (5.23)$$

Setting  $r = 1$  and  $w$  close to zero (maximum phase shift) yields  $\Delta\theta \approx 10^{-68}$ . Hence, the phase shift at the observable range of modes should be negligible, meaning the phases of the relevant large modes can be assumed coherent. Note that the larger size of the physical universe the more suppressed the phase shift is. Also, the stiffer the cosmological fluid is the more suppressed the phase shift is.

### 5.3 Brief discussion of results

We studied the final states of the perturbations for the two non-equivalent semi-quantum theories derived in the previous chapters. The performed analysis allowed us to acquire a better understanding of different aspects of the predictions that the obtained solutions yield, in terms of physical quantities, and from different points of view. We found that the primordial amplitude can be written in terms of physical parameters, permitting an improved interpretation and allowing us to constraint our results with observations.

Quantum bouncing cosmological models being an incipient alternative to the standard inflationary scenario, very little is yet known about the characteristic features of the inherent bounce. By testing the model with cosmological observations, we can obtain an estimate of the scale of the bounce, at the same time we are able to shed light on attributes of the physical universe, such as its size. We found that, in order for the model of quantum spacetime to be fitted to observational data, the quantum bounce must possess an anomalously large strength  $\mathfrak{R}$ , as can be observed in Figs. 5.7c and 5.7a.

<sup>5</sup>The value  $z_{tr} = 10^{28}$  corresponds to the redshift of the “end-of-inflation” [94].

The conformal spectrum depends on both the parameter  $\mathfrak{K}$ , coming from quantization of the background, as well as the ratio  $r$  between the 3D compact manifold and the observable universe. Since there exists some amount of degeneracy between those, the tensor index should be calculated to raise this degeneracy. It is to be expected that a similar behaviour will be observed in the latter, as predicted in [27].

On the other hand, the fluid parametrization was deduced to show an unphysical behaviour in terms of the mentioned parameters. In addition, its relatively low particle production compared to the conformal case, due to the narrow spread of the probability distribution along the phase space of the amplified perturbations, can reaffirm it as an unconvincing theory, leading us to interpret these results as the resolution of the quantization ambiguity.

Moreover, we found that our bouncing model is able to explain the constancy of the primordial amplitude of the comoving curvature perturbations, with all the modes emerging coherently, what is a requirement in order to get predictions with potential to match the observations that give as a result the CMB spectrum.

In principle, we studied a model which eventually needs to be improved, as it yields unphysical blue-tilted spectral index. However, some of its properties are expected to be valid in a more realistic model still to be constructed.



# 6

## Can a quantum mixmaster universe undergo a spontaneous inflationary phase?

**DISCLAIMER:** The material presented in this Chapter is originally included in a paper submitted for publication in *Phys. Rev. D* (Ref. [35]) of which I am a coauthor. Part of it was also included in a paper published in *Acta Physica Polonica B Proceedings Supplement 16, 6-A20* [arXiv:2302.01111] (Ref. [95]) of which I am the only author. My contributions to this publication can be summarised as follows: I participated in the analytical examination of the dynamics of the model presented in the article. I numerically searched for the inflationary dynamics in the semiquantum mixmaster model and studied the global dynamics over a few cosmic cycles. I produced all the plots that illustrate the dynamics of the model and make an integral part of the result. I participated in the discussion of the obtained results. I participated in the preparation of the paper for publication. I gave talks presenting these results in: "The 8th Conference of The Polish Society on Relativity" (Warsaw, Poland in Sep. 2022), "Cosmology on Safari" (Hluhluwe, South Africa in Mar. 2023) and "NCBJ PhD Seminar 2023" (National Centre for Nuclear Research, Poland in Apr. 2023).

Thus far, we studied alternative bouncing cosmological models to cosmic inflation for the primordial universe, in which the generation of primordial structure occurs during the contraction and the bounce that stops contraction and initiates the present expansion. Unfortunately, we proved that these simple bouncing models tend to generate blue-tilted spectrum for primordial perturbations contrary to the observational evidence. We note that the both types of models, bouncing and inflation, share a very restrictive assumption of a slightly perturbed isotropic and homogeneous universe. That is, they are based on Friedmann cosmology, assuming from the very beginning the approximate isotropy and homogeneity in the primordial space. Such assumption is in accordance with the fact that CMB observations [8] indicate that the universe can be considered approximately isotropic at the time of decoupling. However, substantial amounts of inhomogeneities and anisotropies could play an important role in the primordial universe: on one hand, they could hinder the cosmic inflation driven by inflaton while, on the other hand, they themselves could spontaneously generate an accelerated expansion phase. The latter possibility was discussed, e.g., in [96]. Unfortunately, a non-perturbative investigation into the inhomogeneous primordial universe remains a very challenging problem.

Nevertheless, a less demanding question, though still utterly important, of whether a sufficient amount of anisotropy in the primordial universe could spontaneously generate a cosmic inflation turns out to be tractable. To our best knowledge, this question has never been studied apart from a few related works that we mention below.

In order to address the stated question, we study the most generic anisotropic Bianchi Type IX universe, also known as the mixmaster universe, whose classical model was derived in section 2.2.3 (see Eqs. (2.56), (2.53), and (2.54)). We postpone the study of perturbations to future works, only noticing that some studies of CMB [17] suggest some anomalies at large angular scales that might require this kind of anisotropic extensions to the standard theories in order to explain their origin. Presently, we focus our full attention on the issue of dynamics of anisotropic cosmological quantum background. We quantize the Bianchi IX model and introduce its semiquantum framework in which its dynamics is more accessible, though far from trivial. Hence, we employed the quantization procedure of section 2.4.2 (similar to the one applied in the work presented in section 3.1 for the quantum FLRW model), since it is convenient and encompasses many quantization ambiguities, which makes our study more general.

The classical dynamics of the mixmaster universe is widely known to be very complex. The employed quantization combined with our semiquantum formalism produce a model of similar, if not higher, complexity. Therefore, we address our specific question about the mixmaster dynamics in qualitative terms, which permits to avoid the mathematical and numerical difficulties of finding the full solution. Previous result [39, 40] suggests that as the universe emerges from the bounce the anisotropy continues to be strongly excited, forcing the isotropic geometry of the universe to expand in an accelerated way and for a long period of time. In other words, the quantum mixmaster universe seems to spontaneously generate an inflationary phase. The use of the words ‘suggests’ and ‘seems’ is fair as for deriving that result, in those works crude approximation to the anisotropy potential was used, though the analyzed model was fully quantum. In the present work we resolve this issue in a semiquantum framework without making any approximation to the anisotropy potential [35].

## 6.1 Quantum mixmaster model and semiquantum portrait

Let us recall the Hamiltonian constraint for the classical model of the mixmaster universe (2.56),

$$\begin{aligned} \mathbf{C} &= -\mathbf{C}_{iso} + \mathbf{C}_{ani} \\ \mathbf{C}_{iso} &= \frac{N}{24} \left( \frac{9}{4} p^2 + 36q^{\frac{2}{3}} \right), \quad \mathbf{C}_{ani} = \frac{N}{24} \left( \frac{\mathbf{p}^2}{q^2} + 36q^{\frac{2}{3}} V(\boldsymbol{\beta}) \right), \end{aligned} \quad (6.1)$$

where  $\boldsymbol{\beta} = (\beta_+, \beta_-)$ ,  $\mathbf{p} = (p_+, p_-)$ , and the classical potential reads:

$$V_{IX}(\boldsymbol{\beta}) = \frac{1}{2} e^{4\beta_+} \left( \left[ 2 \cosh(2\sqrt{3}\beta_-) - e^{-6\beta_+} \right]^2 - 4 \right) + 1. \quad (6.2)$$

The phase space range for the two pairs of anisotropic variables is the full plane:  $(\beta_{\pm}, p_{\pm}) \in \mathbb{R}^2$ , while for the isotropic variables is the half-plane:  $(q, p) \in \mathbb{R}_+ \times \mathbb{R}$  (see Eq. (2.54)). As explained below Eq. (2.45), the variable  $q$  describes the isotropic geometry (with  $p$  its conjugate isotropic momentum) and  $\beta_{\pm}$  the distortions to isotropy,

hence the latter are called the anisotropic variables (with  $p_{\pm}$  their respective conjugate anisotropic momenta). They follow the spacetime line element of Eq. (2.55).

The quantization based on generalised coherent states respects the symmetries of the phase space of the Bianchi IX model and produces a self-adjoint representation of relevant observables such as the Hamiltonian. As before, the main outcome of the employed quantization is the resolution of the big-bang singularity via a bouncing dynamics, complemented now with a modification to the anisotropy potential as well. As we explained in section 2.4.3, the semiquantum framework is derived with the use of GCS that also respect the existing symmetries. For the mixmaster, the latter are given by the product of the Weyl-Heisenberg (for the anisotropic planes) and the affine group (for the isotropic half-plane).

In section 3.1.1, we explicitly computed first the quantization of the isotropic background by means of the integral map of Eq. (2.90), obtaining the quantum Hamiltonian, and secondly, by use of a different family of fiducial vectors, applied the semiquantum approximation (in section 3.1.2) via the expectation values as proposed in Eq. (2.94). Here, we make a direct computation of the lower symbol introduced in Eq. (2.93) combining the two steps to obtain the semiquantum version of our background variables. We use a fiducial vector that has the right properties for both quantization and for making the phase space semiquantum portraits. Based on this more general fiducial we obtain a concise formula for the lower symbol of a given observable. The chosen family of fiducial vectors satisfy the physical centering conditions and, at the same time, it preserves the canonical commutation rule. Moreover, we use the two free quantization parameters in the only family of fiducial vectors to understand the quantization as a smearing of phase space observables, and illustrate the quantum uncertainty as coming from the width of the smearing probability distribution. This helps us to explain below how the quantum uncertainty now causes the breakdown of the 4-dimensional background spacetime.

### 6.1.1 Quantization and Semiquantum portrait of the isotropy

Since the isotropic variables are defined in the half-plane, we make use of affine coherent states and adopt the previously described covariant affine quantization, consistent with the symmetry of the half-plane

$$f(q, p) \mapsto A_f = \int_{\mathbb{R}_+^* \times \mathbb{R}} \frac{dq dp}{2\pi\rho(0)} f(q, p) |q, p\rangle \langle q, p|. \quad (6.3)$$

Its combination with the semiquantum portrait evaluating inside the affine coherent states  $|q, p\rangle$  gives the following lower symbol formula:

$$\check{f}(q, p) = \int_{\mathbb{R}_+ \times \mathbb{R}} \frac{dq' dp'}{2\pi\rho(0)} |\langle q, p | q', p' \rangle|^2 f(q', p'), \quad (6.4)$$

which is the average of the function  $f(q, p)$  with respect to the probability distribution  $(q', p') \mapsto \frac{1}{2\pi\rho(0)} |\langle q, p | q', p' \rangle|^2$ . As a fiducial vector we choose one family of unit vectors depending on two free parameters  $\xi$  and  $\nu$ :

$$\psi_0(x) = \frac{1}{\sqrt{2xK_0(\nu)}} e^{-\frac{\nu}{4}(\xi x + \frac{1}{\xi x})}, \quad (6.5)$$

where  $K_0$  is the modified Bessel function of the second kind. It can be shown that we simplify the calculations and ensure the commutation rule  $[A_q, A_p] = 1$  by fixing  $\xi = K_1(\nu)/K_2(\nu)$  (later for the sake of discussion of the classical limit of physical quantities we restore the arbitrary  $\xi$ ). Summarising, we find the following lower symbols:

$$\begin{aligned} \overline{(p^2)} &= p^2 + \frac{K(\nu)}{q^2}, & K(\nu) &= \frac{K_1(\nu)^2 \left(1 + \nu \frac{K_0(\nu)}{K_1(\nu)}\right)}{4K_0(\nu)K_2(\nu)}, \\ \overline{(q^\alpha)} &= Q_\alpha(\nu)q^\alpha, & Q_\alpha(\nu) &= \frac{K_\alpha(\nu)K_{\alpha+1}(\nu)}{K_0(\nu)K_1(\nu)}. \end{aligned} \quad (6.6)$$

where we decided to change the notation of the semiclassical parameters  $K(\nu)$  and  $Q_\alpha(\nu)$  in order to differentiate them from the ones with gothic-style letters obtained in the Friedmann model of chapter 3, for different families of fiducial vectors.

### 6.1.2 Quantization and semiclassical portrait of the anisotropy

The anisotropic variables cover the full plane. Therefore, we make use of a quantization method based on the Weyl-Heisenberg group of translations, that respect the symmetry of the full plane. We consider a four-dimensional phase space  $\mathbb{R}^4 = \mathbb{R}^2 \times \mathbb{R}^2$  made of two pairs of canonical variables,  $(\beta_+, p_+)$  and  $(\beta_-, p_-)$ , and define the covariant Weyl-Heisenberg integral quantization of a function  $f(\mathbf{r}_\pm)$  in the phase space  $\mathbf{r}_\pm = (\beta_\pm, p_\pm) \in \mathbb{R}^2$  (we omit the index  $\pm$  in the sequel) by looking at the general quantization map of Eq. (2.90), and making the analogy for the current phase space variables  $((q, p) \rightarrow (\beta_\pm, p_\pm))$ :

$$f(\mathbf{r}) \mapsto A_f := \int_{\mathbb{R}^2} f(\mathbf{r}) \mathcal{Q}(\mathbf{r}) \frac{d^2\mathbf{r}}{2\pi c_Q}, \quad (6.7)$$

The family of operators  $\mathcal{Q}(\mathbf{r})$  on  $\mathcal{H} = L^2(\mathbb{R}, dx)$  has the form defined by Eq. (2.91), where now the employed UIR corresponds to that of the Weyl-Heisenberg group:

$$U_W(\mathbf{r}) = e^{i(pQ - \beta P)}, \quad (6.8)$$

and they satisfy the resolution of the identity:

$$\int_{\mathbb{R}^2} \mathcal{Q}(\mathbf{r}) \frac{d^2\mathbf{r}}{2\pi c_Q} = \mathbb{1}_{\mathcal{H}}, \quad (6.9)$$

where  $\mathcal{Q}(\mathbf{r}) = U_W(\mathbf{r}) \mathcal{Q}_0 U_W(\mathbf{r})^\dagger$ , and the chosen  $\mathcal{Q}_0$  are admissible provided that the Weyl-Heisenberg group sets the normalization constant to be  $c_Q = \text{Tr}(\mathcal{Q})(\mathbf{r}) = 1$ , since  $\mathcal{Q}(\mathbf{r})$  is a family of unit-trace operators. Thus, the choice of a quantization procedure is reduced to the choice of a single operator,  $\mathcal{Q}_0$  (i.e., the choice of a family of normalized fiducial states  $|\psi_0\rangle\rangle$ ).

Equivalently, one may use the weight function,  $\Pi(\mathbf{r})$ , which is defined via the Weyl-Heisenberg transform of  $\mathcal{Q}_0$ , (see Eqs. (2.76) and (2.78)),

$$\Pi(\mathbf{r}) := \text{Tr}(U_W(-\mathbf{r}) \mathcal{Q}_0) \implies \mathcal{Q}_0 = \int_{\mathbb{R}^2} U_W(\mathbf{r}) \Pi(\mathbf{r}) \frac{d^2\mathbf{r}}{2\pi}, \quad (6.10)$$

to determine the quantization procedure as suggested in Eq. (2.96) and below, allowing us to use the alternative (more manageable) direct formula for the lower

symbol of Eq. (2.98) to obtain the semiquantum description. Then, the quantization method is reduced to the choice of the appropriate weight function  $\Pi(\mathbf{r})$ . It is straightforward to see that  $\text{Tr}(\mathcal{Q}_0) = \Pi(0)$  and hence we must assume  $\Pi(0) = 1$ . The weight  $\Pi(\mathbf{r}_\pm)$  defines the extent of coarse graining of the phase space  $\mathbf{r}_\pm = (\beta_\pm, p_\pm) \in \mathbb{R}^2$ . Notice that the standard canonical quantization is obtained for  $\Pi(\mathbf{r}) = 1$ , or equivalently for  $\mathcal{Q}_0 = 2P$ , where  $P$  is the parity operator defined as  $PU_W(\mathbf{r})P = U_W(-\mathbf{r})$  [55]. By using the covariant Weyl-Heisenberg integral quantization, the canonical commutation rule is always preserved for the basic canonical pair, independently of the choice of  $\Pi(\mathbf{r})$  (or  $\mathcal{Q}_0$ ), since we get:  $A_\beta = \hat{\beta} + c_0$ ,  $A_p = \hat{p} + d_0$ , with arbitrary  $c_0, d_0 \in \mathbb{R}$ ,  $\rightarrow [A_\beta, A_p] = i\mathbb{1}$ , satisfying the canonical commutation between the anisotropic phase space variables.

Let us then assume the following Gaussian weight function centred in the origin,

$$\Pi(\beta, p) = e^{-\frac{\beta^2}{\sigma^2}} e^{-\frac{p^2}{\omega^2}}, \quad (6.11)$$

where  $\Pi(\beta, p) = \Pi(-\beta, -p)$  and  $\Pi(0, 0) = 1$ . The width parameters  $\sigma$  and  $\omega$  encode the uncertainty in dealing with a given point in the phase space. The symplectic Fourier transform of the weight reads,

$$\mathcal{F}(\Pi)(\beta, p) = \frac{\sigma\omega}{2} e^{-\frac{1}{4}(\omega^2\beta^2 + \sigma^2p^2)}, \quad (6.12)$$

and their convolution reads

$$\mathcal{F}(\Pi) * \mathcal{F}(\Pi)(\beta, p) = \frac{\pi\sigma\omega}{2} e^{-\frac{1}{8}(\omega^2\beta^2 + \sigma^2p^2)}. \quad (6.13)$$

Hence, the lower symbol formula takes the form of regularizing Gaussian convolutions:

$$\check{f}(\beta, p) = \int_{\mathbb{R}^2} \frac{\pi\sigma\omega}{2} e^{-\frac{1}{8}(\omega^2(\beta' - \beta)^2 + (\sigma^2(p' - p)^2))} f(\beta', p') \frac{d\beta' dp'}{4\pi^2}. \quad (6.14)$$

With this formula we find

$$\widetilde{(e^{-\alpha\beta})} = e^{\frac{4\alpha^2}{\omega^2}} e^{-\alpha\beta}, \quad \widetilde{(p^2)} = p^2 + \frac{8}{\sigma^2}, \quad (6.15)$$

and the lower symbol of the semiquantum anisotropy potential,

$$\begin{aligned} \check{V}(\beta_\pm) = & \frac{1}{3} \left( D(4\sqrt{3}, 4) e^{4\sqrt{3}\beta_- + 4\beta_+} + D(4\sqrt{3}, 4) e^{-4\sqrt{3}\beta_- + 4\beta_+} + D(0, 8) e^{-8\beta_+} \right) \\ & - \frac{2}{3} \left( D(2\sqrt{3}, 2) e^{-2\sqrt{3}\beta_- - 2\beta_+} + D(2\sqrt{3}, 2) e^{2\sqrt{3}\beta_- - 2\beta_+} + D(0, 4) e^{4\beta_+} \right) + 1, \end{aligned} \quad (6.16)$$

where the  $D(x, y) = e^{\frac{4x^2}{\omega^2}} e^{\frac{4y^2}{\omega^2}}$  are regularization factors issued from our choice of the Gaussian weights. The semiquantum anisotropy potential (6.16) is plotted in Fig. 6.1, in comparison with the classical (6.2) mixmaster potential.

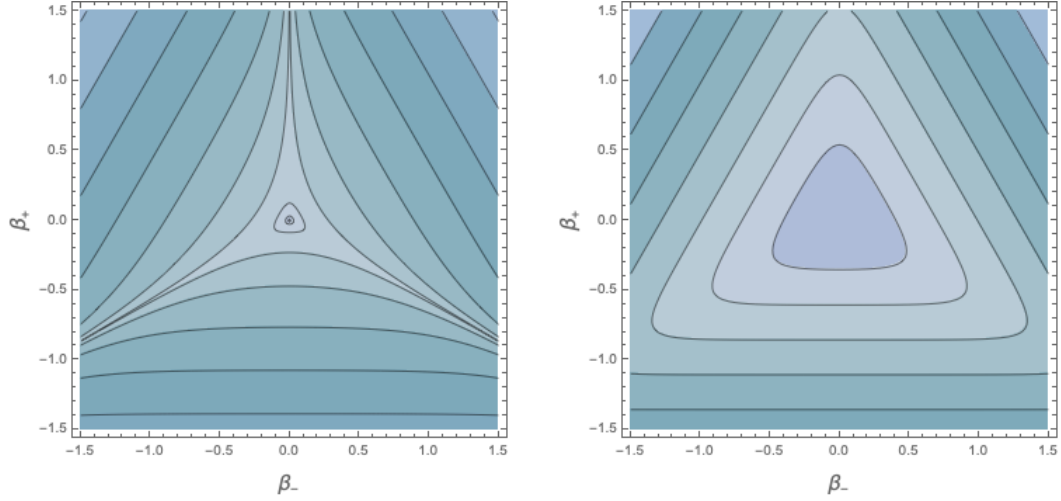


FIGURE 6.1: The classical (left) and semiquantum (right) ( $\tau_{\pm} = 5 = \sigma_{\pm}$ ) anisotropy potential. The classical potential comprises three narrowing channels with their bottoms asymptotically ( $\beta_+ \rightarrow \infty$  or  $\beta_+ \rightarrow -\infty$ ) approaching the zero value. In the semiquantum case the three channels become confined due to the semiquantum corrections as their bottoms raise indefinitely for  $\beta_+ \rightarrow \infty$  or  $\beta_+ \rightarrow -\infty$ .

### 6.1.3 Semiquantum portrait of the total Hamiltonian constraint

The semiquantum portrait of the Hamiltonian constraint (6.1) reads (for  $N = 24$ ) as

$$\check{C} = \frac{9}{4} \left( p^2 + \frac{K(v)}{q^2} \right) - Q_{-2}(v) \frac{\mathbf{p}^2 + \sum_{\pm} \frac{8}{\sigma_{\pm}^2}}{q^2} - 36Q_{\frac{2}{3}}(v)q^{\frac{2}{3}}[\check{V}(\boldsymbol{\beta}) - 1]. \quad (6.17)$$

The quantum potential for the isotropic geometry  $\propto q^{-2}$  is repulsive if and only if  $\frac{9}{4}K(v) > Q_{-2}(v) \sum_{\pm} \frac{8}{\sigma_{\pm}^2}$ , which we assume to hold in sequel. For convenience, we introduce

$$K_{eff}(v, \sigma_{\pm}) := K(v) - \frac{32}{9} \sum_{\pm} \frac{Q_{-2}(v)}{\sigma_{\pm}^2} > 0. \quad (6.18)$$

We derive from the semiquantum Hamiltonian constraint (6.17) the following Hamilton equations:

$$\dot{q} = \frac{9}{2}p, \quad (6.19)$$

$$\dot{p} = \frac{9}{2} \frac{K_{eff}}{q^3} - 2Q_{-2} \frac{\mathbf{p}^2}{q^3} + 24Q_{\frac{2}{3}} q^{-\frac{1}{3}} [\check{V}(\boldsymbol{\beta}) - 1], \quad (6.20)$$

$$\dot{\beta}_{\pm} = -2Q_{-2} \frac{p_{\pm}}{q^2}, \quad (6.21)$$

$$\dot{p}_{\pm} = 36Q_{\frac{2}{3}} q^{\frac{2}{3}} \partial_{\pm} \check{V}(\boldsymbol{\beta}), \quad (6.22)$$

where

$$\begin{aligned} Q_{-2} &= Q_{-2}(\nu) = \frac{K_2(\nu)}{K_0(\nu)}, \\ Q_{\frac{2}{3}} &= Q_{\frac{2}{3}}(\nu) = \frac{K_{\frac{2}{3}}(\nu)K_{\frac{5}{3}}(\nu)}{K_0(\nu)K_1(\nu)}. \end{aligned} \quad (6.23)$$

We have thus obtained a dynamical system in the full phase space  $\mathbb{R}_+^* \times \mathbb{R} \times \mathbb{R}^4$  to be now examined. It involves six positive otherwise arbitrary quantization parameters:  $\nu, \sigma_{\pm}, \omega_{\pm}$  (degree of confidence...) and defines dynamical trajectories as a function of five initial conditions.

We find the semiquantum model to be invariant under the following scalings:

$$\begin{aligned} t' &= \frac{t}{\delta^{1/2}}, \quad q' = \frac{q}{\delta^{3/4}}, \quad p' = \frac{p}{\delta^{1/4}}, \\ \beta'_{\pm} &= \beta_{\pm}, \quad p'_{\pm} = \frac{p_{\pm}}{\delta}, \quad K'_{eff} = \frac{K_{eff}}{\delta^2}. \end{aligned} \quad (6.24)$$

We note that unlike the classical scale transformations (2.58), the above scalings involve  $K_{eff}$ , a non-dynamical quantum repulsion coefficient. This was to be expected as the quantization introduces a new scale into the system, i.e. the Planck scale, and thereby destroying the exact scaling symmetry present in the classical model. Nonetheless, if a solution to the semiquantum model with a fixed value of  $K_{eff}$  is known, then respective solutions to the model for all the other values of  $K_{eff}$  are also known.

It is straightforward to find the semiquantum versions of the geometric quantities (2.59),

$$\begin{aligned} \check{R}_{iso} &= \frac{3Q_{\frac{2}{3}}}{2q^{\frac{4}{3}}}, \quad \check{R}_{ani} = -\frac{3Q_{\frac{2}{3}}\check{V}(\beta)}{2q^{\frac{4}{3}}}, \\ \check{\sigma}^2 &= \frac{Q_{-2}\mathbf{p}^2}{48q^4}, \quad \check{R}_Q = \frac{3K_{eff}}{32q^4}, \end{aligned} \quad (6.25)$$

as well as the semiquantum version of the generalized Friedmann equation (2.60):

$$H^2 = \frac{1}{6}\rho_r - \frac{1}{6}\check{R}_{iso} + \frac{1}{3}\check{\sigma}^2 - \frac{1}{6}\check{R}_{ani} - \frac{1}{6}\check{R}_Q, \quad (6.26)$$

where we added radiation as the only matter component, in concordance with the classical mixmaster model introduced in section 2.2.3 (see below Eq. (2.60)).

We interpret the difference between the obtained semiquantum and the initial classical expressions to be the effect of quantum dispersion imposed on the geometry of the universe. The largest discrepancy between the classical and the semiquantum model is given by the repulsive quantum potential  $\frac{K_{eff}}{q^2}$  (or, equivalently, the quantum curvature  $\check{R}_Q$ ). Another strong quantum feature is given by modifications to the anisotropy potential  $\check{V}(\beta)$ . The remaining quantum features are introduced into the Hamilton equations (6.19)-(6.22) through the constants  $Q_{-2}$  and  $Q_{\frac{2}{3}}$ .

In particular, due to the Hamilton equations coupling between the isotropic and anisotropic degrees of freedom, in Eq. (6.21), the constant  $Q_{-2}$  alters the *classical* relation between the time derivative of the intrinsic three-metric variables  $\beta_{\pm}$  and their respective momenta  $p_{\pm}$  that define the embedding of the intrinsic geometry

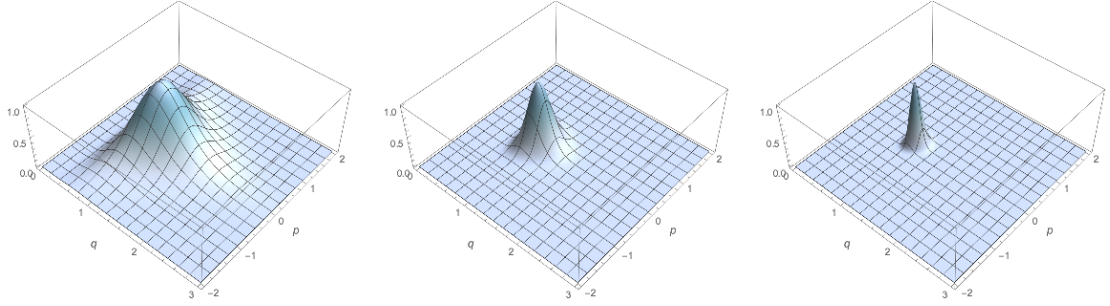


FIGURE 6.2: The smearing probability distribution producing quantum corrections for  $\nu = 30, 150, 660$  (from left to right). For small values of  $\nu$  our quantization procedure yields a very quantum system with large quantum uncertainties. On the other hand, for  $\nu \rightarrow \infty$  our quantization procedure reproduces the exact classical system with vanishing uncertainties.

into a spacetime (extrinsic curvature), which must hold in any 4-d spacetime. Therefore, with  $Q_{-2} \neq 1$ , a 4-d spacetime no longer exists<sup>1</sup>. This comes from the fact that the momenta  $(p, p_{\pm})$  do not commute with the three-geometry variables  $(q, \beta_{\pm})$ . The probability distribution smearing the isotropic 4-geometry (introduced in Eq. (6.4)) reads (after restoring the arbitrary parameter  $\zeta$ )

$$\frac{1}{2\pi c_{-1}} \left| \frac{K_0 \left( \nu \frac{q+q'}{2\sqrt{qq'}} \sqrt{1 + \frac{4iqq'(p'-p)}{v\zeta(q+q')}} \right)}{K_0(\nu)} \right|^2, \quad (6.27)$$

where the parameters  $\nu$  and  $\zeta$  control the quantum dispersion induced by the affine coherent states. For  $\zeta = 1/\nu$  and  $\nu \rightarrow \infty$ , the regularizing probability distribution converges to the Dirac delta  $\delta(q - q')\delta(p - p')$  (in distributional sense) and all the physical quantities obtained from (6.4) remain classical and satisfy the classical relations. However, the non-vanishing quantum uncertainty between  $q$  and  $p$  requires  $\nu < \infty$ , which produces a *smearred geometry*. In order to visualize the quantization process the probability distribution for the state  $(q', p') = (1, 0)$  for three different values of  $\nu$  is plotted in Fig. 6.2.<sup>2</sup>

Analogously, the probability distribution associated with the lower symbol formula for anisotropic geometry (6.14) is a Gaussian with the arbitrary parameters  $\sigma_{\pm}$  and  $\omega_{\pm}$ . Taking  $\sigma_{\pm} \rightarrow \infty$  and  $\omega_{\pm} \rightarrow \infty$  removes the quantum uncertainty between  $\beta_{\pm}$  and  $p_{\pm}$ , the Gaussian probability distribution converges to the Dirac delta  $\delta(\beta_{\pm} - \beta'_{\pm})\delta(p_{\pm} - p'_{\pm})$  and all the physical quantities obtained from (6.14) retain their classical properties.

<sup>1</sup>However, the requirement for the existence of the classical limit for the anisotropic variables equation of motion (6.21) in this semiquantum model could be satisfied by renormalization of  $\beta_{\pm}$  by the constant  $Q_{-2}$ , or the convenient choice of  $\nu$ .

<sup>2</sup>In these plots we can also observe how selecting the physical origin of the classical phase space  $(q', p') = (1, 0)$ , the chosen fiducial vector (6.5) preserves the centering for the expectation values of  $\hat{Q}$  and  $\hat{P}$  in the semiquantum phase space around  $(q, p) = (1, 0)$  independently of the value of  $\nu$ , however with non-negligible smearing.

## 6.2 Semiquantum dynamics

The semiquantum phase space exhibits a generic quantum bounce, replacing the big-bang and big-crunch singularities, and a classical late-time re-collapse. The anisotropy energy fuels the isotropic contraction and expansion. Moreover, the expansion and contraction can be fuelled by various matter contributions. In this model, for simplicity, we keep only one matter term that we chose to be radiation, that enters into the Hamiltonian as  $-\frac{M_r}{q^{2/3}}$ , with  $M_r$  a positive constant. We now proceed to examine the dynamics of the semiquantum mixmaster model, starting with the simplest case, the fully isotropic Friedmann case, in order to later observe in a clearer way the effects caused by non-negligible anisotropy.

### 6.2.1 Isotropic dynamics

Let us start by assuming perfectly spherical spatial sections with  $\beta_{\pm} = 0 = p_{\pm}$ . Then, the isotropic part of the constraint is the only non-trivially vanishing,

$$\check{C}_{iso} = \frac{9}{4} \left( p^2 + \frac{K_{eff}}{q^2} \right) + 36Q_{\frac{2}{3}} q^{\frac{2}{3}} - \frac{M_r}{q^{2/3}}. \quad (6.28)$$

For convenience, we introduce  $L := 36Q_{\frac{2}{3}}$ . Making use of the equation (6.19) and the vanishing of the constraint (6.28) we express the conformal time as a function of  $q$ ,

$$\int d\eta = \int q^{-\frac{2}{3}} dt = \int \frac{dq}{q^{\frac{2}{3}} \dot{q}} = \frac{1}{4\sqrt{L}} \times \ln \left( 2\sqrt{L} \sqrt{Lq^{\frac{8}{3}} + M_r q^{\frac{4}{3}} - \frac{9}{4} K_{eff}} + 2Lq^{\frac{4}{3}} + M_r \right). \quad (6.29)$$

The above relation is easily inverted if we neglect the intrinsic curvature,  $L = 0$ , yielding the approximate solution

$$q(\eta) = \left( 4M_r \eta^2 + \frac{9}{4} \frac{K_{eff}}{M_r} \right)^{\frac{3}{4}}. \quad (6.30)$$

where the above approximation breaks down for large universes with non-negligible isotropic curvature. For negligible  $L$  we find that the amount of time needed for the universe to bounce back to the same volume  $q^2$  reads,

$$\Delta\eta = \frac{1}{\sqrt{R}} \sqrt{q^{\frac{4}{3}} - \frac{9}{4} \frac{K_{iso}}{R}},$$

$$\Delta t = \frac{1}{2\sqrt{R}} \left[ q^{\frac{2}{3}} \sqrt{q^{\frac{4}{3}} - \frac{9K_{iso}}{4R}} + \frac{9K_{iso}}{4R} \ln \left( \frac{q^{\frac{2}{3}} + \sqrt{q^{\frac{4}{3}} - \frac{9K_{iso}}{4R}}}{\sqrt{\frac{9K_{iso}}{4R}}} \right) \right],$$

which is useful for numerical integrations.

The quantum bounce and the classical re-collapse both occur when  $p = 0 = \dot{q}$ , where the Hamiltonian constraint yields

$$\frac{9}{4} K_{eff} + Lq^{\frac{8}{3}} - M_r q^{\frac{4}{3}} = 0. \quad (6.31)$$

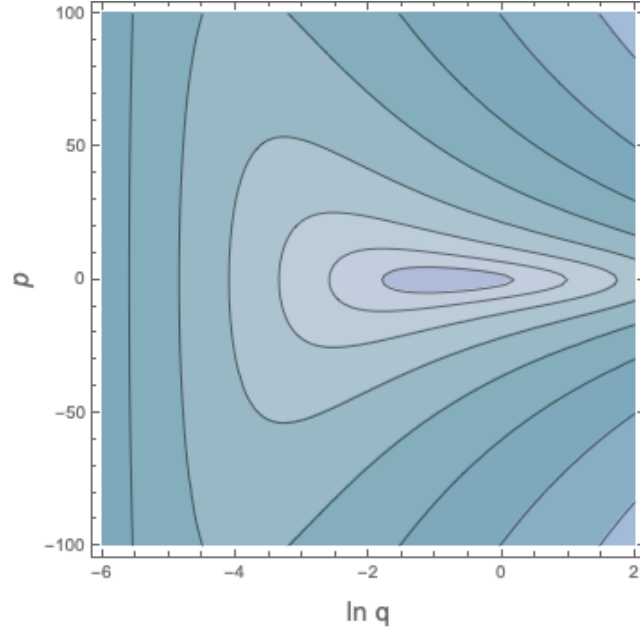


FIGURE 6.3: The isotropic bouncing solutions for  $\nu = 10$  and various values of  $M_r$  ( $\sigma_{\pm} = 5 = \omega_{\pm}$ ).

If we assume that at the quantum bounce the intrinsic curvature is negligible, i.e.  $L = 0$  as before, whereas at the classical re-collapse the quantum repulsion is negligible, i.e.  $K_{iso} = 0$ , then we find the minimal and maximal  $q$  to read,

$$q_{min} = \left( \frac{9K_{eff}}{4M_r} \right)^{\frac{3}{4}}, \quad q_{max} = \left( \frac{M_r}{L} \right)^{\frac{3}{4}}. \quad (6.32)$$

Furthermore, the maximum  $p = p_{max}$  occurs for  $q$  such that

$$\frac{\partial \check{C}_{iso}}{\partial q} \propto \frac{9}{2} K_{eff} - \frac{2}{3} M_r q^{\frac{4}{3}} - \frac{2}{3} L q^{\frac{8}{3}} = 0, \quad (6.33)$$

which after neglecting  $L$  gives  $q = (27)^{\frac{1}{4}} q_{min}$ , at which

$$p_{max} = \frac{4}{3(27)^{\frac{1}{4}} \sqrt{2}} \frac{M_r^{3/4}}{K_{eff}^{1/4}}. \quad (6.34)$$

A few bouncing trajectories are plotted in Fig. 6.3. In the isotropic case, the only term of the generalized-Friedmann equation that can cause accelerated expansion is the quantum curvature  $\check{R}_Q$ , just after finishing the contraction phase and initiating the expanding one. We note that in this case the phase of accelerated expansion is very brief and clearly insufficient from the point of view of the process of structure formation at a substantial range of cosmological scales. Indeed, combining the minimal value  $q_{min}$  (6.32) with the value of  $q$  at which the acceleration terminates (defined in Eq. (6.38) to be discussed later) we find that  $\Delta N = \ln \left( \frac{a_{end}}{a_{min}} \right) = \ln(\sqrt{2})$  e-folds. This is due to the fact that the term  $\check{R}_Q$  dominates the dynamics during a brief amount of time.

### 6.2.2 Anisotropic dynamics

The anisotropy makes the dynamics of the universe too complex to be solved analytically. In order to reduce the complexity of the system it is common to employ the adiabatic approximation [37, 38]. In this approximation the complicated, oscillatory motions of the anisotropic variables are replaced with their energy averaged over many oscillations under the assumption that the value of the isotropic variable  $q$  does not change significantly during this time. Moreover, the anisotropy potential that is responsible for the oscillations also requires an approximation such as the harmonic approximation or the steep-wall approximation. Unfortunately, these approximations have a rather restricted regime of applicability. Therefore, in the present work we choose to combine numerical computations with some analytical estimates, while keeping fully the potential and the anisotropic oscillations.

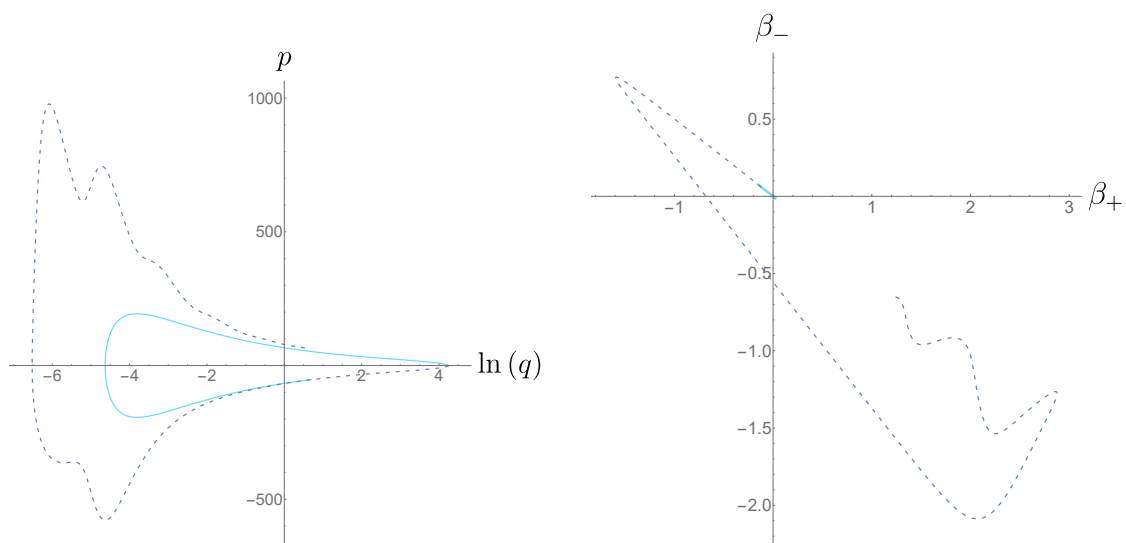


FIGURE 6.4: Two cycles in the evolution of an anisotropic universe plotted in the  $(q, p)$ - and  $(\beta_-, \beta_+)$ -planes. The first and the second cycle are given by solid and dashed curves, respectively. Despite the fact that the first one is very isotropic and resembles the solutions of Fig. 3, the second one accumulates anisotropy on the approach to the bounce that now happens at a smaller volume. The dynamics around the second bounce is very asymmetric in the  $(q, p)$ -plane. The trajectory in the  $(\beta_-, \beta_+)$ -plane starts around the minimum where it remains for the first cycle. Then during the second cycle it moves to larger values of  $\beta_{\pm}$  where it bounces off the potential walls producing oscillations. We set the following initial data:  $q = 2.0$ ,  $p = -52.6579$ ,  $\beta_+ = -0.01$ ,  $\beta_- = 0.005$ ,  $p_+ = 0.0$ ,  $p_- = 0.0$ . We set the parameters as follows:  $\omega_{\pm} = 50$ ,  $\sigma_{\pm} = 100$ ,  $\nu = 37.5$  ( $K_{eff} = 9.255$ ),  $R = 10^4$ .

In Fig 6.4 we present numerically integrated two cycles of a generic semiquantum mixmaster solution. As in the isotropic case, the anisotropic universe avoids the singularity through bounces. The quantum potential diminishes rapidly after the bounces and the anisotropy takes over the dynamics, leaving some imprints. Finally, the matter density exceeds the anisotropic energy density, and the standard Friedmann cosmology begins. Note that the two cycles (one given by the solid curve and the other by the dashed curve) are very different. The first one follows closely the isotropic solution and the  $\beta_{\pm}$ 's remain very small, whereas in the next cycle anisotropy develops as the universe contracts and the  $\beta_{\pm}$ 's start oscillating inside

one of the channels. It results in an asymmetric bounce, leading to the destruction of the cosmic periodicity with each new cosmic cycle being different from the previous one. One typically observes a few oscillations in the expansion rate right after the bounce. Moreover, a high rate of post-bounce expansion can last for an extended period of time as seen from the behavior of the dynamical variable  $p$ . In [39] a similar behavior was observed and explained by the growth of the anisotropic energy triggered by the bounce. By the virtue of the Hamiltonian constraint, this newly produced anisotropic energy has to be balanced by the growth of the isotropic energy. During the bounces, the entire isotropic energy takes the form of the repulsive potential. As the universe starts to re-expand, the entire isotropic energy is transferred back to isotropic expansion. The observed dynamics points to the possibility for a phase of sustained accelerated post-bounce expansion lasting for some e-folds. We shall investigate this issue in the following section.

Let us show now that a bounce exists in the generic semiquantum dynamics of the mixmaster universe. We note that the bounce must occur in the following subset of the constrained surface:

$$p = 0, \quad \dot{p} = \frac{6K_{eff}}{q^3} - \frac{8Q_{-2}}{3} \frac{\mathbf{p}^2}{q^3} > 0. \quad (6.35)$$

The above set of conditions defines a 4-dimensional subspace in the 5-dimensional constraint surface. A generic trajectory must pass through that region or even cross it infinitely many times. To see that in fact any trajectory should bounce let us follow the dynamics of  $p$  along a typical trajectory in the constraint surface<sup>3</sup>:

$$\dot{p} = \frac{\frac{9}{2}K_{eff}}{q^3} - \frac{2Q_{-2}}{q^3} \left\{ \mathbf{p}^2 - 12 \frac{Q_{\frac{2}{3}}}{Q_{-2}} q^{\frac{8}{3}} [\check{V}(\boldsymbol{\beta}) - 1] \right\}. \quad (6.36)$$

We note that the first and the third terms are positive while the second one negative, and their absolute values grow as the universe contracts with  $q \rightarrow 0$  and  $p < 0$ . As the anisotropic variables oscillate inside the potential walls the anisotropy energy (or, its part) is being transferred back and forth between the second (the kinetic) and the third (the potential) term. Initially, the sum of these two terms is negative and the first term is negligible as the universe is contracting more and more rapidly ( $\dot{p} < 0$ ). However, because of the oscillatory energy transfer, the absolute value of the two terms must grow slower than  $q^{-3}$ . Hence, down the line at some value of  $q > 0$  their sum must become dominated by the first term that is positive and grows as  $q^{-3}$ . As a result, for sufficiently small value of  $q$  (provided that the bounce has not occurred before) the dynamics is sufficiently well-approximated by

$$\dot{q} = \frac{9}{2}p, \quad \dot{p} \approx \frac{\frac{9}{2}K_{eff}}{q^3}, \quad (6.37)$$

leading to essentially the isotropic dynamics that we showed previously to be non-singular. Hence, the bounce must eventually happen for any trajectory.

The set of semiquantum Hamilton equations constitutes a non-linear system whose dynamics is chaotic. Therefore, although the standard solution in general

<sup>3</sup>The difference between  $\dot{p}$  in Eqs (6.35) and (6.36) is vanishing at the constraint surface.

follows a evolution like the one described above for Fig. 6.4, the form of the cycles in the plots of the isotropic phase space trajectories can vary a lot depending on both the initial values of the six dynamical degrees of freedom and the values of the semiquantum parameters. For each initial condition in the isotropic half-plane there remains a huge amount of freedom in determining the initial data for the anisotropic variables inside the anisotropic potential. This leads to infinitely many trajectories for the isotropic geometry from a given point  $(q, p)$ . These trajectories can differ from each other a lot, in particular, they can exhibit very different post-bounce dynamics with widely varying inflationary phases depending on how strong and long-lasting is the influence of each of the anisotropic terms ( $\tilde{R}_{ani}$  or  $\check{\sigma}^2$ ).

## 6.3 Accelerated expansion

The quantum dynamics of the mixmaster universe is very rich and could, for instance, exhibit a prolonged phase of accelerated expansion during which the local structure inside the mixmaster universe is amplified in the same way as it happens for inflationary phase driven by a scalar field. The investigated issue is thus important. The existence of a robust inflationary phase in a bouncing anisotropic model could provide a serious challenge to the hypothesis of inflaton and its paramount role in the primordial evolution. On the other hand, the non-existence of such a phase in our model should in principle strengthen the existing arguments in favour of inflaton as another attempt at challenging its exceptional status fails.

### 6.3.1 General remarks

The accelerated expansion takes place when  $\ddot{a} > 0$ , or

$$\frac{d}{d\eta} \mathcal{H} > 0, \quad (6.38)$$

where  $\mathcal{H} = \dot{a}/a = \dot{\eta}$  is the conformal Hubble parameter<sup>4</sup>. When the conformal Hubble horizon  $\mathcal{H}^{-1}$  is shrinking, perturbation modes of fixed co-moving wavelengths leave the horizon and become amplified. It is often assumed that the span of wavelengths that exit the horizon during the inflationary phase is such that  $k_{fin}/k_{ini} \gtrsim 10^8$ . This is equivalent to say that the increase in orders of magnitude of the conformal Hubble rate  $\mathcal{H}$  during the inflationary accelerated expansion is assumed to be at least  $10^8$ . The growth in the number of wavelengths that cross the horizon reads:

$$\frac{dk}{k_{ini}} = \frac{d\mathcal{H}}{\mathcal{H}_{ini}} = \frac{1}{\mathcal{H}_{ini}} \frac{d\mathcal{H}}{dN} dN, \quad (6.39)$$

where we have expressed the growth of the superhorizon scales as a function of the number of e-folds:  $N = \ln(a/a_{ini})$ . We find this unit of time to be very convenient. It measures the number of times the space grows during expansion (or shrinks during contraction). The range of scales that leave the horizon during a finite number of e-folds  $\Delta N$  can be estimated from the initial state of the system via the Taylor

<sup>4</sup>Differentiation with respect to cosmic and conformal time are denoted by  $'$  and  $''$ , respectively.

expansion:

$$\frac{k_{fin}}{k_{ini}} = \frac{1}{\mathcal{H}} \frac{d\mathcal{H}}{dN} \Big|_{ini} \Delta N + \frac{1}{2} \frac{d}{dN} \left( \frac{1}{\mathcal{H}} \frac{d\mathcal{H}}{dN} \right) \Big|_{ini} (\Delta N)^2 + \mathcal{O}(\Delta N^2). \quad (6.40)$$

If we assume that the second- (and any higher-) order term is much smaller than the first one, i.e.,  $\left| \frac{(\Delta N)^2}{2} (\ln \mathcal{H})_{,NN} \Big|_{ini} \ll k_{fin}/k_{ini}$ , then for most of the inflationary phase the Hubble horizon remains more or less constant and the phase lasts for  $\Delta N = \frac{k_{fin}}{k_{ini}} \left( \frac{1}{\mathcal{H}} \frac{d\mathcal{H}}{dN} \right)^{-1} \Big|_{ini}$  of e-folds.

### 6.3.2 Proper analysis

If an inflationary phase occurs in the semiquantum mixmaster model it must be driven by either the quantum curvature  $\frac{1}{6}\check{R}_Q$  or the anisotropy energy  $\frac{1}{3}\check{\sigma}^2 - \frac{1}{6}\check{R}_{ani}$ , or a combination of both. We therefore neglect the radiation and the isotropic curvature and re-write the generalized Friedmann Eq. (6.26) as

$$H^2 = \frac{1}{6}\check{\rho}_{ani} - \frac{1}{6}\check{R}_Q > 0, \quad (6.41)$$

where we introduced the notion of the anisotropy energy density  $\frac{1}{6}\check{\rho}_{ani} = \frac{1}{3}\check{\sigma}^2 - \frac{1}{6}\check{R}_{ani}$ .

We use the above equation to derive the Raychaudhuri equation (the equation describing the rate of change of expansion<sup>5</sup> [97]) with the expansion parameter replaced by the conformal Hubble parameter. Let us assume that at each moment of time the right-hand side terms are well-approximated by power functions in the scale factor,

$$\frac{1}{6}\check{\rho}_{ani} = \frac{\lambda_{ani}}{a^{n_{ani}+2}}, \quad \frac{1}{6}\check{R}_Q = \frac{\lambda_Q}{a^6}, \quad (6.42)$$

( $\lambda_{ani} > 0$ ,  $\lambda_Q > 0$ ), i.e., their logarithms are approximately linear in the number of e-folds,  $N \propto \ln a$ . Note that the anisotropy effectively acts as a barotropic fluid with  $\frac{p}{\rho} = w_{ani} = (n_{ani} - 1)/3$ . We find

$$\frac{d}{d\eta} \mathcal{H} = \frac{a}{2} \frac{d}{da} \mathcal{H}^2 = -\frac{n_{ani}\lambda_{ani}}{2a^{n_{ani}}} + \frac{2\lambda_Q}{a^4}. \quad (6.43)$$

In order for the accelerated expansion to occur the condition (6.38) must hold, that is,

$$0 < \lambda_Q - \frac{n_{ani}\lambda_{ani}}{4a^{n_{ani}-4}}, \quad (6.44)$$

<sup>5</sup>The Raychaudhuri equation express the rate of change for the expansion of of a congruence of timelike geodesics in a given spacetime. We derive an analogue to such equation by fixing the correspondence between our semiquantum geometric quantities expressed in terms of the canonical variables and the geometrical concepts related to the congruence of geodesics (expansion, shear, curvature).

which must be consistent with the Friedmann equation (6.41),

$$0 < \frac{\lambda_{ani}}{a^{n_{ani}-4}} - \lambda_Q. \quad (6.45)$$

Let us first assume that  $\lambda_Q = 0$ , that is, the influence of the quantum curvature on the expansion is negligible. By Eq. (6.44), it is possible only if  $n_{ani} < 0$ . This behaviour coincides with the barotropic fluid behaviour with  $w_{ani} < -\frac{1}{3}$ . We will see below that this behaviour of the anisotropy energy density is impossible neither in the classical nor in the semiquantum model.

Since we neglect the radiation it is impossible to neglect anisotropy by putting  $\lambda_{ani} = 0$ , i.e., it has to be present in the expanding universe if the condition (6.45) is to hold. Moreover, we already proved in the isotropic case that, if quantum curvature is the only possible source of accelerated expansion, such phase lasts for very short time. Therefore, the anisotropic energy cannot be neglected when the quantum curvature stops driving the dynamics in order to sustain the accelerated expansion.

The remaining possibility is that both the anisotropy and the quantum curvature are important in the expanding universe. In this case the above conditions are combined into ( $n_{ani} > 0$ ):

$$n_{ani}\lambda_Q < \frac{n_{ani}\lambda_{ani}}{a^{n_{ani}-4}} < 4\lambda_Q, \quad (6.46)$$

from which we see immediately that  $0 < n_{ani} < 4$ . Upon dividing the above inequality by  $n_{ani}\lambda_Q$  and fixing  $\frac{\lambda_{ani}}{\lambda_Q} e^{N_i(4-n_{ani})} = 1$ ,  $\frac{\lambda_{ani}}{\lambda_Q} e^{N_f(4-n_{ani})} = \frac{4}{n_{ani}}$ , we obtain

$$e^{\Delta N(4-n_{ani})} = \frac{4}{n_{ani}}, \quad (6.47)$$

where  $\Delta N = N_f - N_i$ . One may verify that there are two solutions to the above equation for  $n_{ani}$  if  $\Delta N > \frac{1}{4}$ . The accelerated expansion must occur at least for around  $\Delta N \gtrsim 60$  e-folds in order to enough number of modes become super-horizon and match the current observations as the standard inflationary predictions do [26, 98]. This means that  $n_{ani}$  must be very small and close to  $n_{ani} = 4e^{-4\Delta N}$  during the accelerated expansion phase. This behavior coincides with the barotropic fluid behavior for the barotropic index  $w_{ani} \approx -\frac{1}{3}$ , which, as we show below, can not last sufficiently long to yield a robust inflationary phase. Another solution is  $n_{ani} = 4$ , which lies in the closure of the admissible values but does not belong to them. Hence, we exclude this solution.

Note that we may also interpret Eq. (6.47) as yielding the number of e-folds for a given value of  $n_{ani}$  assumed to be constant during the accelerated expansion phase. Since  $n_{ani} < 4$  we conclude that the lower bound for the number of e-folds reads  $\Delta N = 0.25$ . This lower bound implies that anisotropy can in fact reduce the duration of the inflationary phase with respect to the isotropic radiation-filled universe, for which the number of e-folds  $\Delta N = \ln \sqrt{2} \approx 0.347 \ll 60$  is clearly above the found lower bound (see Sec. 6.2.1), though still much too small to reproduce the inflationary scenario.

### Numerical analysis

Let us now re-express the generalized Friedmann equation (6.41) in terms of the mean scale factor:

$$H^2 = -\frac{1}{64} \frac{K_{eff}}{a^6} + \frac{Q_{-2}}{144} \frac{\mathbf{p}^2}{a^6} + \frac{Q_{\frac{2}{3}}}{4} \frac{\check{V}(\beta)}{a^2}, \quad (6.48)$$

Looking at the approximation (6.42) of the anisotropy energy density as a power of the scale factor  $n_{ani} + 2$ , requiring  $n_{ani}$  to be maintained very small means that the last term of the above Friedmann equation is the one that must dominate the dynamics during the phase of accelerated expansion, when anisotropy takes over after the quantum curvature diminishes. In other words, the anisotropic intrinsic curvature ( $-\frac{1}{6}\check{R}_{ani}$ ) must be much larger than the kinetic term ( $\frac{1}{3}\check{\sigma}^2$ ) for sufficiently long time for the above model to potentially generate enough e-folds of accelerated expansion. However, the semiquantum anisotropic potential  $\check{V}(\beta_{\pm}(t))$ , cannot be assumed to remain at a constant value. Therefore, the evolution of the position of the fictitious particle in the  $(\beta_-, \beta_+)$  plane inside the potential plays a crucial role in fuelling the inflationary behaviour [95].

The semiquantum anisotropic potential (6.16) is roughly triangular, with three canyons (or channels) in each of the vertices that now become confined (closed) due to the semiquantum corrections (see Fig.6.1-right). A study of the canyons shows that their profiles can be flattened, i.e, made grow less steeply, by increasing the value of the free quantization parameters  $\omega_{\pm}$ . That is, choosing a higher value of  $\omega_{\pm}$  makes the semiquantum potential look more like its classical version in the sense that the channels' length is extended, allowing the particle to penetrate into higher values in the  $(\beta_-, \beta_+)$  plane. However, the semiquantum regularization does not allow to make the bottoms of the canyons asymptotically ( $\beta_{\pm} \rightarrow \pm\infty$ ) approach to zero value, as in the classical potential. On the contrary, their bottoms always raise indefinitely as  $\beta_{\pm} \rightarrow \pm\infty$ . Thus, the most likely scenario, with the longest phase of inflationary dynamics, assumes the particle to be placed deep inside one of the channels shortly after the anisotropy energy takes over the dynamics. Along with the latter situation, we make the bottom of the channels as flat as possible, with a suitable choice of  $\omega_{\pm}$ . Then, we seek the anisotropic potential to consistently dominate for the largest number of e-folds over the kinetic term. If the potential is sufficiently flat inside the channels, the particle should be rolling down the potential very slowly.

We performed multiple numerical simulations of the above scenario. A typical example of the post-bounce evolution is plotted in Fig. 6.5. As one can observe, the model is not able to generate inflationary dynamics lasting sufficiently long. Therefore, we conclude that the semiquantum mixmaster universe cannot undergo a robust phase of accelerated expansion. This is due to the fact that, as we explain in the next section with analytical investigation, the anisotropy power law  $n_{ani}$  value cannot be maintained close to zero during enough time, because the semiquantum anisotropy potential is everywhere (besides the origin where it takes very small values) too steep for the slow roll of the anisotropy variables.

### Analytical analysis

Let us now inspect the equations of motion for anisotropy. We use the analogy between scalar fields in isotropic universe and the anisotropy variables. Upon dividing

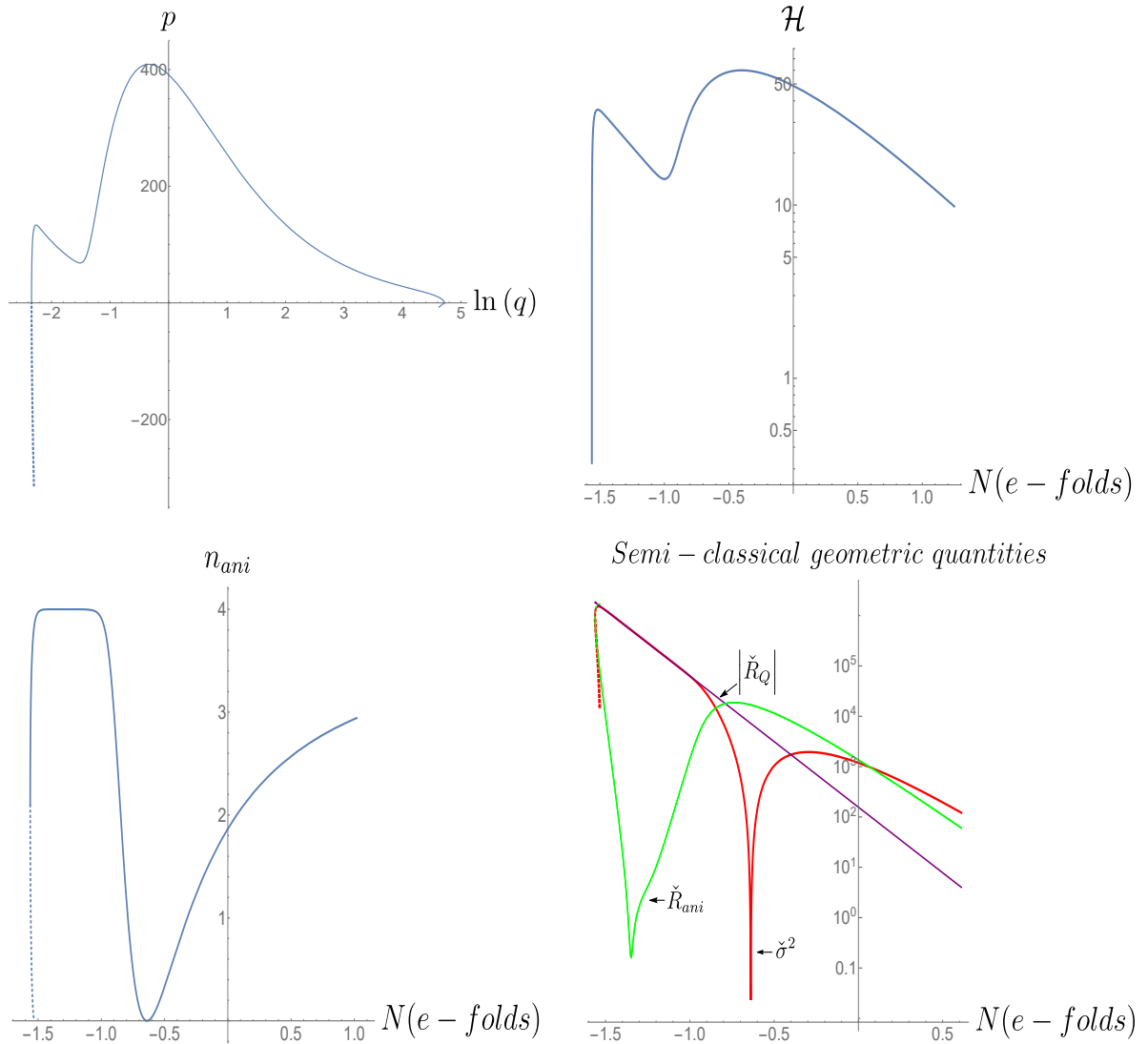


FIGURE 6.5: A typical solution to the semiquantum mixmaster universe close to the bounce, with extended inflationary dynamics. In the  $(q, p)$ -plane the accelerated expansion is initially driven by the semi-quantum curvature correction as the universe bounces, then it ends and appears again driven by the anisotropic curvature. In the  $(N, \mathcal{H})$ -plane the inflationary dynamics is exhibited in the growth of the conformal Hubble rate  $\mathcal{H}$ , which takes place at the beginning of expansion, around  $N \approx -1.5$ , and from around  $N \approx -1$  to  $N \approx -0.5$ . In the  $(N, n_{ani})$ -plane the inflationary dynamics is reflected in the small values of  $n_{ani} \approx 0$ , which happens at the bounce and during the anisotropy-driven inflation (recall that  $n_{ani}$  describes the behaviour of the anisotropy energy,  $\check{\rho}_{ani} \propto \frac{1}{a^{2+n_{ani}}}$ ). As the bottom-right panel shows, the dynamics is initially driven by the quantum curvature responsible for the bounce, then it is taken over by the anisotropy: first there is a lot of shear and little of anisotropic curvature so the dynamics is not inflationary (what yields  $n_{ani} \approx 4$ ). The inflationary dynamics begins once the energy of shear is transferred to the anisotropy potential, when the particle is slowing down deep inside one of the potential channels, which takes place around  $N \approx -1$ . We set the following initial data:  $q = 0.1$ ,  $p = -312.895$ ,  $\beta_+ = 0.0$ ,  $\beta_- = -1.71$ ,  $p_+ = 0.0$ ,  $p_- = 15.0$ . We set the parameters as follows:  $\omega_{\pm} = 56.23$ ,  $\sigma_{\pm} = 100$ ,  $\nu = 40008$  ( $K_{eff} = 10001.7$ ),  $R = 10^2$ .

the anisotropic part of the semiquantum Hamiltonian (6.17) by  $-36Q_2q^{\frac{2}{3}}$  (or, by setting  $1/N := -36Q_2q^{\frac{2}{3}}$ ) it acquires the following form:

$$H_{ani} = \frac{\mathbf{p}^2}{2m} + \check{V}(\boldsymbol{\beta}), \quad (6.49)$$

where the mass  $m(q) = 18Q_2q^{\frac{8}{3}}/Q_{-2}$  depends on the size of the universe in such a way that  $m$  grows as the universe expands. The equation of motion for  $\beta_{\pm}$  reads

$$\ddot{\beta}_{\pm} = -\frac{1}{m}\check{V}_{,\beta_{\pm}} - \frac{\dot{m}}{m}\dot{\beta}_{\pm}. \quad (6.50)$$

This dynamics is conservative only when  $\dot{q} = 0$ . However,  $\dot{q} > 0$  as the universe expands, and hence the energy  $H_{ani}$  may only decrease. Given that the anisotropy energy density at each moment of time behaves as a power function of the scale factor (see Eq. (6.42)), we have

$$\check{\rho}_{ani} \propto \frac{H_{ani}}{a^2} \propto \frac{1}{a^{n_{ani}+2}}, \quad (6.51)$$

with  $n_{ani} > 0$  as was to be shown. Upon inspecting the Hamiltonian (6.49) we clearly see that the kinetic energy scales as  $a^{-4}$ , whereas the potential energy is independent of the scale factor. Hence, we conclude that  $0 < n_{ani} < 4$ .

In order to reproduce the inflationary dynamics, we must have  $n_{ani} = 4e^{-4\Delta N}$ , which is positive and very small for  $\Delta N \approx 60$  e-folds. This requires the dynamics to be dominated by the anisotropy potential with a negligible kinetic energy  $\dot{\beta}_{\pm} \approx 0$ . In other words, the relative change of the potential during that number of e-folds must be very small. We find

$$d\check{V} = \check{V}_{,\pm}d\beta_{\pm} = \check{V}_{,\pm}\frac{\dot{\beta}_{\pm}}{H}\Delta N = -\check{V}_{,\pm}p_{\pm}\frac{Q_{-2}\Delta N}{12q^2H}, \quad (6.52)$$

where  $H$  is the Hubble rate. Let us assume  $d\check{V} = -\frac{\mathbf{p}^2}{2m}\Big|_{fin}$  (i.e., the difference between total energy and potential energy transferred to the kinetic term at the end of inflation, with  $\check{V}$  assumed to dominate the anisotropy energy until the end of accelerated expansion phase) and combine it with the last relation to obtain

$$d\check{V} = \left[ \check{V}_{,\pm} \frac{\sqrt{2m}Q_{-2}\Delta N}{12q^2H} \right]^2. \quad (6.53)$$

Thus, the condition  $d\check{V}/\check{V} \ll 1$  implies

$$\frac{\check{V}_{,\pm}}{\check{V}} \ll \frac{2\mathcal{H}/\sqrt{\check{V}}}{\sqrt{Q_2^2/Q_{-2}\Delta N}}, \quad (6.54)$$

where the conformal Hubble rate reads roughly  $\mathcal{H} \approx \frac{Q_2}{2} \sqrt{\check{V}}$  (by the virtue of the constraint equation) yielding

$$\frac{\check{V}_{,\pm}}{\check{V}} \ll \frac{\sqrt{Q_2 Q_{-2}}}{\Delta N}. \quad (6.55)$$

The right hand side of the above expression is very small. In our semiquantum model model we have  $2 < \frac{|\check{V}_{,\pm}|}{|\check{V}|} < 8$  except close to the point of origin  $\beta = 0$ , where the potential  $\check{V}$  has the minimum. We see that neither classical nor semiquantum potential can satisfy the above requirement and hence a sustained inflationary phase is excluded from this model. It is the exponential character of  $\check{V}$  that disallows anisotropy-driven inflation.

At this point it is interesting to note that the inflationary phase might occur in the harmonic approximation of the anisotropy potential as

$$\frac{|V_{,\pm}|}{V} = \frac{|2\beta|}{\beta^2} = \frac{2}{|\beta|}, \quad (6.56)$$

can be smaller than any value provided that the particle is placed sufficiently far away from the point of origin  $\beta = 0$ . This explains the previous result obtained in a full quantum framework in [39], where the harmonic approximation to the anisotropy potential was used.

### Comparison with simple inflaton model replacing anisotropy

It is instructive to compare the anisotropy Hamiltonian to that of a minimally coupled scalar field in a closed universe. The scalar field Hamiltonian constraint reads:

$$C_\phi = N \left( \frac{1}{2q^2} \pi_\phi^2 + q^2 V(\phi) \right), \quad (6.57)$$

which can be brought to the form of Eq. (6.49) by setting  $N := 1/q^2$ :

$$H_\phi = \frac{1}{2m'} \pi_\phi^2 + V(\phi), \quad (6.58)$$

where  $m'(q) = q^4$ . Now, we see clearly that the key difference lies in the respective masses  $m(q)$  and  $m'(q)$ . The energy density of the scalar field now reads

$$\rho_\phi \propto H_\phi \propto \frac{1}{a^{n_\phi}}, \quad (6.59)$$

where  $6 > n_\phi > 0$  following from the same reasoning as before. We clearly see that because of the minimal coupling the requirements for the inflationary potential are much milder than for anisotropy potential. Furthermore, given a complete (or, almost complete) freedom in proposing the inflationary potential, one may choose the harmonic one that easily produces the desired accelerated expansion. The numerical comparison of inflaton- (with quadratic potential) and anisotropy-driven dynamics in the post-bounce evolution is given in Fig. 6.6.

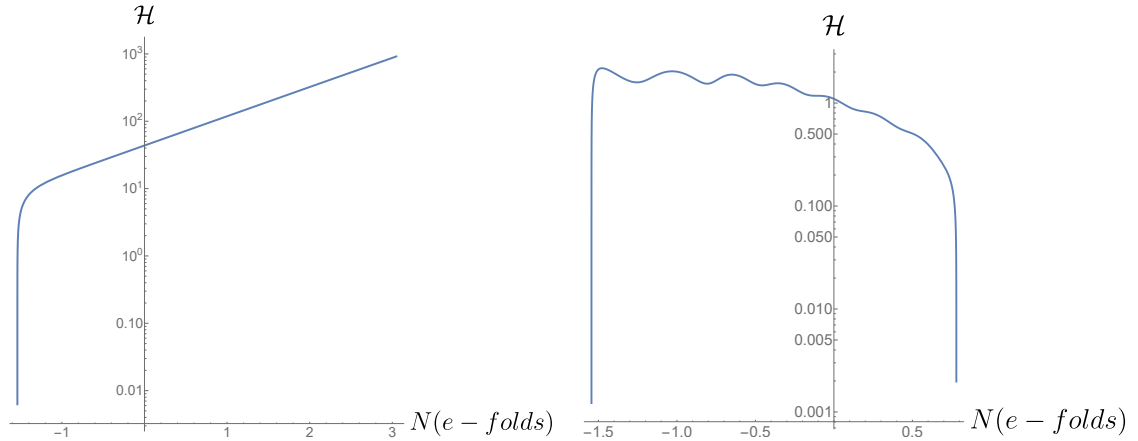


FIGURE 6.6: The evolution of the conformal Hubble rate in the anisotropy- and inflaton-dominated universes. On the left we see a robust exponential growth of the conformal Hubble rate generated by inflaton in a quadratic potential. On the right we see how the anisotropic curvature (just after the bounce ends) increases the conformal Hubble rate only by little and in an oscillatory manner (due to the oscillating anisotropic deformations  $\beta_{\pm}$ ). We set the following initial data:  $q = 0.1$ ,  $p = -5.139$ ,  $\beta_+ = 0.579$ ,  $\beta_- = 0.748$ ,  $p_+ = 0.175$ ,  $p_- = 0.15$ ,  $\phi = 2615121.8$ ,  $\pi_{\phi} = 0.01$ . We set the parameters as follows:  $\omega_{\pm} = 177.83$ ,  $\sigma_{\pm}^2 = 0.04738$ ,  $\nu = 350$  ( $K_{eff} = 11.9083$ ),  $R = 1.0$ , the mass of inflaton  $m_{\phi} = 0.0000578$ .

## 6.4 Brief discussion of results

In this chapter we investigated whether a quantum anisotropic primordial universe can spontaneously induce a phase of inflationary dynamics. We first derived a very generic quantum model of mixmaster universe via integral covariant quantization and coherent states methods. Thanks to these methods we were able to cover a wide range possible quantization ambiguities and semiquantum frameworks parametrized by a set of arbitrary constants. Then, using the equations of motion we found the reasons for why anisotropic universe, neither classical nor quantum, can not induce a sustained inflationary phase. In order to state these reasons clearly we compared the anisotropic model to the single-field inflationary model.

Both the anisotropy and the inflaton energy are declining as the universe expands. However, a minimally coupled field can produce effective pressure with  $w_{\phi} \in (-1, 1)$  while anisotropy produces effective pressure with  $w_{ani} \in (-\frac{1}{3}, 1)$ . It is well-known that  $w_{eff} < -\frac{1}{3}$  is required in order for accelerated expansion to take place. Therefore, pure anisotropy fails to induce inflation. Nevertheless, if one adds to the system a quantum correction in the form of repulsive potential, then any contribution, including anisotropy, can induce inflation for  $w_{ani} \approx -1/3$ . Thus, in principle, anisotropy could induce a sustained inflationary phase if its potential allowed for it. The crucial property is that in order for its effective pressure to remain minimal the relative change of the potential along a dynamical trajectory must be very small and slow. For the anisotropy potential this is however impossible because the potential is fixed by general relativity to be exponential. The inflationary potential does not have this limitation and could be, e.g., quadratic. We note that even quantization of the anisotropy potential does not change its exponential character.

# 7

## Conclusions and prospects for the future

Notwithstanding the fact that the results presented in this doctoral thesis do not constitute a new complete alternative theory, they provide a basis for the construction of such a theory in the future and set down the direction to be followed. This thesis contributes to the study of the effects that a quantum background can introduce on the evolution of the primordial universe. We found that, in the cosmological perturbation theory over a fluid-filled FLRW universe, there exist two, and only two, inequivalent ways of quantizing the model. This is in contrast with inflationary models, where the quantization is unique and the basic perturbation variable choice is made by convenience. The ambiguity that we find requires a background with a strong departure from the classical evolution on which inflationary models are based. The finding that the choice of basic variables matters is important as it affects the construction of the proposed quantum bouncing models. One might be tempted to reject one of the solutions of this simple model as unphysical and interpret that their predictions do not have a big significance. However, for the moment it is not clear how consequential it can be for more complex models. In other words, the second solution being too peculiar to be viable in comparison with the generic one may not be the case in more intricate quantum cosmologies.

In those isotropic bouncing models, even though their background does not experience a long-lasting inflationary dynamics, we proved that their quantization gives rise to a bounce that, solves the big-bang singularity, and produces a mechanism to generate cosmological structures by amplification of primordial vacuum fluctuations, which is the relevant physical outcome to look forward. The model, however, could in principle be improved to match the observations. The main issue is that the generated power spectrum is slightly blue tilted (for the assumed  $w > 0$ ).

The introduction of a significantly more generic model (mixmaster universe) including primordial anisotropy was proved to be not sufficient to make the bouncing semiquantum background generate enough inflationary dynamics. This means, we concluded, that the combination of anisotropic and quantum background cannot reproduce the accelerated expansion behaviour of a universe filled with a scalar (inflaton) field. It is tempting to speculate that, since anisotropy can produce an effective cosmological fluid pressure with  $w \approx -1/3$ , the mixmaster universe could still be a promising model for a cosmological scenario in which anisotropy plays a key role in the generation of primordial structure. That would be a bouncing cosmology in which the structure generation starts in the contracting phase and then is

smoothly transferred through a bounce to the expanding phase, such as in the perturbed isotropic models studied here, with the anisotropy modifying the contraction and the bounce and leading to the primordial perturbations with the correct spectrum. In this scenario, one could expect, there is more anisotropy in the contracting phase than in the expanding. The proposed scenario would require to apply perturbation theory in the anisotropic background, in order to study how the anisotropic oscillations interplay with the contracting and expanding phase and influence the propagation of primordial perturbations, leaving their new imprints in the spectrum above certain scale. We note that, in an anisotropic model, the dynamics of perturbation modes would be direction dependent ( $v_k \rightarrow v_{\vec{k}}$ ). Whether the resultant gravitational potentials modified by anisotropy can amplify the perturbations properly in each direction is a really interesting as well as challenging question to investigate. The suggested research would involve highly non-trivial calculations very likely uncovering new and rich physics of cosmological perturbations that interact in more sophisticated ways, e.g. via couplings between different modes of perturbations.

It would be an honour for me to be part of the research dedicated to such ambitious and exciting cosmological scenario.

# Bibliography

- [1] A. Einstein. On the General Theory of Relativity. *Reports of the meetings of the Prussian Academy of Sciences in Berlin* (4 Nov. 1915), pp. 778–786. English translation in *The Collected Papers of Albert Einstein*. Vol. 6. (English translation supplement) *Princeton University Press* (1997), pp. 98–107.
- [2] A. Einstein. On the General Theory of Relativity (Addendum). *Reports of the meetings of the Prussian Academy of Sciences in Berlin* (11 Nov. 1915), pp. 799–801. English translation in *The Collected Papers of Albert Einstein*. Vol. 6. (English translation supplement) *Princeton University Press* (1997). pp. 108–110.
- [3] A. Einstein. Explanation of the Perihelion Motion of Mercury from the General Theory of Relativity. *Reports of the meetings of the Prussian Academy of Sciences in Berlin* (18 Nov. 1915), pp. 831–839. English translation in *The Collected Papers of Albert Einstein*. Vol. 6. (English translation supplement) *Princeton University Press* (1997). pp. 112–116.
- [4] A. Einstein. The Field Equations of Gravitation. *Reports of the meetings of the Prussian Academy of Sciences in Berlin* (25 Nov. 1915), pp. 844–847. English translation in *The Collected Papers of Albert Einstein*. Vol. 6. (English translation supplement) *Princeton University Press* (1997). pp. 117–120.
- [5] A. Einstein. Cosmological considerations on the general theory of relativity. *Reports of the meetings of the Prussian Academy of Sciences in Berlin* (8 Feb. 1917), pp. 142–152. English translation in H.A. Lorentz, et al. *The principle of relativity*. *Dover Publications* (1952). pp. 175–188.
- [6] E. Hubble. A Relation Between Distance and Radial Velocity Among Extra-Galactic Nebulae. *Proceedings of the National Academy of Sciences of the United States of America* 15.3 (15 March 1929), pp. 168–173.
- [7] V. M. Slipher. Further Notes on Spectrographic Observations of Nebulae and Clusters. *Publications of the American Astronomical Society* 4 (1922), pp. 284–286.
- [8] Planck Collaboration. Planck 2015 results. XX. Constraints on inflation. *A&A* 594 (2016).
- [9] S. W. Hawking and R. Penrose. The Singularities of gravitational collapse and cosmology. *Proc. Roy. Soc. Lond.* A314 (1970), pp. 529–548.
- [10] Alan H. Guth. The Inflationary Universe: A Possible Solution to the Horizon and Flatness Problems. *Phys. Rev.* D23 (1981), pp. 347–356.
- [11] Chris J. Isham. Canonical quantum gravity and the problem of time. *Integrable systems, quantum groups and quantum field theories*. Springer (1993), pp. 157–287.
- [12] J. B. Hartle and S. W. Hawking. Wave function of the Universe. *Phys. Rev. D* 28 (1983), pp. 2960–2975.
- [13] P. Peter, E. J. C. Pinho, and N. Pinto-Neto. Gravitational wave background in perfect fluid quantum cosmologies. *Phys. Rev. D* 73.104017 (2006).
- [14] P. Peter, E. J. C. Pinho, and N. Pinto-Neto. A non inflationary model with scale invariant cosmological perturbations. *Phys. Rev. D* 75.023516 (2007).
- [15] W. Nelson, I. Agullo, and A. Ashtekar. Perturbations in Loop Quantum Cosmology. *Phys. Rev. D* 86.103505 (2012).

- [16] W. Nelson, R. Gambini, I. Agullo, and A. Ashtekar. Loop Quantum Cosmology and the Primordial Power Spectrum. *Physical Review Letters* 107.041301 (2012).
- [17] A. Durakovica, P. Hunt, S. Mukherjee, S. Sarkar, and T. Souradeepf. Reconstruction of a direction-dependent primordial power spectrum from Planck CMB data. *JCAP* 02.012 (2018).
- [18] S. Deser R. L. Arnowitt and C. W. Misner. The dynamics of general relativity, (in *Gravitation: an introduction to current research*, chapter 7, L. Witten ed., Wiley, U.S.A., (1962), pp. 227-264). *Gen. Relativ. Gravit* 40 (2008), pp. 1997–2027.
- [19] P. Małkiewicz. Hamiltonian formalism and gauge-fixing conditions for cosmological perturbation theory. *Classical Quantum Gravity* 36.215003 (2019).
- [20] B. F. Schutz. Perfect Fluids in General Relativity: Velocity Potentials and a Variational Principle. *Phys. Rev. D* 2 (1970), pp. 2762–2773.
- [21] B. F. Schutz. Hamiltonian theory of a relativistic perfect fluid. *Phys. Rev. D* 4.12 (1971), p. 3559.
- [22] F. G. Alvarenga, R. Fractalossi, R. G. Furtado, and S. V. B. Gonçalves. Dynamics of a perfect fluid through velocity potentials with application in quantum cosmology. *Braz.J.Phys.* 47.1 (2017), pp. 96–105.
- [23] J. d. C. Martin, P. Małkiewicz, and P. Peter. Unitarily inequivalent quantum cosmological bouncing models. *Phys. Rev. D* 105.023522 (2022).
- [24] H. Bergeron, A. Dapor, J-P. Gazeau, and P. Małkiewicz. Smooth big bounce from affine quantization. *Phys. Rev. D.* 89.083522 (2014).
- [25] K. Kuchar. A bubble-time canonical formalism for geometrodynamics. *J. Math. Phys.* 13.768 (1972).
- [26] P. Peter and J-P. Uzan. *Primordial Cosmology*. Oxford Graduate Texts (Oxford University Press, Oxford, UK) (2013).
- [27] P. Małkiewicz and A. Mroczewski. Dynamics of primordial fields in quantum cosmological spacetimes. *Phys. Rev. D* 103.083529 (2021).
- [28] P. A. M. Dirac. *Lectures on Quantum Mechanics*. Vol 2 (1964). (New York: Belfer Graduate School of Science).
- [29] V. A. Belinskii, I. M. Khalatnikov, and E. M. Lifshitz. Oscillatory approach to a singular point in the relativistic cosmology. *Adv. Phys.* 19 (1970), pp. 525–573.
- [30] R. Kantowski and R.K. Sachs. Some Spatially Homogeneous Anisotropic Relativistic Cosmological Models. *Journal of Mathematical Physics* 7.443 (1966).
- [31] M. P. Ryan and L. C. Shepley. Homogeneous Relativistic Cosmologies. *Physics Today* 29.4 (1976), p. 67.
- [32] G. F. R. Ellis and M. A. H. MacCallum. A class of homogeneous cosmological models. *Commun. Math. Phys.* 12.108 (1969).
- [33] C. W. Misner. Quantum Cosmology. I. *Phys. Rev.* 186.1319 (1969).
- [34] J. H. Bae. Mixmaster revisited: wormhole solutions to the Bianchi IX Wheeler–De Witt equation using the Euclidean-signature semi-classical method. *Class. Quant. Gravity* 32.075006 (2015).
- [35] H. Bergeron, J. d. C. Martin, J-P. Gazeau, and P. Małkiewicz. Can a quantum anisotropic universe spontaneously generate an inflationary phase? (2023). [arXiv:2303.07873].
- [36] C. W. Misner. Mixmaster Universe. *Phys.Rev.Lett.* 22.1071 (1969).
- [37] H. Bergeron, E. Czuchry, J-P. Gazeau, P. Małkiewicz, and W. Piechocki. Smooth Quantum Dynamics of Mixmaster Universe. *Phys. Rev. D* 92.061302(R) (2015).
- [38] H. Bergeron, E. Czuchry, J-P. Gazeau, P. Małkiewicz, and W. Piechocki. Singularity avoidance in a quantum model of the Mixmaster universe. *Phys. Rev. D* 92.124018 (2015).

- [39] H. Bergeron, E. Czuchry, J-P. Gazeau, and P. Małkiewicz. Nonadiabatic bounce and an inflationary phase in the quantum mixmaster universe. *Phys. Rev. D* 93.124053 (2016).
- [40] H. Bergeron, E. Czuchry, J-P. Gazeau, and P. Małkiewicz. Vibronic framework for quantum mixmaster universe. *Phys. Rev. D* 93.064080 (2016).
- [41] H. Bergeron, E. Czuchry, J-P. Gazeau, and P. Małkiewicz. Spectral properties of the quantum Mixmaster universe. *Phys. Rev. D* 96.043521 (2017).
- [42] H. Bergeron, E. Czuchry, J-P. Gazeau, and P. Małkiewicz. Integrable Toda system as a quantum approximation to the anisotropy of the mixmaster universe. *Phys. Rev. D* 98.083512 (2018).
- [43] A. H. Guth. The Inflationary Universe: A Possible Solution to the Horizon and Flatness Problems. *Phys. Rev. D* 23 (1981), pp. 347–356.
- [44] A. Linde. Hybrid inflation. *Phys. Rev. D* 49 (1994), pp. 748–754.
- [45] A. D. Linde. Chaotic Inflation. *Physics Letters B* 129 (1983), pp. 177–181.
- [46] R. D. Klauber. Horizons in Cosmology (2018).
- [47] A. Hämäläinen. Cosmic Perturbation Theory and Inflation. *Department of Physics, University of Jyväskylä* (2015). Master’s Thesis.
- [48] Y. Akrami et al. (Planck collaboration). Planck 2018 results. X. Constraints on inflation. *Astron. Astrophys.* 641.A10 (2020).
- [49] P. Peter. Observing alternatives to inflation. *PoS Cosmology2009. Contribution to: International Workshop on Cosmic Structure and Evolution* 003 (2009).
- [50] E. Schrödinger. Der stetige Übergang von der Mikro zur Makromechanik. *Naturwissenschaften* (1926), pp. 664–666.
- [51] I. R. Senitzky. Harmonic oscillator wave functions. *Phys Rev.* 95 (1954), pp. 1115–1116.
- [52] A. M. Perelomov. Coherent states for arbitrary Lie group. *Communications in Mathematical Physics* 26.3 (1972), pp. 222–236.
- [53] L. A. Takhtaja. Quantum mechanics for mathematicians. *American Mathematical Society* (2008).
- [54] T. M. van Haeringen. Generalized Coherent States. *Bachelor Project Physics and Mathematics, University of Groningen* (2016).
- [55] H. Bergeron, E. M. F. Curado, J-P. Gazeau, and L. M. C. S. Rodrigues. Weyl-Heisenberg integral quantization(s): a compendium (2017). [arXiv:1703.08443].
- [56] E. W. Aslaksen and J. R. Klauder. Unitary Representations of the Affine Group. *J. Math. Phys.* 15.206 (1968).
- [57] J-P. Gazeau and R. Murenzi. Covariant Affine Integral Quantization(s). *J. Math. Phys* 57.052102 (2016).
- [58] E. Berge, S. M. Berge, F. Luef, and E. Skrettingland. Affine quantum harmonic analysis. *Journal of Functional Analysis* 282.109327 (2022).
- [59] H. Bergeron and J.-P. Gazeau. Integral quantizations with two basic examples. *Annals of Physics (NY)* 344 (2014), pp. 43–68.
- [60] L. Van Hove. Sur le probleme des relations entre les transformations unitaires de la mécanique quantique et les transformations canoniques de la mécanique classique. *Bulletin de la Classe des sciences. Académie royale de Belgique* 37 (1951), pp. 610–620.
- [61] M. Reed and B. Simon. Methods of Modern Mathematical Physics, II. Fourier Analysis, Self-Adjointness, Vol 2. *Academic Press, New York* 2 (1975), pp. 43–68.
- [62] S. T. Ali, J-P. Antoine, and J-P. Gazeau. Coherent States, Wavelets and their Generalizations. Second edition. *Theoretical and Mathematical Physics, Springer, New York* (2013).

- [63] J. R. Klauder. Continuous-Representation Theory. II. Generalized Relations between Quantum and Classical Dynamics. *Journal of Mathematical Physics* 4 (1963), pp. 1058–1073.
- [64] J. d. C. Martin. The primordial structure from Quantum Cosmological bouncing models. *Contribution to the 2022 Cosmology session of the 56th Rencontres de Moriond* (2022). [arXiv:2203.03924].
- [65] D. Battefeld and P. Peter. A critical review of classical bouncing cosmologies. *Phys. Rep.* 571.1 (2015).
- [66] R. Brandenberger and P. Peter. Bouncing cosmologies: Progress and problems. *Found. Phys.* 47.797 (2017).
- [67] J. Grain and V. Vennin. Bouncing cosmologies: Progress and problems. *J. Cosmol. Astropart. Phys.* 02.022 (2020).
- [68] C. Kiefer and M. Kramer. Quantum Gravitational Contributions to the Cosmic Microwave Background Anisotropy Spectrum. *Phys. Rev. Lett* 108.021301 (2012).
- [69] A. Vilenkin. Boundary conditions in quantum cosmology. *Phys. Rev. D* 33.12 (1986).
- [70] J. R. Klauder. The Affine quantum gravity program. *Classical Quantum Gravity* 19.817 (2002).
- [71] J. R. Klauder. Enhanced Quantization: Particles, Fields and Gravity. *World Scientific, Hackensack* (2015).
- [72] H. Bergeron, J. P. Gazeau, and P. Małkiewicz. Primordial gravitational waves in a quantum model of big bounce. *J. Cosmol. Astropart. Phys.* 05.057 (2018).
- [73] A. Vilenkin. Quantum cosmology and the initial state of the Universe. *Phys. Rev. D* 37.888 (1988).
- [74] F. Olver, D. Lozier, R. Boisvert, and C. Clark. The NIST Handbook of Mathematical Functions. *Cambridge University Press, New York, NY* (2010).
- [75] V. F. Mukhanov, H. A. Feldman, and R. H. Brandenberger. Theory of cosmological perturbations. *Physics Reports* 215 (1992). Master’s Thesis, pp. 203–333.
- [76] P. Małkiewicz. What is dynamics in quantum gravity. *Classical Quantum Gravity* 34.205001 (2017).
- [77] J. Martin and P. Peter. On the “Causality Argument” in Bouncing Cosmologies. *Phys. Rev. Lett.* 92.061301 (2004).
- [78] J. Martin. Inflationary Perturbations: The Cosmological Schwinger Effect. *Springer, Berlin, Heidelberg* (2008).
- [79] P. Peter and N. Pinto-Neto. Has the Universe always expanded? *Phys. Rev. D* 65.023513 (2001).
- [80] V. F. Mukhanov and S. Winitzki. Introduction to Quantum Fields in Classical Backgrounds (2004). Lecture notes.
- [81] L. Chataignier and M. Krämer. Unitarity of quantum gravitational corrections to primordial fluctuations in the Born-Oppenheimer approach. *Phys. Rev. D* 103.066005 (2021).
- [82] A. Y. Kamenshchik, A. Tronconi, and G. Venturi. The Born–Oppenheimer approach to quantum cosmology. *Classical and Quantum Gravity* 38.15 (2021).
- [83] H. Bergeron, P. Małkiewicz, and P. Peter (2023). [Under preparation].
- [84] J. d. C. Martin, P. Małkiewicz, and P. Peter. Ambiguous power spectrum in a quantum bounce (2023). [arXiv:2212.12484].
- [85] P. Małkiewicz. Clocks and dynamics in quantum models of gravity. *Class. Quant. Grav.* 34.145012 (2017).
- [86] P. Małkiewicz and A. Miroszewski. Internal clock formulation of quantum mechanics. *Phys. Rev. D* 96.046003 (2017).

- [87] P. Małkiewicz, P. Peter, and S. D. P. Vitenti. Quantum empty Bianchi I space-time with internal time. *Phys. Rev. D* 101.046012 (2020).
- [88] P. Małkiewicz, P. Peter, and S. D. P. Vitenti. Clocks and Trajectories in Quantum Cosmology. *Universe* 8.71 (2022).
- [89] V. Mukhanov and S. Winitzki. Introduction to quantum effects in gravity. *Cambridge University Press* (2007).
- [90] J. d. C. Martin and P. Małkiewicz. Physical predictions and final quantum state of perturbations in quantum bouncing cosmology (2023). [In preparation].
- [91] J. Haro and E. Elizalde. Gravitational particle production in bouncing cosmologies. *JACP* 10.028 (2015).
- [92] G. Gubitosi and J. Magueijo. The phenomenology of squeezing and its status in non-inflationary theories. *JCAP* 11.014 (2017).
- [93] S. Dodelson. Coherent Phase Argument for Inflation. *AIP Conf. Proc.* 689.184 (2003).
- [94] S. Dodelson. Modern Cosmology. *Academic Press* 11.014 (2003).
- [95] J. d. C. Martin. Mixmaster universe: semiclassical dynamics and inflation from bouncing. *Acta Physica Polonica B Proceedings Supplement* 16.6-A20 (2023). [arXiv:2302.01111].
- [96] T. Buchert and N. Obadia. Effective inhomogeneous inflation: curvature inhomogeneities of the Einstein vacuum. *Class. Quantum Grav.* 28.162002 (2011).
- [97] S. W. Hawking and G. F. R. Ellis. The large scale structure of spacetime. *Cambridge University Press* (1973).
- [98] A. D. Linde. A new inflationary universe scenario: A possible solution of the horizon, flatness, homogeneity, isotropy and primordial monopole problems. *Physics Letters B* 108 (1982), pp. 389–393.